UNIVERSIDAD DE ANTIOQUIA

DYNAMICS OF CONTINENTAL WATER STORAGE IN REGIONS OF HYDROGEOLOGICAL INTEREST IN COLOMBIA WITH IMPLICATIONS FOR WATER SECURITY

Silvana Bolaños Chavarría

Universidad de Antioquia

Facultad de Ingeniería, Escuela Ambiental

Medellín, Colombia

2020

DYNAMICS OF CONTINENTAL WATER STORAGE IN REGIONS OF HYDROGEOLOGICAL INTEREST IN COLOMBIA WITH IMPLICATIONS FOR WATER SECURITY

A Dissertation
Submitted to the Faculty of Engineering
Universidad de Antioquia

By

Silvana Bolaños Chavarría

In Partial Fulfillment
of the Requirements for the Degree
Doctor of Environmental Engineering

Supervised by
PhD Teresita Betancur Vargas
PhD Juan Fernando Salazar Villegas

Environmental School
Faculty of Engineering
Universidad de Antioquia
Medellín, Colombia

2020

"Water is the driving force of all nature."

Leonardo da Vinci

This study is dedicated to my family who always believed in me, to my professors who always taught me, to God my guide, and to you, my love...

ACKNOWLEDGEMENTS

LIST OF FIGURES

LIST OF TABLES

CHAPTER 1
INTRODUCTION AND BACKGROUND

Some aspects of the understanding of the hydrological cycle, including its flows and stocks, are largely based on in situ measurements leading to long time series from dense gauging networks. While this "high density" is common in some regions of the world mainly in developed countries (Chen, Wilson, Tapley, Scanlon, & Güntner, 2016b), developing countries still struggle with limited availability of data from e.g. rain and discharge gauges (Gründemann, Werner, & Veldkamp, 2018; Seyoum & Milewski, 2016). Further, although an accurate assessment the water balance components depends on the quantity and quality of the available data, these measurements are generally sparse (Zhang, 2017).

Groundwater is among the main components of hydrological systems, and it contributes to the maintenance of terrestrial and aquatic ecosystems. Groundwater constitutes the largest reservoir of liquid fresh water of the planet (accounting for 95%, ignoring polar ice caps and glaciers). In contrast, water in rivers accounts for approximately 0.006% (Šiklomanov, 1997). Groundwater is an important source of drinking water for almost half of the world's population, including provision of water for human consumption, agriculture, industry and a variety of ecosystems (Döll et al., 2012). Further, groundwater plays an important role in the capacity of societies to adapt to climate change and variability because it is generally less sensitive to the effects of climate change relative to surface water (Resende et al., 2019). However, climate change has significant impacts on groundwater, including decreases in aquifer recharge and intensification of water extraction from aquifers due to climatic extremes such as severe droughts (Green et al., 2011; Taylor et al., 2013; Zaveri et al., 2016).

Piezometric data from wells provide useful but limited information because of, for instance, their limitations in depth (typical depths rarely exceed 100 meters) and spatial coverage (Fatolazadeh, Voosoghi, & Naeeni, 2016). Lack of groundwater observations limits our understanding of the dynamic relationship between groundwater and climate, as well as of the effect of the use of the this resource, especially in areas in which it is intensively exploited (Taylor et al., 2013). Enhancement of in situ measurements and use of new data from advances in satellite instrumentation is fundamental for improving our understanding of the dynamics of water storages.

In 2005, the Hydrogeology Journal released a special edition entitled "The future of hydrogeology" (Voss, 2005) in which, from the perspective of different authors, they question and discuss how hydrogeology will be in the coming decades. In one of these papers, Hoffmann (2005) discuss how advances in satellite instrumentation and models contribute to answer important open questions in the field of hydrogeology. Gleeson and Cardiff (2013) summarize this discussion and list several questions that focus on the spatio-temporal variability of the flows and storages of groundwater at continental scales, also called "megascales". They note that in recent years there has been a growing interest on the use of satellites that provide continuous (both over space and time) descriptions of groundwater variability.

The performance and utility of satellite data have been continuously improving (Hoffmann, 2005). One of the main developments has been the Gravity Recovery and Climate Experiment (GRACE), which is the first satellite mission dedicated to monitoring the Earth's gravitational field. The GRACE mission consists of a pair of NASA satellites that have been in the low Earth orbit since 2002, and produce detailed measurements of changes in the Earth's gravitational field, which in turn provides information for research on the variability of continental and oceanic water, as well as on earthquakes and crustal deformation. GRACE measures gravity by relating it to the distance between the two satellites, which use a precise microwave system that measures variations in the distance between satellites due to variations in the acceleration of gravity. These satellites are about 220 km apart and can detect changes of less than one micrometer per second in relative speed. These changes in the Earth's gravitational field are directly related to changes in surface mass. The surface mass signal reflects the total water storage (TWS), which in land corresponds to the sum of groundwater, soil moisture, surface water, snow, and ice (Fig. 1.1) (Shamsudduha et al., 2017).

GRACE data have been widely used in hydrological sciences (Fig. 1.2). Applications are concentrated in two aspects: first, the evaluation of TWS that involves evaluation of groundwater change; and second, the assimilation of GRACE in hydrological models (Ning, Ishidaira, & Wang, 2014). Recent studies have shown that the conjoint use of TWS data from GRACE and other hydrological data sets can provide estimates of the water balance components that are useful for mega-scale water management (Chen, Wilson, Tapley, Scanlon, & Güntner, 2016b; Famiglietti et al., 2011; Yeh, Swenson, Famiglietti, & Rodell, 2006; Zaitchik, Rodell, & Reichle, 2008).
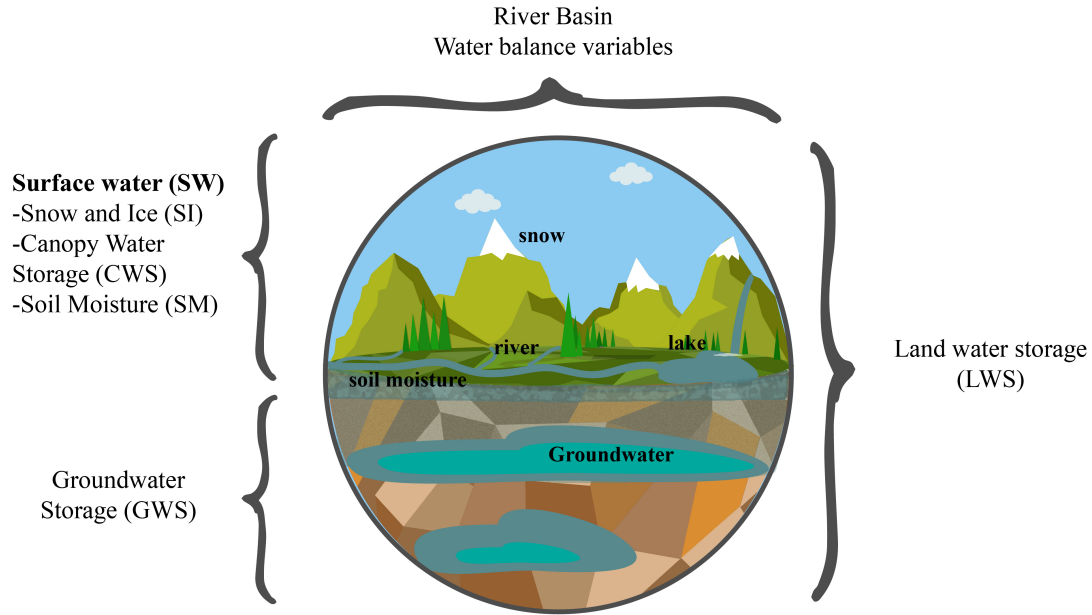
Figure 1.1: Schematic description of TWS and water balance.

There are unsolved challenges and limitations that limit the application and interpretation of GRACE data (Alley & Konikow, 2015; Chen, Famigliett, Scanlon, & Rodell, 2016a). Some of the main limitations of GRACE data arise from their spatial resolution that ranges between 0.5°and 1°. These resolutions can be excessively coarse for some aquifers that are small relative to a GRACE cell. Overall, it has been estimated that GRACE can detect changes in TWS with an accuracy of 1.5 cm in the equivalent water thickness for areas that are larger than 200,000 km^2 (Famiglietti & Rodell, 2013). Further, GRACE does not separate the components of water storage, such as groundwater and soil moisture. This separation can be accomplished by using models (e.g. from GLDAS) and combining GRACE data with hydrological data from different sources. Validation of GRACE data, and particularly of TWS estimates, is challenging due to the uncertainty and limitations that are inherent to observations themselves (Chen, Wilson, Tapley, Scanlon, & Güntner, 2016b).

In Colombia, the Magdalena-Cauca river basin (Fig. 1.3) is among the most relevant and complex units of study. Most of the societal and economical dynamics of the country develops and/or depends on this basin. The Magdalena-Cauca includes a complex terrain characterized by the presence of three mountain ranges (so-called western, central, and eastern branches of the Colombian Andes) that correspond to the northern edge of the Andes. The Magdalena River has a length of 1,540 km, and crosses from South to North
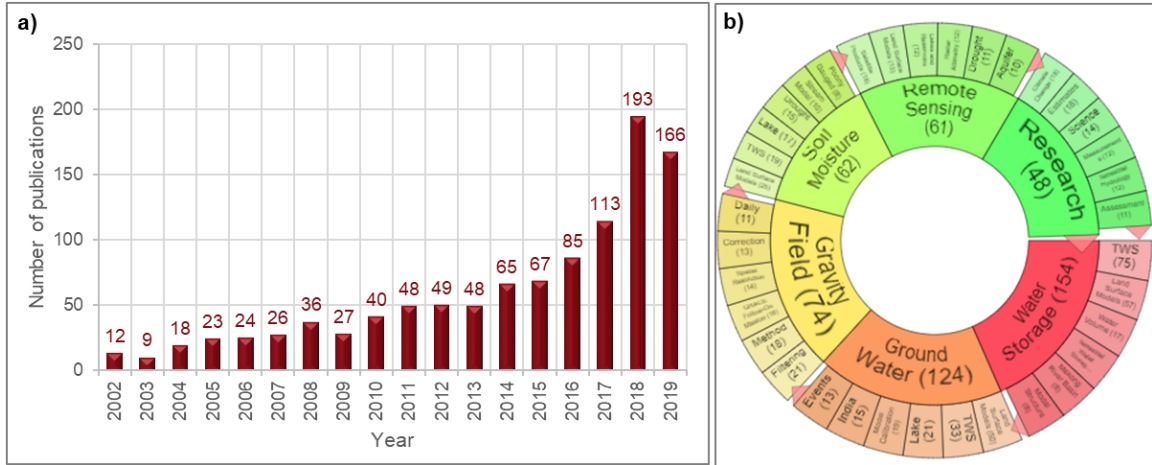
Figure 1.2: Evolution of GRACE studies since its launch. Data based on the academic search engine World Wide Science using the keywords GRACE satellite and hydrology. a) Number of publications per year; b) most representative issues in which GRACE is applied. Information is directly taken from https://worldwidescience.org.

almost the entire territory of Colombia. It receives in the Momposina depression the waters of the Cauca river and 300 km beyond it empties into the Caribbean Sea. With heights between 0 and more than 5,000 meters above sea level, all thermal floors and a wide climatic variability are recorded (IDEAM & CORMAGDALENA, 2001).

The Magdalena and Cauca rivers are key elements in the context of the Andean orogeny in Colombia; the basin is formed by rocks with ages from the Precambrian to the Tertiary. These rocks are partially covered by unconsolidated Quaternary deposits. Lithologically, the territory presents igneous, sedimentary, and metamorphic rocks, with a great variety of types and textures. Above the surface formations, the outermost part of the earth's crust stands out, which are the soils, forming the basis for the sustenance of the vegetation cover and biotic ecosystems. The soils fulfill functions and provide services, associated with the exchanges and flows of matter and energy between the components of the ecosystem, the availability of these elements guarantees the sustainability of the environment (IDEAM & CORMAGDALENA, 2001). The characteristics of the soils of the morphogenic macro-units determine sustainable alternative uses; on the other hand, they are key factors in the water cycle and offer storage capacities and water regulation (see Appendix A for a detailed geological and hydrogeological description of the basin in Spanish).

While the upper part of the basin is characterized by a complex topography and the presence of different ecosystems such as montane wetlands (Páramo) (Rodríguez & Ar-

4

menteras, 2005), the lower part of the basin is characterized by the presence of extensive wetlands. The largest wetlands system is known as La Mojana, which is close to the confluence of the Cauca and Magdalena rivers, and is characterized by a complex network of swamps and channels (IDEAM & CORMAGDALENA, 2001). Further, several regions within the basin have been describes as "regions of hydrogeological interest" (National Study of Water or ENA for its acronym in Spanish, versions 2014 and 2018), meaning that they have been prioritized by national authorities for the study and potential use of groundwater. These regions of interest include 8 hydrogeological provinces which in turn include 34 aquifer systems (Fig. A.7 in Appendix A) (IDEAM, 2015, 2019). Some of these hydrogeological systems are the most intensively used in Colombia (located in Valle del Cauca, Middle Upper Magdalena, and the Cordillera Oriental), mainly for agriculture and human consumption.

Although several studies have investigated these aquifer systems in Colombia, the country lacks a sufficiently dense and adequate national monitoring network of groundwater resources. Currently, the National Institute of Hydrology, Meteorology, and Environmental Studies (IDEAM, Instituto de Hidrología, Meteorología y Estudios Ambientales) is leading an initiative that seeks to establish a national hydrogeological monitoring network, but its scope is still limited due to insufficient information and dispersion of studies on water resources. In the last decades, the number of hydrological and meteorological monitoring stations has been decreasing in the entire national area (Rodríguez et al., 2019), which limits the advances in the understanding of the national water resources. This situation highlights the potential and relevance of using GRACE data for studying TWS and related variables and dynamics in Colombia. This satellite-based data may provide information that would otherwise not be available. This is of particular importance because of the role of TWS in the dynamics of hydrological processes on land, including variations in surface and groundwater availability and related impacts on water resources management (Syed, Famiglietti, Rodell, Chen, & Wilson, 2008).

Here we test the hypothesis that GRACE data provide a realistic representation of both surface and groundwater storage in Colombia, which is relevant for informing decisions on water resources management in the Magdalena-Cauca basin. From this perspective, the general objective of this dissertation is to study the dynamics of continental water storages in regions of particular interest for hydrogeological studies in Colombia, while discussing the implications for future water availability. The specific objectives point to: (i) assessing the performance of the fifth release of GRACE in the representation of the dynamics of
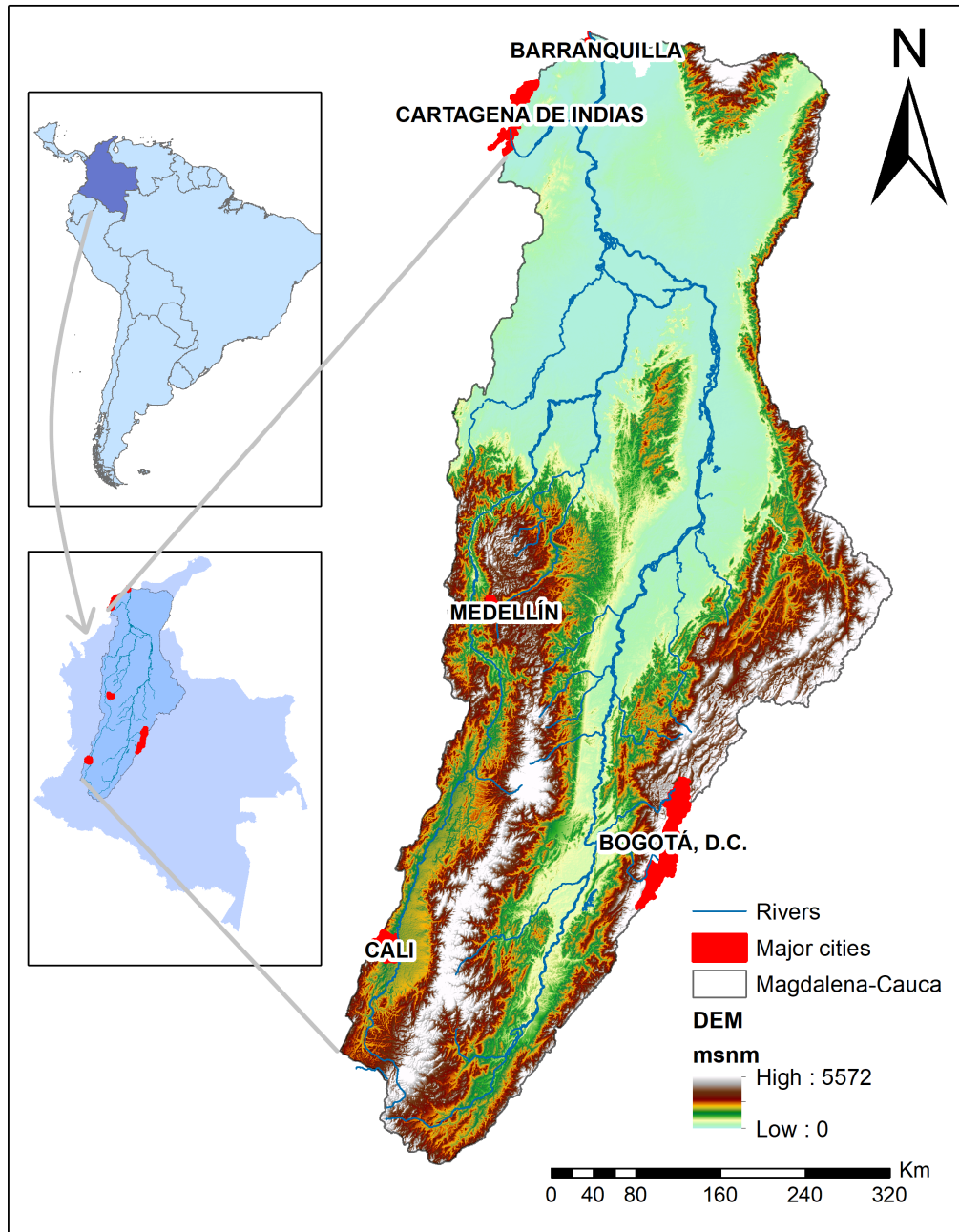
Figure 1.3: Location of the Magdalena-Cauca basin in Colombia, in northwestern South America. The digital Elevation Model (DEM) represents topographical elevation in meters above the sea level.

TWS in the Magdalena-Cauca river basin; (ii) characterizing the dynamics of water storage in the regions of interest; and (iii) discussing the mechanisms behind these dynamics. This is accomplished through a combination of theoretical discussions and data analyses that seek to find meaningful relationships between variables related to multiple processes,

including recharge, large-scale climatic effects, and surface water dynamics. Further, after evaluating GRACE data and taking into account the increasing use of global models to support water resources studies, we compare TWS in the study basin from GRACE and a set of different global models.

It is worth mentioning that there are very few applications of GRACE to studies in Colombia. Guarín Giraldo and Poveda (2013) studied the spatio-temporal variability of water storage in the soil and precipitation in the Colombian territory between August 2002 and February 2008, as well as its potential relationship with the El Niño/Southern Oscillation (ENSO). They found good agreement between GRACE data, simulated moisture results from the NCEP/NCAR Reanalysis, and precipitation from TRMM, and suggest that there may be an inverse relationship between TWS from GRACE and the Oceanic Niño Index (ONI). Ospina M and Vargas J (2018) used GRACE data along with the Global Land Data Assimilation System (GLDAS) and hydrometeorological gauges to study the spatial and temporal variability of groundwater accumulation in the Eastern Llanos of Colombia for a period between 2003 and 2014. They suggest that GRACE data provide valuable insight for monitoring recharge changes. Overall, With around 15 years of monthly data, the GRACE mission has proven that it can provide valuable information for decision making in site-specific studies.

The methodological approach of this research can be divided in two parts. First, we use different precipitation, evaporation, and river flow datasets from gauging stations and remote sensing to evaluate the consistency of GRACE data products through water balance computations. This comparison led to the identification of one of the GRACE products, the one from the Jet Propulsion Laboratory mass-concentration (JPL mascon), as the bets performing in the representation of changes of water storage in the Magdalena-Cauca basin. Then we perform a trend analysis of GRACE data that reveals temporal and spatial shifts in the TWS fields. In particular, we identify a growing trend in TWS between 2002 and 2010, and a decreasing trend afterwards. This trends are consistent with changes in precipitation and temperature over the basin that coincide with ENSO-induced variability over the region. Finally, we analyze the spatial patterns of GRACE and find meaningful relationships with topography and the presence of wetlands at the Mompós Depression zone. The results of this first part are presented in Chapter 2, in the form of an article entitled "Spatial and temporal shifts of total water storage fields in a medium-size tropical basin inferred from GRACE data" that is currently under review.

In the second part we assess the ability of six global hydrological models (GHM) and four land surface models (LSM) to represent the dynamics of TWS in the Magdalena-Cauca. These models were provided by the EartH2Observe (E2O) project. Based on results from the first part, the assessment was based on a comparison between simulated (by the set of models) and observed (through GRACE) TWS in the Magdalena-Cauca basin. We compare monthly TWS changes obtained from each model with the corresponding value from GRACE for the 2002–2014 period, considering monthly variability, seasonality, and long-term trends. The assessment considered the Magdalena-Cauca basin as a whole, as well as some of its major sub-basins. Overall, we found that the models have a poor performance in representing TWS at the monthly timescale, and that this performance improves for seasonality and long-term trends. Results highlight the sensibility of performance to scale. The details and results of this part are presented in Chapter 3 in the form of an article that is in the submission process.

Finally, in Chapter 4, we present a general discussion and the main conclusions of the thesis, including implications for water security in Colombia. Figure 1.4 schematically shows the flow of the thesis chapters, including the main scientific question to be answered in each one in order to achieve the proposed objectives.
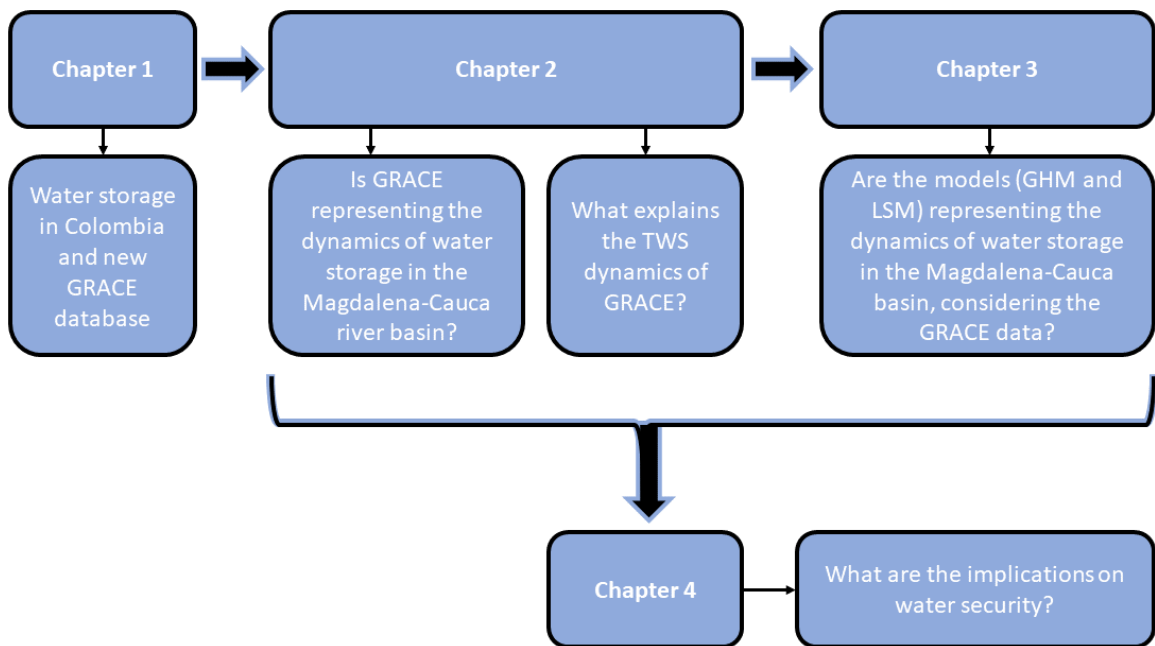
Figure 1.4: Flowchart of the thesis content.

CHAPTER 2
GRACE REVEALS DEPLETION IN WATER STORAGE IN NORTHWESTERN SOUTH AMERICA BETWEEN ENSO EXTREMES

Silvana Bolaños[1], Teresita Betancur[1], Juan F. Salazar[1], Micha Werner[2]

[1]Grupo de Ingeniería y Gestión Ambiental - GIGA, Escuela Ambiental, Facultad de Ingeniería, Universidad de Antioquia, Medellín, Colombia

[2]Water Science and Engineering Department, IHE Delft Institute for Water Education, Delft, the Netherlands

Key Points:

- GRACE and water balance-based estimates of water storage are comparable in northern South America.

- Trends in water storage shift from positive to negative as a result of ENSO variability.

- Spatial heterogeneity of trends is related to the presence of wetlands and the Andean mountains.

Abstract

Dynamics of terrestrial water storage are determinant for many natural and social phenomena, with implications for water security and environmental sustainability. Here we use 2002–2017 data from the Gravity Recovery and Climate Experiment (GRACE) to study these dynamics in the Magdalena-Cauca river basin in northwestern South America. Through comparison with water balance-based estimates we assess the performance of multiple GRACE products in representing water storage dynamics in the basin, identifying the Mascon product from the Jet Propulsion Laboratory as the best suited for further analysis. We then investigate the existence of long term trends and show that terrestrial water storage in general and groundwater storage in particular have been gradually depleting in the basin since around the end of 2010. GRACE data reveal that this trend is not uniform across the basin but exhibits a clear-cut pattern in which the water depletion rate

is more pronounced in the lower parts of the basin than it is in the upper basin. We explore the mechanisms behind the identified temporal trends and spatial patterns and show that water storage depletion largely coincides with a period between the La Niña and El Niño extreme phases of ENSO. Likewise, the pronounced contrast between depletion rates in the lower and higher parts of the basin largely coincides with marked biophysical differences between these regions, including the presence of major wetland systems in the lowlands, and the highlands of the Andean mountains.

2.1 Introduction

Many natural and social phenomena depend on the dynamics of terrestrial water storage, which plays a major role in the Earth's climate system through its effect on the global water, energy, and biogeochemical cycles (Famiglietti, 2004; Huang et al., 2013; Long et al., 2017; Salazar et al., 2018; Yang, Xia, Zhan, Qiao, & Wang, 2017). The dynamics of terrestrial water storage are, however, sensitive to global change and understanding how and why these dynamics are changing in different regions of the world is critical to the assessing of present and future water security (Long et al., 2014; Voss et al., 2013); and is recognized as a fundamental problem of the hydrological sciences in the Panta Rhei context (Montanari et al., 2013).

A first order explanation of these dynamics is given by the water balance equation,

$$\frac{dS}{dt} = P - E - Q, \tag{2.1}$$

which, for a river basin, determines that temporal variations in terrestrial water storage (dS/dt) depend on the differences between input fluxes of precipitation (P) and output fluxes of evapotranspiration (E) and river discharge (Q). Here S includes all components of water storage at the surface (e.g. water bodies, soil moisture, and snow) and beneath it (groundwater).

Estimation of dS/dt for any given region is challenging, especially when hydrological data is scarce or unavailable (e.g. Hassan and Jin, 2016; Ouma, Aballa, Marinda, Tateishi, and Hahn, 2015; Voss et al., 2013). Monitoring wells provide precise but generally scattered (in space and time) data of groundwater level that can be used to estimate variations in groundwater storage (e.g. Huang et al., 2013; Nanteza, Linage, Thomas, and Famiglietti, 2016). Observations of soil moisture, snow, and surface water provide additional means to directly estimate different components of TWS. The water balance equation

(Eq. 2.1) allows for the estimation of dS/dt indirectly through estimates of fluxes P, E, and Q. Though this is not trivial for large river basins, it can be accomplished through combining multiple observational techniques (e.g. gauging networks and remote sensing) and modelling. The launch of the Gravity Recovery and Climate Experiment (GRACE) twin satellite mission in 2002 has provided an unprecedented way of directly estimating dS/dt through high-precision measurements of the Earth's gravity field. The fundamental idea behind these GRACE-based estimates is that variations in the Earth's gravity field are related with the dynamics of the total terrestrial water storage (TWS) defined as the sum of snow, surface water, soil moisture, and groundwater (Tapley, Bettadpur, Watkins, & Reigber, 2004; Wahr, Swenson, Zlotnicki, & Velicogna, 2004).

Since the launch of the mission, the use of GRACE data to investigate variations in TWS has attracted much attention (Famiglietti, 2014; Wada et al., 2010). It has helped identify different regions of the world in which terrestrial water, mainly groundwater, is being depleted, including northwest India (Rodell, Velicogna, & Famiglietti, 2009; Tiwari, Wahr, & Swenson, 2009), the Central Valley in California (Famiglietti et al., 2011) and Texas (Long et al., 2013), as well as in the United States of America (U.S.) (Yi & Wen, 2016), China (Feng et al., 2013; Long et al., 2014; Shen, Leblanc, Tweed, & Liu, 2015), the Middle East (Voss et al., 2013), and East Africa (Nanteza, Linage, Thomas, & Famiglietti, 2016; Swenson & Wahr, 2009). Such depletion in water storage poses a threat to the water security and environmental sustainability of those regions.

Several studies have demonstrated that water storage variations can be inferred from GRACE with enough resolution and accuracy to benefit water security assessments and water management (Jiang et al., 2014; Landerer & Swenson, 2012; Long, Longuevergne, & Scanlon, 2015; Wang & Li, 2016). However, there is incomplete evidence of the ability of GRACE data to reproduce the dynamics of terrestrial water storage in all continental regions of the world, thus calling for further evaluation and case-specific studies (e.g. Abiy and Melesse, 2017; Long et al., 2016; Seyoum and Milewski, 2016). Moreover, variations in processing of GRACE data have led to multiple GRACE products (e.g. JPL-Mascons and CSR-Mascons; Save, Bettadpur, and Tapley, 2016; Watkins, Wiese, Yuan, Boening, and Landerer, 2015; Wiese, Landerer, and Watkins, 2016; more details in Section 2) the performance of which is not equivalent in every region (e.g. Long et al., 2017; Scanlon et al., 2016; Shamsudduha et al., 2017). The performance of GRACE data can be assessed through comparison of TWS anomalies from GRACE and variations in surface water, soil moisture, snow and groundwater storage (estimated from groundwater level data, if avail-

able) (Scanlon, Longuevergne, & Long, 2012; Seyoum & Milewski, 2016). Alternatively GRACE-based TWS anomalies can be compared with estimates of dS/dt through Equation 2.1 using data of the fluxes data P, E and Q. For instance, water balance estimates have been used to show that GRACE produces a realistic representation of water storage dynamics in California's Sacramento and San Joaquin River basins in the U.S. (Famiglietti et al., 2011) and in East Africa (Nanteza, Linage, Thomas, & Famiglietti, 2016).

Other applications of GRACE data include estimating the water balance of large river basins (Jiang et al., 2014; Seo & Lee, 2016); evapotranspiration (Billah et al., 2015; Lv et al., 2017; Ramillien et al., 2006; Tang & Zhang, 2011); water budget closure (Lv et al., 2017; Sheffield, Ferguson, Troy, Wood, & McCabe, 2009; Wang, Guan, Gutiérrez-Jurado, & Simmons, 2014); basin storage-river flow relationships (Papa et al., 2015; Reager, Thomas, & Famiglietti, 2014; Sproles, Leibowitz, Reager, et al., 2015); groundwater variations (Chen, Wilson, Tapley, Scanlon, & Güntner, 2016b; Famiglietti et al., 2011; Feng et al., 2013; Hachborn, Berg, Levison, & Ambadan, 2017; Nanteza, Linage, Thomas, & Famiglietti, 2016; Rodell, Velicogna, & Famiglietti, 2009); flood forecasting (Chen, Wilson, & Tapley, 2010; Reager, Thomas, & Famiglietti, 2014; Tangdamrongsub, Ditmar, Steele-Dunne, Gunter, & Sutanudjaja, 2016), as well as vegetation greenness and drought characterization (Chen, Wilson, Tapley, Yang, & Niu, 2009; Long et al., 2014; Tang, Cheng, & Liu, 2014), glacier, ice cap changes and snow water equivalent (Chen, Wilson, Tapley, Blankenship, & Ivins, 2007; Frappart, Ramillien, & Famiglietti, 2011; Li, Chen, Ni, Tang, & Hu, 2019). In most of these, GRACE data are combined with measurements of e.g. precipitation and either hydrological or land surface models. Through the combination improved insight is provided into the water balance and fluxes in basins studied, but less so into the performance of GRACE data in representing the dynamics of TWS.

In this paper, we explore the ability with which GRACE data derived products can represent the dynamics of TWS in the tropical Magdalena-Cauca basin (MC basin henceforth) in northwestern South America. We develop five main activities. After describing our data and methods (Sec. 2.2), we first assess the performance of multiple available GRACE products (more details in Sec. 2.2.3) in representing water storage dynamics as compared to independent water balance estimates based on terrestrial observations (Sec. 2.3.1). Second, we use the best performing GRACE product to investigate the existence of long term trends in the MC basin as a whole, as well as in its major sub-basins (Sec. 2.3.2). Third, we use the Global Land Data Assimilation System (GLDAS) to separate surface water (SWS)

and groundwater (GWS) contributions to trends in TWS. Fourth, we use GRACE data to study the spatial variability of temporal trends in order to explore the existence of physically meaningful spatial patterns. This mapping highlights an advantage of using GRACE data, as it would not be possible with water balance estimates that depend on spatially non-continuous and relatively scarce observations of water balance fluxes. Finally, we explore the underlying mechanisms that explain the identified temporal trends and spatial patterns, hypothesising that these are commensurate to ENSO-related variability and pronounced biophysical differences in the basin (Sec. 2.4). We present our main conclusions in Section 2.5.

2.2 Data and Methods

2.2.1 The Magdalena-Cauca basin

The region of interest in this study is the MC basin, located in northwestern South America and draining an area of $276,000$ km^2 (Fig. 2.1). The Magdalena river originates in the Andes at an elevation of approximately $3,700$ m above sea level, and runs for $1,612$ km before flowing into the Western Caribbean in the Atlantic Ocean (López López, Immerzeel, Rodríguez Sandoval, Sterk, & Schellekens, 2018; Restrepo & Kjerfve, 2000). The Cauca River is the main tributary of the Magdalena River, flowing along the western part of the basin, and joining the Magdalena River in a inner-delta wetland area called La Mojana, which is a part of the Mompós Depression. Focus on this basin is motivated by its paramount importance to water security, and related energy and food security, in Colombia. This importance is highlighted by the fact that the MC basin is the largest basin entirely contained within Colombia, covering around 25% of the country's continental area; contains most of the reservoirs of the national hydropower system, as well as multiple wetlands, paramos (montane wetland ecosystems unique to the northern Andes), and small watershed systems, which are critical to water supply across the country (Angarita et al., 2018; IDEAM & CORMAGDALENA, 2001).

The National Water Study (ENA after its Spanish acronym, versions 2014 and 2018) identifies 34 aquifer systems in the MC basin (Fig. A.7 in Appendix A), some of which have been extensively exploited and are critical to the agricultural sector of the country (`http://www.andi.com.co/Uploads/ENA_2018-comprimido.pdf`). These aquifers will likely play a crucial role in safeguarding future water security and environmental sustainability (IDEAM, 2015, 2019). Further, the MC basin is located in a region that is a world biodiversity hotspot (Rangel-Ch, 2015), and has been identified as highly sensitive to ENSO-induced climate variability (Bedoya-Soto, Poveda, Trenberth, & Vélez-
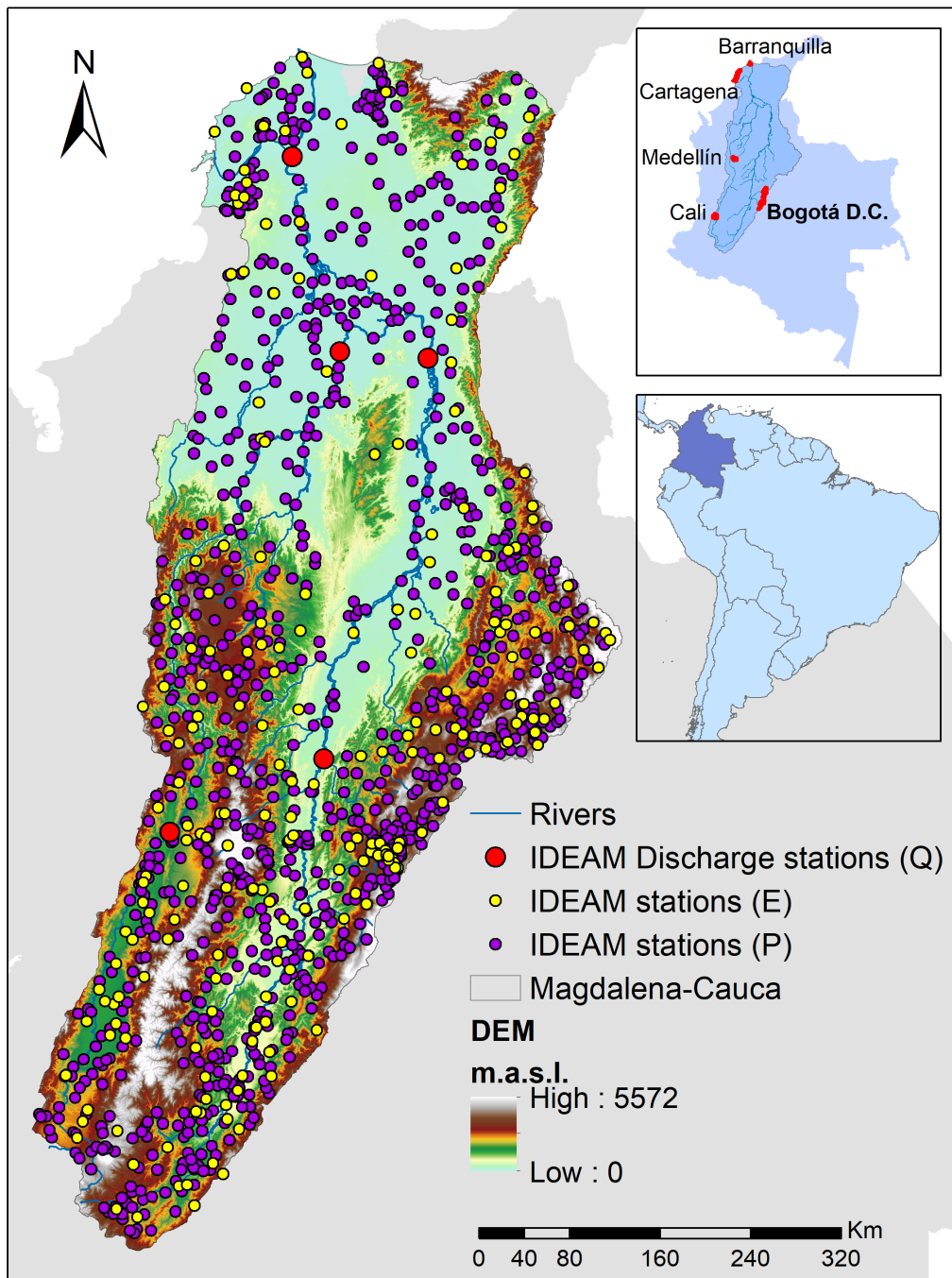
Figure 2.1: The Magdalena-Cauca (MC) river basin in northwestern South America. Points show the gauging stations from the national network (IDEAM) used in this study for discharge (red), evaporation (yellow), and precipitation (purple) . Shading represents topographical elevation in meters above the sea level.

Upegui, 2019; Hoyos, Escobar, Restrepo, Arango, & Ortiz, 2013). The region is regarded to be highly vulnerable to climate change (Magrin et al., 2014; Pabón Caicedo, 2012).

2.2.2   GRACE and water balance components data

We use 183 months from April 2002 to June 2017 of GRACE-derived monthly anomalies of TWS from three different products. The first product is constructed from post-processed GRACE RL05 level-3 land (L3-land) data, gridded at 1°($\sim$ 110 km near the Equator) and based on the RL05 Spherical Harmonics (SH) basis function. Datasets are obtained from three sources; the Center for Space Research at University of Texas (CSR, Austin); the Jet Propulsion Laboratory (JPL), and Geoforschungs Zentrum Potsdam (GFZ) processing centers (Landerer & Swenson, 2012; Swenson & Wahr, 2006). The ensemble mean of these three post-processed GRACE datasets is used to balance the bias of any single post-processing technique (e.g. Sakumura, Bettadpur, and Bruinsma, 2014; Voss et al., 2013). The second and third products are JPL-Mascons and CSR-Mascons, which are solutions gridded at 0.5°($\sim$ 55 km) that use regional mass concentration functions (i.e. Mascons) to parameterize the gravity field. These Mascon products have become operational within the last years (Save, Bettadpur, & Tapley, 2016; Watkins, Wiese, Yuan, Boening, & Landerer, 2015; Wiese, Landerer, & Watkins, 2016). All five solutions of GRACE land used in this study (CSR, JPL, GFZ, JPL mascon and CSR mascon) are available through the GRACE Tellus page `http://grace.jpl.nasa.gov` supported by the NASA Measures Program.

In order to restore the energy lost through processing, we use the scaling factors provided by each processing center to scale GRACE data, following standard processing steps (Landerer & Swenson, 2012; Ouma, Aballa, Marinda, Tateishi, & Hahn, 2015). TWS anomalies are estimated as the difference between monthly values and the mean of these values over the period from 2004 to 2009 (details in GRACE Tellus website). All other anomalies used in this study were calculated with respect to the same period. Missing data (e.g. due to battery management) were directly remedied by linear interpolation (e.g. Liesch and Ohmer, 2016; Ouma, Aballa, Marinda, Tateishi, and Hahn, 2015; Shamsudduha, Taylor, and Longuevergne, 2012; Xiao, He, Zhang, Ferreira, and Chang, 2015). Variations in water storage are always expressed as an equivalent water thickness (e.g. cm of water).

We estimate the water balance components in the MC basin using a combination of data from the national network of gauging stations and global re-analysis and satellite datasets. In all cases, these data correspond to the period 2002–2015, with the original

values converted into anomalies by subtracting the mean values for the 2004–2009 period. Data from gauging stations of the national network were provided by the National Institute of Hydrology, Meteorology and Environmental Studies of Colombia (IDEAM for its Spanish acronym; available in `http://www.ideam.gov.co/`), and include time series of precipitation from 1084 gauges, evaporation from 199 gauges, and river flow from 5 gauges for 5 subbasins considered below (Fig. 2.1). Precipitation data were also obtained from four products: the Tropical Rainfall Measuring Mission —TRMM 3B43 level 3 version 7 (Huffman et al., 2007)—, the Global Precipitation Climatology Centre —GPCC which provides gridded gauge-analysis products derived from quality controlled station data (Schneider, Fuchs, Meyer-Christoffer, & Rudolf, 2008)—, the Climate Research Unit —CRU (Harris & Jones, 2017)—, and the Centre for Medium-Range Weather Forecasts (ECMWF) ReAnalysis-Interim —ERA-Interim (Dee et al., 2011). For evapotranspiration, we use data from the MODIS Global Evapotranspiration Project (MOD16) (Running, Mu, & Zhao, 2017), ERA-Interim reanalysis, and the Global Land Evaporation Amsterdam Model (GLEAM). GLEAM combines multi-satellite observations to estimate daily actual evaporation through a process-based methodology. We use both GLEAM versions v3A and v3B (Martens et al., 2017; Miralles et al., 2011). GLEAM v3A is based on satellite-observed soil moisture, vegetation optical depth, and snow-water equivalent, air temperature and radiation from reanalysis, and a multi-source precipitation product; whereas GLEAM v3B is largely driven by satellite data. Taking advantage of the multiple available data sources, we produce an ensemble of estimates of the variation in terrestrial water storage through the water balance (Eq. 2.1). Table 2.1 summarizes the GRACE and water balance components data used in this study.

Table 2.1: Summary of GRACE and water balance components used in this study.

Source	Variable	Resolution	Time period	References
GRACE (CSR, JPL, GFZ)	EWT	1°x 1°	Apr 2002–Jan 2017	Swenson & Wahr, 2006 Landerer & Swenson, 2012
JPL, CSR mascons	EWT	0.5°x 0.5°	Apr 2002 – Jun 2017	Watkins et al., 2015 Wiese et al., 2016
GLDAS	EWT	0.25°x 0.25°	Jan 2000 – Dec 2017	Rodell et al., 2004
TRMM	P	0.25°x 0.25°	Jan 2000 – Dec 2016	Huffman et al., 2007

Table 2.1 – continued from previous page

Source	Variable	Resolution	Time period	References
GPCC	P	0.5°x 0.5°	Jan 2000 – Oct 2016	Schneider et al., 2008
CRU	P	0.5°x 0.5°	Jan 2000 – Dec 2015	Harris & Jones, 2017
ERA Interim	P E	0.75°x 0.75°	Jan 2000 – Dec 2015	Dee et al., 2011
MODIS	E	0.5°x 0.5°	Jan 2000 – Dec 2014	Running et al., 2017
GLEAM v3A	E	0.25°x 0.25°	Jan 2000 – Dec 2014	Martens et al., 2017 Miralles et al., 2011
GLEAM v3B	E	0.25°x 0.25°	Jan 2003 – Dec 2015	Martens et al., 2017 Miralles et al., 2011
IDEAM	P E Q	1084 stations 199 stations 5 stations	Jan 2000 – Dec 2015	n/a

EWT: equivalent water thickness. P: precipitation. E: evapotranspiration. Q: river discharge. n/a: not applicable.

2.2.3 Comparing GRACE and water balance derived estimates of TWS variation

Comparison between GRACE-derived and water balance-based estimates of TWS variation has been widely used as a procedure for assessing GRACE data (e.g. (Becker, LLovel, Cazenave, Güntner, & Crétaux, 2010; Famiglietti et al., 2011; Nanteza, Linage, Thomas, & Famiglietti, 2016; Scanlon et al., 2018; Voss et al., 2013)). Using all sources of data for P and E, as well as records of Q near the outlet of the MC basin, we first estimate monthly values of dS/dt from the water balance equation (Eq. 2.1). Then we compare these water balance-based estimates of dS/dt with the time derivative of TWS anomalies, expressed as a forward difference derivative (TWSC) of the form

$$\frac{dS}{dt}_n \approx TWSC_n = TWS'_n - TWS'_{n-1}, \qquad (2.2)$$

where $n-1$ and n denote consecutive months, and the primes indicate anomalies. We use this comparison to differentiate between GRACE products, with all further analyses using only the GRACE product that exhibits best agreement with water balance-based estimates of TWS variations.

2.2.4 Isolation of GWS contribution from GRACE-Derived TWS variation

TWS anomalies derived from GRACE can be understood as the result of adding anomalies in groundwater storage (GWS') and all forms of surface water storage (SWS') (e.g. Chen, Wilson, Tapley, Scanlon, and Güntner, 2016b; Famiglietti et al., 2011; Shamsudduha, Taylor, and Longuevergne, 2012, and others) as expressed by

$$TWS' = GWS' + SWS'. \tag{2.3}$$

Therefore, anomalies of groundwater storage GWS' can be estimated as the residual of TWS' after subtracting SWS'. SWS' includes multiple components, though some may be negligible for a given region. For instance, the snow water equivalent can be assumed as negligible for the MC basin due to its tropical climate regime. In contrast, soil moisture (SM) arguably accounts for a considerable portion of SWS variations.

Another TWS component that may be large is the storage of surface water in major water bodies such as reservoirs and lakes (e.g. Becker, LLovel, Cazenave, Güntner, and Crétaux, 2010; Shamsudduha et al., 2017; Swenson and Wahr, 2009). Indeed, most of the major reservoirs and some large wetland systems in Colombia are located within the MC basin (Angarita et al., 2018). In some studies, this component is subtracted from TWS to isolate GWS (e.g. Famiglietti et al., 2011; Fatolazadeh, Voosoghi, and Naeeni, 2016; Huang, Pavlic, Rivera, Palombi, and Smerdon, 2016; Liesch and Ohmer, 2016 and others). However, this requires an estimation of water storage dynamics in such water bodies, which is not always possible due to the available data (e.g. surface water altimetry data from LEGOS, Voss et al., 2013). These data of the dynamics of water storage in large water bodies is not available for the MC basin. Further, water storage dynamics in large water bodies is often tightly coupled to GWS dynamics through sub-surface flows (Ouma, Aballa, Marinda, Tateishi, & Hahn, 2015; Winter, 1999). From this perspective, as with several other studies (e.g. Hachborn, Berg, Levison, and Ambadan, 2017; Moiwo, Lu, and Tao, 2012; Ouma, Aballa, Marinda, Tateishi, and Hahn, 2015; Rodell et al., 2007) we calculate GWS' as;

$$GWS' = TWS' - SM', \tag{2.4}$$

where SM' can be estimated by means of hydrological or land surface models. Here we use the Global Land Data Assimilation System (GLDAS) to estimate SM'. GLDAS is a robust simulation system that incorporates satellite and ground-based observational data products using advanced land surface modeling and data assimilation techniques with the

purpose of generating optimal fields of land surface states for soil moisture, snow, and fluxes, at global scales and high spatial resolution (0.25–1°) in near-real time (Rodell et al., 2004). GLDAS outputs have been widely used in GRACE studies (e.g. Ni et al., 2018; Ospina M and Vargas J, 2018; Ouma, Aballa, Marinda, Tateishi, and Hahn, 2015; Yang and Chen, 2015). We use GLDAS outputs from the Noah land surface model (Ek et al., 2003). We select this particular model for two reasons. First, compared to the other available models; Community Land Model (CLM), MOSAIC, and the Variable Infiltration Capacity (VIC) model, the Noah model has a finer resolution (0.25°), which is important given the size of the MC basin. Second, previous studies have demonstrated that SWS estimates from Noah are consistent with seasonal variations in GRACE estimates (Eom, Seo, & Ryu, 2017; Han et al., 2009).

2.2.5   Detection of trends and breakpoints

To analyse trends, we first remove seasonality from GRACE data, and then apply linear regression and the nonparametric Mann-Kendall (MK) test. The MK test is a standard rank-based procedure which allows assessing the significance of trends (Huang et al., 2013). Further, we use the Segmented package in R (Muggeo et al., 2008) to study whether the water storage records are better described by one or two trend lines, i.e. whether there are breakpoints at which a trend is reduced (e.g. the slope is reduced without changing its sign) or even reversed (the sign of the slope changes). This trend analysis was performed for the whole MC basin and its main tributaries, as well as for each GRACE grid cell in order to explore the existence of spatial patterns in TWS variability.

2.2.6   Optical and Synthetic Aperture Radar (SAR) images

To support our discussion of the spatial variability of trends, we use images acquired by the PALSAR sensor onboard the ALOS satellite, and Landsat data of Climate Data Record (CDR) from the Science Processing Architecture System of the U.S. Geological Survey (USGS) Earth Resources Observation and Science (EROS) Centre. The ALOS-PALSAR system was launched on June 2006 and operated until May 2011. We processed 43 images in the form of high-resolution Radiometric Terrain Correction (RTC) based on Single Look Complex (SLC) data in strip map mode, with single polarization HH available for the Mompós Depression wetlands area between 2010 and 2011. We adopted the L-band HH polarized mode images because it is known to be sensitive to water level change beneath the vegetation (Grings et al., 2009; Pope, Rejmankova, Paris, & Woodruff, 1997; Rosenqvist, Shimada, Ito, & Watanabe, 2007) while maintaining coherence for interfero-

metric processing (Kim et al., 2009). These SAR images have been used in several studies to delimit floodplains and wetlands in different regions of the world (e.g. Arnesen et al., 2013; Dabrowska-Zielinska et al., 2014; Palomino-Ángel, Anaya-Acevedo, Simard, Liao, and Jaramillo, 2019; Yuan, Lee, and Jung, 2015. Using these images, we are able to obtain a map of the extent of flooding during the 2010–2011 wet season in which there was extensive flooding in the basin. Obtaining such a map would otherwise be very difficult to obtain due to the cloud cover. ALOS data was obtaind from the Alaska Satellite Facility online portal (`https://vertex.daac.asf.alaska.edu/`)

Optical images acquired during the dry season are reported to be better suited for classification purposes in tropical environments (Deus, 2016; Liesenberg, Galvão, & Ponzoni, 2007). Data used here were acquired by Landsat 8 satellites. The bands 4, 5, and 6 corresponding to Red ($0.64 - 0.67 \mu m$), Near-Infrared ($0.85 - 0.88 \mu m$) and SWIR 1 ($1.57 - 1.65 \mu m$), were acquired at 16 day intervals and $30m$ resolutions. The combination of bands 4-5-6 of these bands is useful to identify water bodies. The Landsat scene of World Reference System path-row 9-53, 9-54, 8-54, and 8-55 were chosen as these cover the inundation area within Mompós Depression wetlands during the ENSO event of 2015–2016. In total we processed 36 images corresponding to dry months where the cloud cover was less than 30%. The steps used for the identification of floodplains are described in detail in Escobar Martínez (2011) and Anaya-Acevedo et al. (2017). The Landsat data is available through the USGS EarthExplorer online portal (`https://earthexplorer.usgs.gov/`).

2.3 Results

2.3.1 Comparison between GRACE products and water balance-based estimates

Figure 2.2 shows a comparison between the multiple GRACE-based estimates of TWSC and the corresponding estimates of dS/dt based on the water balance (equations 2.1 and 2.2). Figures 2.2a and 2.2b depict, respectively, the time series of monthly values and the average annual cycle for the whole period. Three different GRACE-based estimates are included; the mean of the Spherical Harmonics (SH) basis functions from the CSR, JPL, and GFZ processing centers (GRACE Mean SH); and the Mascon products from JPL (JPL-Mascon) and CSR (CSR-Mascon). Estimates derived from the water balance are established with all combinations of sources of data for P, E, and Q (Table 2.1). This ensemble is depicted by its mean value (black solid line in Figs. 2.2a,b) and the corresponding envelope (gray shade). We highlight the estimates of dS/dt based only on gauging data from

20
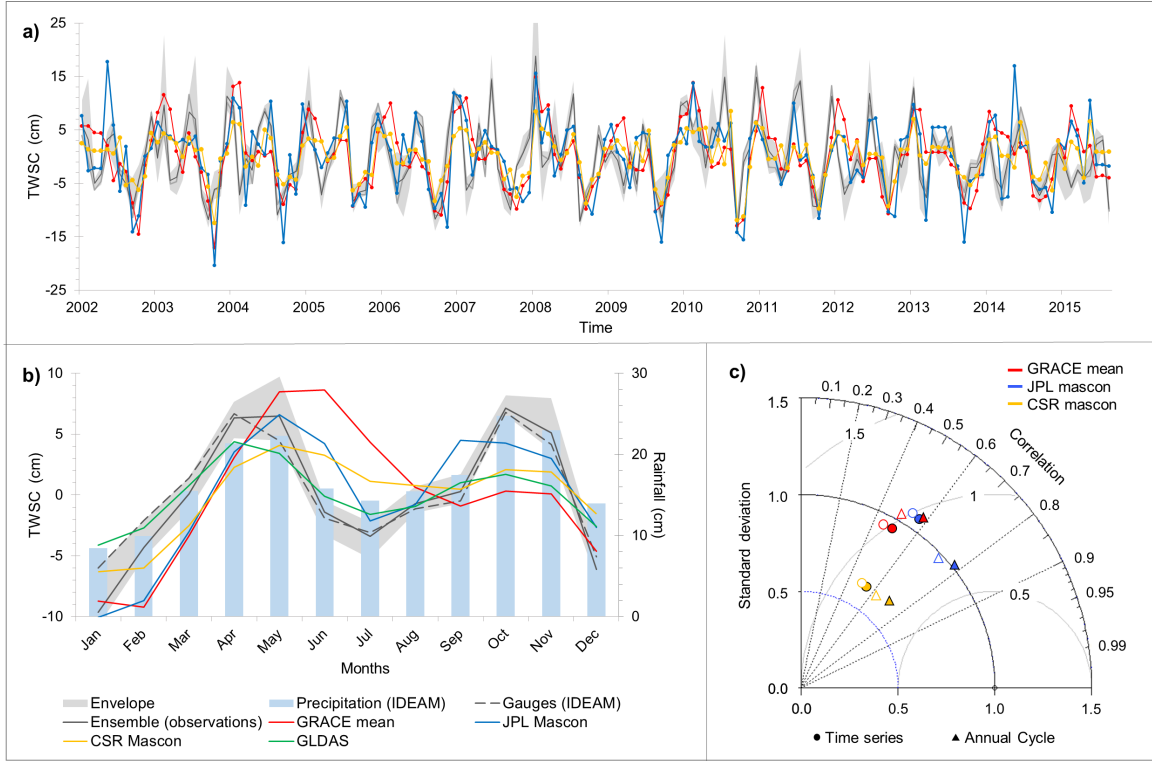
Figure 2.2: Comparison between the three GRACE-based estimates of TWSC and the corresponding estimates of dS/dt based on the water balance. (a) Time series of monthly values during 2002–2015; (b) 14-years (2002–2015) average annual cycle; and (c) Taylor diagrams relating observation-based estimates (ensemble: filled points, gauging stations from IDEAM: unfilled points) and TWSC (GRACE) for both the time series in (a) and the annual cycle in (b). Grey shading in panels (a) and (b) shows the envelope of dS/dt estimates (Eq. 2.1) using multiple data sources for the water balance components. Blue bars show the network-averaged annual cycle of precipitation for the same period. Green line shows the 14-years (2002–2015) average annual cycle of surface water storage change (SWS' in Eq. 2.3)

the national network (black dashed line in Fig. 2.2c, Gauges IDEAM). Additionally, Figure 2.2c shows a Taylor diagram summarizing the agreement between the different GRACE- and water balance-based estimates in reproducing the temporal variability of terrestrial water storage (either TWSC or dS/dt) in the MC basin.

Agreement between GRACE- and water balance-based estimates varies among the three GRACE products. There are three clear differences. First, correlation is worst for the GRACE Mean SH product (red in Fig. 2.2), both for the time series and the annual cycle. The poor correlation is particularly as a results of the lag in the first peak of the bi-modal climate, which for the GRACE Mean SH product occurs between May–June, while all other estimates indicate the peak in April–May. This lag is evident in the average annual

21

cycle (Fig. 2.2b) as a result of the pronounced lags that are observed in several years of the time series, e.g. 2004, 2006, 2009, 2012 and 2013 (Fig. 2.2a).

Second, the bi-modality of the annual cycle is less pronounced in estimates of CSR-Mascon (yellow in Fig. 2.2) than it is for all other estimates. Although this is not easy to detect by visual examination of the time series (Fig. 2.2a), it is evident in the average annual cycle (Fig. 2.2b), and results in the worst representation of temporal variance (standard deviation) obtained with this product (yellow points in Fig. 2.2c).

Third, better agreement between GRACE- and the water balance-based estimates is found for the JPL-Mascon product (blue in Fig. 2.2). In particular, JPL-Mascon is clearly best in representing the average annual cycle (Fig. 2.2b), with the highest correlation, lowest error, and best standard deviation (blue triangle in Fig. 2.2c). As for the time series of monthly values (Fig. 2.2a), JPL-Mascon is comparable with GRACE mean SH in error and standard deviation but better in correlation (blue vs. red circles in Fig. 2.2c), and comparable with CSR-Mascon in correlation but much better in standard deviation (blue vs. yellow circles in Fig. 2.2c). The only statistics in which JPL-Mascon is clearly worse than other product is in the error for the time series which is best for CSR-Mascon (blue vs. yellow circles in Fig. 2.2c). In summary, JPL-Mascon produces better or comparable results with respect to other GRACE-based estimates in almost all cases (five out of six statistics). This indicates that JPL-based estimates are closer to water balance-based estimates in the MC basin, and hence we choose this product for further analysis.

2.3.2 Trends in water storage

GRACE data (JPL-Mascon henceforth) reveals the existence of two different trends in terrestrial water storage (TWS') during the study period for the whole MC basin (Fig. 2.3). There is a positive trend (i.e. an increase in water storage, 0.14 ± 0.02 cm/month) before 2010 and a negative trend (i.e. a decrease or depletion of water storage, -0.37 ± 0.04 cm/month) afterwards. This positive (negative) trend is equivalent to an increase (decrease) of TWS of 41.04 ± 5.19 km^3 (77.68 ± 7.57 km^3) during 2002–2010 (2011–2017) in the MC basin. In all cases, reported trends are statistically significant meaning that the corresponding p-value is lower than 0.05, and break points are identified by using the objective method described in Section 2.2.

The pattern consisting in a positive trend of water storage that is reversed in recent years is also present in major tributaries of the MC basin and for surface and groundwater storage
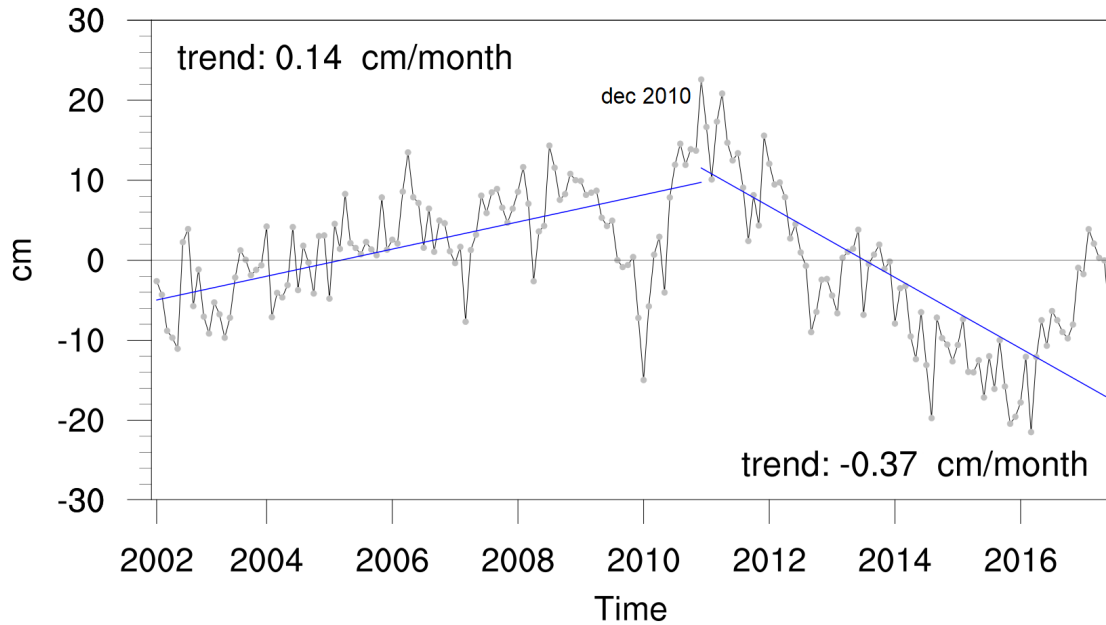
Figure 2.3: Monthly anomalies of TWS from JPL Mascon for the whole MC basin. Solid lines show statistically significant trends ($p < 0.05$) which are positive before December 2010 and negative afterwards. Seasonality is removed from data.

(Fig. 2.4 shows GWS' and SM' while Fig. B.1 in Appendix B shows the same map but for TWS'). Here we introduce the major sub-basins of the whole MC basin, and refer to them as the *middle sub-basins*: the Upper-Middle Magdalena (UMM) and Cauca (C), and *upper sub-basins*: the Upper Cauca (UC) and Upper Magdalena (UM). Soil moisture (SM') and groundwater (GWS') storage contribute differently to trends in total terrestrial water storage (TWS'). At the scale of the whole basin (MC), as well as in its *middle sub-basins* (UMM and C), trends in groundwater are more pronounced than for soil moisture. During the decreasing trend in 2011–2017, the UMM basin lost around 27.64 km^3 and 12.73 km^3 of groundwater and soil moisture, respectively. During the same period, the corresponding losses of groundwater storage and soil moisture in the C basin were close to 6.30 km^3 and 4.78 km^3, respectively.

The upper sub-basins (Fig. 2.4e,d) exhibit contrasting patterns when compared to the middle sub-basins (Fig. 2.4c,b) as well as the whole MC basin (Fig. 2.4a). Two main differences are that in the upper sub-basins depletion rates during recent years have been more pronounced for soil moisture than for groundwater, and break-point may be located in 2008, i.e. earlier than the break-point identified in 2010 for the other basins. Despite these differences, two findings are still common to the whole MC basin and all of its ma-

23
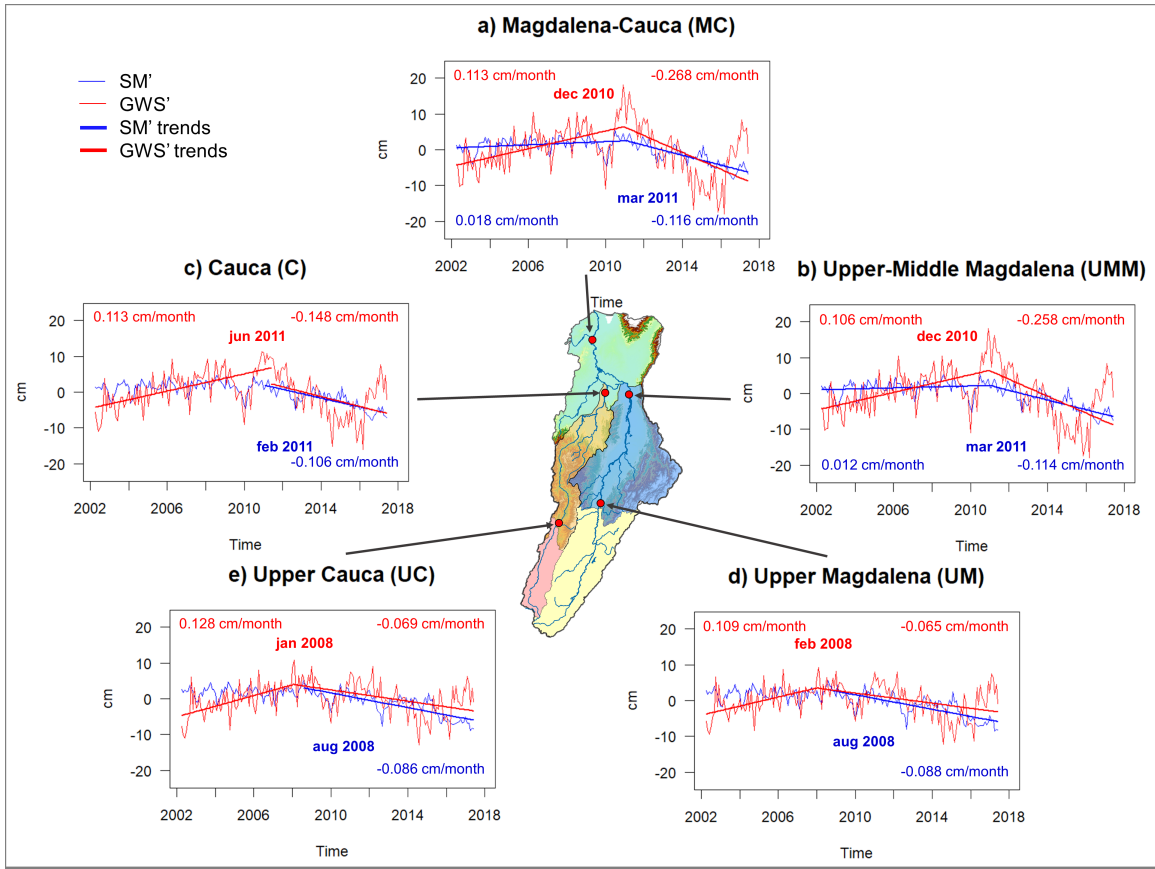
Figure 2.4: Monthly anomalies of SM (blue) and GWS (red) and their corresponding trends (solid lines) at the MC basin as a whole and its major sub-basins. Seasonality is removed from data. Only statistically significant trends ($p < 0.05$) are plotted. Separation of TWS into GWS and SM is obtained through GLDAS, details in Section 2.2.4

jor sub-basins: (i) there has been a water storage depletion trend in recent years, which in most cases (only exceptions are for soil moisture in the upper sub-basins, Fig. 2.4e,d) was preceded by a positive trend; and (ii) the depleting trend coincides with a period between ENSO extremes. Common patterns and differences between sub-basins are further discussed in Section 2.4.

Temporal trends in water storage are not uniformly distributed across space in the MC basin. There is a marked difference between the higher (upstream, south of ~ 7.5 latitude) and lower (downstream, north of ~ 7.5 latitude) parts of the basin (Fig. 2.5). Note that this partition of the MC basin around ~ 7.5 latitude (this is not an arbitrary selection but a result based on Fig. 2.5) implies that the upper sub-basins are in the upper part of the basin, while the middle sub-basins include areas in both the higher and lower parts of the basin. Average trends have the same sign in both parts of the basin (positive during 2002–2010

24
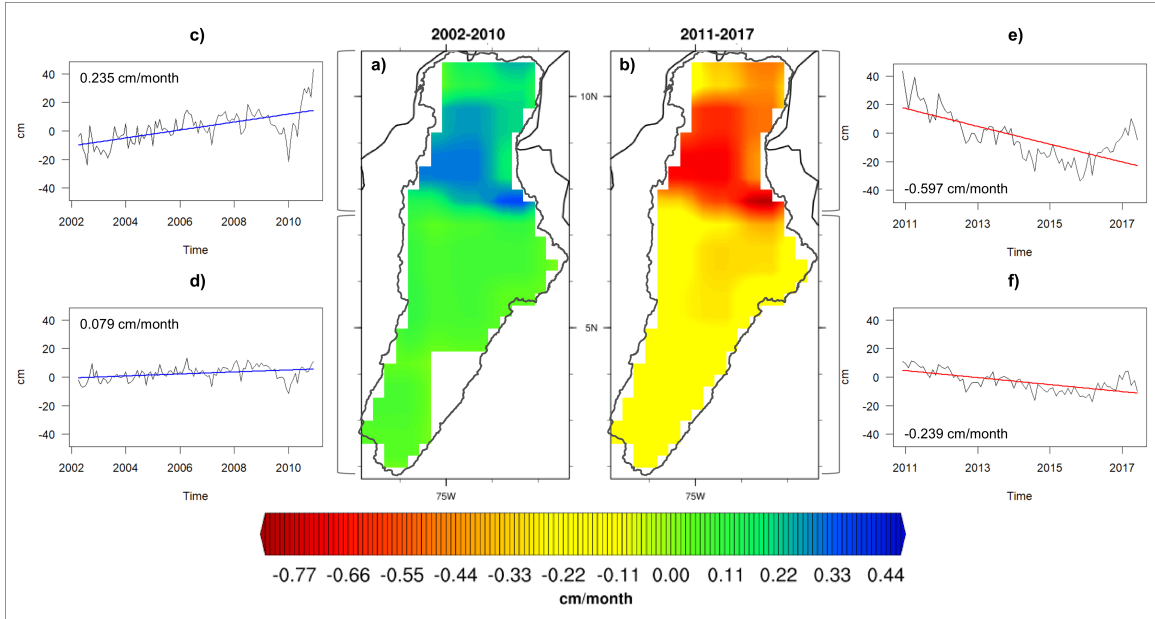
Figure 2.5: Maps of statistically significant ($p < 0.05$) trends in TWS anomalies for time periods 2002–2010 (a) and 2011–2017 (b). Panels c–f show the temporal evolution of TWS anomalies averaged over the northern (c,e: downstream, lower part of the MC basin) and southern (d,f: upstream, higher part of the MC basin) parts of the basin during 2002–2010 (c,d) and 2011–2017 (e,f). Solid lines represent statistically significant ($p < 0.05$) trends.

and negative for 2011–2017) but are much more pronounced in the lower part. During the positive trend period, water storage increased about 26.14 km^3 (trend is 0.23 ± 0.03 cm/month) in the lower part of the basin, whereas it increased around 13.99 km^3 (trend is 0.08 ± 0.02 cm/month) in the higher part. Likewise, the decreasing trend in the lower part (-0.60 ± 0.06 cm/month) is equivalent to a loss of ~49.96 km^3 during the period, while in the higher part (-0.24 ± 0.03 cm/month) the corresponding loss is about 31.80 km^3.

2.4 Discussion

In this section we explore the reasons and/or mechanisms behind our three main findings, as well as their implications for water security and environmental sustainability. The first finding is that among different GRACE-based products the JPL-Mascon product exhibits a closer agreement with water balance-based estimates of water storage dynamics in the MC basin (Sec. 2.3.1). This finding generally agrees with Scanlon et al. (2016) who describe several advantages of Mascon solutions relative to SH such as the increase of signal amplitude due to the reduction of leakage from land to ocean, and the application of geophysical data constraints during processing with little empirical post processing required. In contrast

to the SH approach in which noise reduction and signal restoration are applied as post processing steps, noise is reduced during Mascon processing by applying constraints (Scanlon et al., 2016). The use of mass concentrations leads to better signal-to-noise ratios of the Mascon fields as compared to the SH solutions (Shamsudduha et al., 2017; Watkins, Wiese, Yuan, Boening, & Landerer, 2015). In contrast to SH products used to produce our GRACE ensemble, JPL-Mascon does not require the use of scaling factors in post-processing, which are needed in SH products to restore the signal lost during the processing of the truncation of the gravity coefficients and filtering (Landerer & Swenson, 2012). JPL-Mascon (as well as CSR-Mascon) estimates terrestrial mass changes directly from inter-satellite acceleration measurements and can be used without further post-processing (Rowlands et al., 2010; Shamsudduha et al., 2017; Watkins, Wiese, Yuan, Boening, & Landerer, 2015). Another difference between SH and Mascons is that SH solutions are global whereas Mascons can be applied at regional to global scales (Scanlon et al., 2016). This difference is important because in the global SH solutions one cannot distinguish between land and ocean areas; hence, the generally higher land signals leak into the lower ocean signals, thereby reducing signal amplitudes. In contrast, land and ocean areas can be explicitly defined during Mascon processing, reducing leakage errors relative to the SH solutions (Scanlon et al., 2016). Also, gridded Mascon fields are provided at the improved spatial resolution of $0.5° \times 0.5°$, while SH solutions are available at a resolution of $1° \times 1°$.

As compared to the other Mascon-type product, i.e. CSR-Mascon, JPL-Mascon has two differences that we consider consistent with the better performance found. First, these Mascon products differ in their spatial resolution. JPL-Mascon samples the gravity field at approximately the native resolution of the GRACE mission at the Equator, whereas CSR-Mascon deliberately oversamples the gravity field at the Equator to increase the solution resolution at higher latitudes (Save, Bettadpur, & Tapley, 2016; Scanlon et al., 2016; Watkins, Wiese, Yuan, Boening, & Landerer, 2015). This may be why CSR maps present a spatial distribution smoother than JPL maps, so that it is difficult to identify areas with special interest (e.g. Figure B.2 in Appendix B). The second difference between JPL-Mascon and CSR-Mascon solutions is that they represent two fundamentally different approaches to applying constraints. Among these differences JPL-Mascon constraints are based on both GRACE data and geophysical models, whereas CSR-Mascon constraints are based on GRACE data only (Save, Bettadpur, & Tapley, 2016; Watkins, Wiese, Yuan, Boening, & Landerer, 2015). Scanlon et al. (2016) also show that CSR-Mascon has slightly higher errors than all the other solutions for large basins. For further comparison between SH and Mascon GRACE products we refer the reader to Scanlon et al. (2016) and Shamsudduha et

al. (2017). Overall, our results suggest that JPL-Mascon is preferrable than other products for the assessments of water storage dynamics in the MC basin.

The second finding is the existence of significant temporal trends in water storage that shift from positive (increase in water storage) to negative (water storage depletion) during the study period (Sec. 2.3.2). In the MC basin as a whole, as well as in its middle sub-basins (C and UMM), this shift occurs during the 2010–2011 La Niña (Figs. 2.3 and 2.4a–c). The resulting negative trend continues until the 2015–2016 El Niño. This is further clarified by Figure 2.6 which shows the evolution of TWS anomalies along with precipitation anomalies and the Multivariate ENSO Index (MEI; Wolter and Timlin, 1993).

Several other similar concepts are highlighted in Figure 2.6. The depleting trend occurs between two strong ENSO extremes that had extensive impacts in the MC basin: The 2010–2011 La Niña was related with severe flooding (Hoyos, Escobar, Restrepo, Arango, & Ortiz, 2013), while the 2015–2016 El Niño was linked with the most severe drought in recent years (Hoyos et al., 2017; Martínez, Zambrano, Nieto, Hernández, & Costa, 2017). Indeed, the maximum (TWS'= 22.60 cm in December, 2010) and minimum (TWS'= -21.48 cm in March, 2016) values of TWS anomalies found during the whole study period occurs during these ENSO extremes.
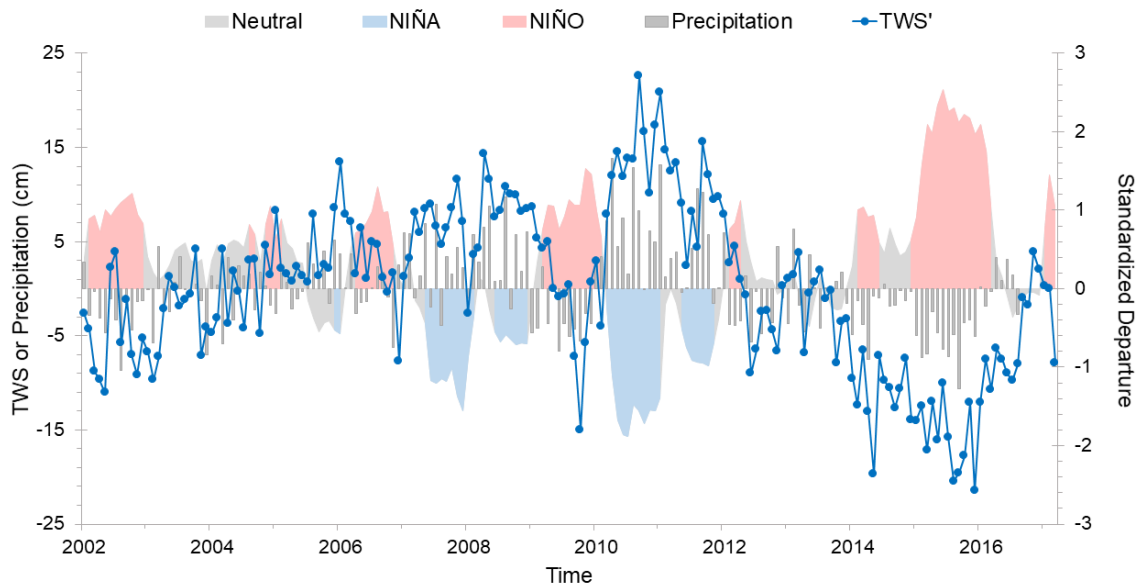
Figure 2.6: Monthly values of TWS anomalies (blue line, left axis), precipitation anomalies (gray bars, left axis), and Multivariate ENSO Index (right axis). Shading indicates whether the ENSO phase is Neutral (gray), El Niño (red), or La Niña (blue).

Figure 2.6 also shows that weaker La Niña (e.g. 2007–2008) and El Niño (e.g. 2009–2010) events can be related with positive and negative anomalies of TWS, respectively. This is consistent with La Niña and El Niño being typically associated with positive and negative anomalies of precipitation in this region, witnessed by the positive/negative anomalies of precipitation mirroring negative/positive values of MEI. The correlation between deseasonalized TWS anomalies and MEI is also negative (-0.71), indicating that negative (positive) values of MEI during La Niña (El Niño) are related with positive (negative) anomalies of TWS. This correlation between MEI and TWS anomalies exhibits the same pattern as the correlation between MEI and precipitation found for northern South America (Guarín Giraldo & Poveda, 2013; Poveda, 2004; Waylen & Poveda, 2002), as well as in other tropical regions in which La Niña and El Niño are related with positive/negative precipitation anomalies (Awange, Forootan, Kuhn, Kusche, & Heck, 2014; Phillips, Nerem, Fox-Kemper, Famiglietti, & Rajagopalan, 2012; Zhang, Chao, Chen, & Wilson, 2015). The correlation between TWS and MEI improves slightly (up to -0.73) if the time series are lagged by two months, consistent with the notion that the effects of ENSO on the hydrology of the region are lagged (Guarín Giraldo & Poveda, 2013; Ni et al., 2018). These results concur with the conclusion that the MC basin is in a region highly sensitive to ENSO extremes (Poveda, 2004), and are consistent with the premise that the observed trends in water storage (Figs. 2.3 and 2.4) are strongly modulated by ENSO extremes.

It is notable that in the upper sub-basins the objective method does not identify the break-point in the trend in 2010 but rather in 2008 (Fig. 2.4d,e). The depleting trend in these sub-basins is significant if starting at 2010 as well (results not shown). That the objective method identifies this break-point in 2008 may, however, be related to physically meaningful differences between the upper and middle sub-basins. There were two La Niña years around 2008 (Fig. 2.6), and the effect of La Niña 2010–2011 on TWS was less pronounced in the upper sub-basins (Fig. 2.4d,e) than in the middle sub-basins (Fig. 2.4b,c) or the whole basin (Fig. 2.4a). This is evident from comparison between peak values of TWS anomalies which occur in 2008 for the upper sub-basins. Despite this difference in the start of the depleting trend, there is a clear pattern common to all sub-basins and the MC basin as a whole: a depleting trend which starts during La Niña (around either 2008 or 2010) and continues until El Niño 2015–2016, i.e. that occurs between ENSO extremes.

Although our results indicate that climate variability plays a major role in water storage dynamics, they do not allow to relate the water storage depletion trends found with climate change. Near the end of our study period there is an evident positive trend in TWS after

around 2016. This may be interpreted as recovery of the TWS after the strong El Niño of 2015–2016. We do not isolate this trend in our analysis because it occurs during a very short period of time given the available period of record. The period of record available also means that we cannot be conclusive on the existence of a climate change signal in water storage dynamics in the MC basin (e.g. long-term persistent water storage depletion). This highlights the importance of long term monitoring of water storage dynamics, which in the case of GRACE and the MC basin depends on international efforts beyond the reach of Colombia. Such continued monitoring is critical for distinguishing between climate variability and the potential effects of climate change. The implications for water security and environmental sustainability are quite different for positive/negative trends in TWS modulated by ENSO, than for a persistent depletion rate as a result of climate change (e.g. Buytaert and De Bièvre, 2012; IDEAM, PNUD, MADS, DNP, and CANCILLERÍA, 2015). More frequent and/or intense El Niño events as a result of climate change (Cai et al., 2014; Cai et al., 2015; Duque-Villegas, Salazar, & Rendón, 2019) could, however, exacerbate longer term depletion rates in the region. Other signals of climate change have been identified in the region, including the shrinkage of tropical glaciers (Poveda & Pineda, 2009) and long-term trends in monthly hydro-climatic series including streamflow, precipitation, and temperature (Carmona & Poveda, 2014).

The third finding is that the magnitude (not the sign) of temporal trends exhibit a pronounced difference between the lower and higher parts of the basin (Fig. 2.5). This spatial heterogeneity largely coincides with the pronounced differences between these parts of the basin. The higher part of the basin (to the South) is in the Andes mountains and is characterized by complex terrain with pronounced elevation gradients (elevation ranges from approximately 41 to 5500 m.a.s.l). There are also pronounced gradients in biophysical properties including biodiversity (Josse et al., 2011), weather and climate regimes (IDEAM & CORMAGDALENA, 2001; Poveda, 2004), and marked differences in the geology, hydrogeology, geomorphology, and soils (see Appendix A). This Andean part of the MC basin is also characterized by the presence of dams and reservoirs (Angarita et al., 2018), strategic ecosystems including paramos (Ortiz, González, & López, 2005) and tropical forests (Rodríguez & Armenteras, 2005), as well as tropical glaciers on the highest peaks (Rabatel et al., 2013); all of which can exert a significant influence on the hydrology of the basin at multiple scales. Indeed, the progressing loss of paramos, tropical forests and glaciers has raised concerns on how these changes will affect future water security in the tropical Andes (Bradley, Vuille, Diaz, & Vergara, 2006; Buytaert, Cuesta-Camacho, & Tobón, 2011; Vuille, 2013).

Compared to the higher part of the MC basin, the lower part constitutes much flatter terrain characterized by the presence of extensive wetland systems, mainly in the Mompós depression (Angarita et al., 2018), and a drier climate with some areas experiencing increasing aridity and desertification processes (Etter, McAlpine, & Possingham, 2008; Jaramillo-Mejía & Chernichovsky, 2019). Figure 2.7 illustrates how the spatial extent of these wetlands was largely reduced between 2010 and 2016, consistent with water depletion during the same period. The Mompós wetlands system are severely impacted by droughts and floods related to ENSO extremes. Indeed, while the 2010-–2011 La Niña caused severe flooding and concomitant damage due to e.g. the breach of a large artificial levee in the Cauca River (Nardini & Franco Idarraga, 2016), the 2015–2016 El Niño caused a severe drought with significant impacts on local water security and related economic impacts (Martínez, Zambrano, Nieto, Hernández, & Costa, 2017).
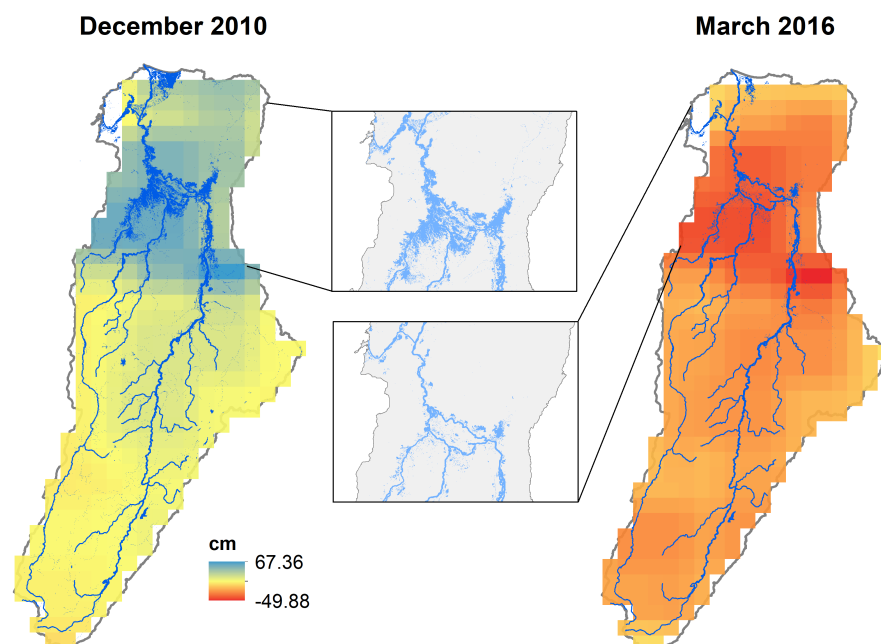
Figure 2.7: Wetlands area superimposed over anomalies of TWS around the beginning (2010) and end (2016) of the water depletion trend in the MC basin. Wetlands areas are based on Palsar and Landsat images (see Sec. 2.2.6 for details).

We interpret the result of the more pronounced positive (before 2010) and negative (after 2010) trends in the lower part of the basin as a higher sensitivity of water storage in this region to external forcing due to ENSO variability. This higher sensitivity can be related to the high variability of water storage in the extensive wetlands of the region (Fig.

30

2.7). Indeed, previous studies have found a close relation between wetland dynamics and TWS (Lee et al., 2011; O'Loughlin, Neal, Schumann, Beighley, & Bates, 2018; Xie et al., 2016). Wetlands are inextricably linked to other key players of the terrestrial water balance such as rivers and aquifers (Fig. A.7 and Appendix A). During wet conditions, extensive wetlands in a flat terrain or depression (e.g. the Mompós depression) can enhance TWS via retention of water from increased precipitation and river discharges including floods. La Niña, and particularly the strong 2010-2011 event, exacerbated the wet conditions in the lower part of the MC basin. In contrast, during dry conditions, wetlands can enhance the reduction of TWS via direct evaporation from extensive areas of free surface water, especially if the availability of energy is relatively high, such as in tropical regions.

2.5   Conclusions

Three main conclusions emerge from this study. First, GRACE-based estimates of water storage dynamics in northern South America, more specifically in the Magdalena-Cauca (MC) basin in Colombia, are comparable to estimates obtained through the water balance equation using multiple independent (and also independent from GRACE) sources of the constituent components of the water balance; precipitation, evaporation, and river discharge. The performance of the different available GRACE products is, however, not uniform. Our analysis indicates that the JPL-Mascon product is best suited for describing the spatial and temporal variability of Terrestrial Water Storage (TWS) in the tropical MC basin. These results provide an unprecedented quantitative assessment of GRACE data for this basin, which can serve as a basis for future applications. More generally, our results contribute to the global assessment of GRACE as a reliable source of data for the study of terrestrial water resources.

Second, GRACE data (JPL-Mascon) reveals the existence of trends in terrestrial water storage that have shifted from positive (i.e. increase of water storage) to negative (i.e. water storage depletion) during the study period. These trends and shifts are evident not only in the total terrestrial water storage but also in soil moisture and groundwater, and have not only occurred in the MC basin as a whole but are also evident in its major sub-basins. Compared to soil moisture, the contribution of groundwater to these trends in total water storage is generally larger. We find that identified shifts in trends are clearly related to ENSO. The most pronounced trend in water storage depletion occurs between the strong 2010–2011 La Niña and 2015–2016 El Niño events. This conclusion is a contribution to the general understanding of the influence of ENSO on continental water resources and their

variability. This has implications for future planning and management of water resources, particularly considering projections of increased frequency and severity of ENSO events. Further, this conclusion highlights the importance of continuing monitoring efforts like GRACE, which are beyond the reach of most countries (e.g. Colombia) but is of benefit to all.

Third, we show that trends in water storage are not uniform across the MC basin. The spatial variations of trends exhibit a pronounced contrast between the higher and lower parts of the basin, i.e between the mountainous (Andean) and flatter (near the Caribbean sea) parts of the basin. We interpret the more pronounced trends in the lower part of the basin as a higher sensitivity of water storage to ENSO variability, related with the presence of extensive wetlands that can exacerbate both water retention during wet conditions (La Niña) and water loss during dry conditions (El Niño).

CHAPTER 3
COMPARATIVE ASSESSMENT OF GLOBAL MODELS IN REPRESENTING GRACE IN A MEDIUM-SIZE TROPICAL BASIN

Silvana Bolaños[1], Micha Werner[2], Juan F. Salazar[1], Teresita Betancur[1]

[1]Grupo de Ingeniería y Gestión Ambiental - GIGA, Escuela Ambiental, Facultad de Ingeniería, Universidad de Antioquia, Medellín, Colombia

[2]Water Science and Engineering Department, IHE Delft Institute for Water Education, Delft, the Netherlands

Abstract

The increasing reliance on global models to address climate and human stresses on hydrology and water resources underlines the necessity for assessing the reliability of these models. Particularly in river basins where availability of gauging information from terrestrial networks is poor, models and remote sensing are increasingly proving to be a powerful tool to support hydrological studies and water resources assessments, though the lack of information may frustrate rigorous performance assessment. Remotely sensed data of the terrestrial water storage such as that obtained from the GRACE satellite mission can, however, provide independent data against which the performance of such global models can be evaluated. We assess the reliability of six global hydrological models (GHM) and four land surface models (LSM) provided by the EartH2Observe (E2O) research project, comparing modelled dynamics of Total Water Storage (TWS) with TWS derived from GRACE data over the Magdalena basin in Colombia. This is a medium sized tropical basin, with a reasonably well developed gauging network. We compare monthly TWS changes obtained from each model with GRACE data for the 2002-2014 period, evaluating monthly variability, seasonality and long-term trends. These are evaluated at basin level, as well as for selected sub-basins with decreasing basin size. Our results show that the models have a poor representation of TWS for the monthly series, but they improve in representing seasonality and long-term trends. The best representation at almost all basin scales is obtained with the GHM W3RA forced by the Multi Source Weighted Ensemble Precipitation (MSWEP). Results highlight the importance of basin scale in the representation of TWS,

as with decreasing basin area we note a commensurate decrease in the model performance. However, as basin area decreases the GRACE measurement and leakage uncertainties increase. We show that GRACE is sensitive to very different model physics found in different basins, and conclude that it provides a valuable validation dataset for the global simulation of TWS and offers useful information for the continuous improvement of large-scale numerical models of the global terrestrial water cycle.

3.1 Introduction

Total Water Storage (TWS) is an important and fundamental variable of the global hydrological cycle. Representing the sum of all water storage components including; water in rivers; lakes and reservoirs; wetlands; soil and aquifers, TWS plays a key role in the Earth's water, energy, and biogeochemical cycles (Syed, Famiglietti, Rodell, Chen, & Wilson, 2008). It reflects the partitioning of precipitation into evaporation and runoff, partitioning of available energy at the surface between sensible and latent heat (Kleidon, Renner, & Porada, 2014). Current interest in TWS not only involves the knowledge of the redistribution of the current body of water in the hydrological cycle, but is also essential for forecasting and gaining insight into the impacts of extreme events such as droughts and floods (Zhang, 2017). As an integrated measure of water availability, (surface and groundwater), the dynamic of TWS has significant implications for water resources management (Syed, Famiglietti, Rodell, Chen, & Wilson, 2008). For this reason, the monitoring of changes in TWS is critical for characterising water resources variability, and to improve the prediction of regional and global water cycles and interactions with the Earth's climate system (Famiglietti, 2004). Despite the acknowledged importance of this variable, integrated observations of TWS are largely unavailable, further confounded by the global decline in gauging networks (Hassan & Jin, 2016). Given the heterogeneity of the hydrology of river basins, comprehensive observation of TWS is very difficult due to insufficient insitu observations of the diverse water storages and fluxes. For example, the number of rain gauges with good quality data in the Magdalena-Cauca river basin, the socio-economically most important and most extensively monitored basin in Colombia, has reduced from about 1,500 in the 1980's to around 1,000 in the 2010's (Rodríguez et al., 2019). Estimation of TWS and its change is commonly done through water balances and the use of models, and is often underestimated. Even many traditional analyses have assumed that at longer timescales and over large regions, change in TWS can be approximated as zero. This implies that in water balance studies it is common to ignore the long-term trends of TWS (Reager & Famiglietti, 2013).

34

One way to estimate TWS is through using hydrological models. At the global scale, there are two categories of such models: Land Surface Models (LSM) and Global Hydrology Models (GHM). LSM focus on describing the vertical exchange of heat and water by solving the surface energy and water balance. These were originally developed by the atmospheric modelling community to simulate fluxes from the land to the atmosphere because of the crucial linkages between the land surface and climate. As the emphasis of LSM's is on simulation of energy fluxes, these may not provide accurate simulation of water storage changes (Scanlon et al., 2018). GHM in contrast focus on solving the water balance equation and simulating catchment outlet streamflow to assess basin water resources or for supporting flood forecasting (Gudmundsson, Wagener, Tallaksen, & Engeland, 2012). One of the primary differences between LSM and GHM is the more physical basis for LSM, including water and energy balances, compared to the more empirical water budget approaches included in most GHM. Additionally, many GHM model anthropogenic influences, including human water use and water resources infrastructure, which most LSM do not (Scanlon et al., 2018). The performance of these models varies because the different physical representation of land-surface processes, differences in model structure and physics, parameterization, and atmospheric forcing data (Zhang et al., 2017). The greatly increased use of hydrological models to support water resources assessments and as a tools to forecast water resources raises questions on the reliability of these models, as reliable representation of short and long-term variations in TWS are critical for assessing water scarcity, estimating response to climate extremes, and for adequate water resources management.

Remote sensing products are also used as a way to observe TWS changes, such as is the case for the Gravity Recovery and Climate Experiment (GRACE) satellite data (Tapley, Bettadpur, Watkins, & Reigber, 2004). The GRACE set of satellites are able to detect changes in the Earth's gravity, that is influenced mainly by large-scale water storage variations and transport on Earth. Since 2002, the GRACE satellites have monitored monthly changes in water mass as TWS increase or decrease as a consequence of climate variability and anthropic impacts. These satellites through monitoring the time variable gravity field provide a more direct estimate of global changes in TWS anomalies than that which can be obtained from models (Scanlon et al., 2018; Tapley, Bettadpur, Watkins, & Reigber, 2004). GRACE has been shown to provide the opportunity to observe water storage dynamics for large river basins and can contribute to better understanding of hydrology at larger temporal and spatial scales, such as are important for climate studies (Lettenmaier & Famiglietti, 2006). Although GRACE has important limitations due to its resolution (Chen, Famigliett,

Scanlon, & Rodell, 2016a), data from GRACE may well be the only way to independently estimate TWS as distributed values, because water balance and models require gauging data (which are often deficient or insufficient) or data from reanalysis that sum uncertainties in its estimation. Advances in GRACE processing from traditional spherical harmonics to more recent mass concentration (mascon) solutions have increased the signal-to-noise ratio and reduced uncertainties (Scanlon et al., 2016). Since these valuable data have become available, GRACE data have been used to validate global model outputs in several studies (see Scanlon et al., 2018 for an overview).

Through the comparison of averaged TWS from models with GRACE-based estimates for a medium size tropical basin, we intend to identify the potential and as well as possible deficiencies of a set of 10 models comprising both of GHM and LSM, analyse the reasons for different model behaviours. We investigate the performance of this set of models for the Magdalena-Cauca river basin (MC basin henceforth) as a whole, as well as for selected sub-basins progressively decreasing in catchment area, using GRACE data from the Jet Propulsion Laboratory mass-concentration (JPL mascon) solution. This was evaluated in a previous study for the area of interest and found to provide the best representation of TWS dynamics in the basin among the available GRACE products (see Chapter 2 Sec. 2.3.1). With the purpose to contribute to the understanding of the dynamic nature of TWS as well as to contribute to future LSM and GHM development and improvement, this study highlights the value of using water storage from GRACE, in addition to traditional water fluxes, in assessing global models. The relatively large set of LSM and GHM models considered in this study are obtained through the open access global Water Resources Reanalysis dataset developed in the eartH2Observe (E2O) research project, a collaborative project funded under the European Union's Seventh Framework Programme (EU–FP7) (Schellekens et al., 2017).

3.2   Data and Methods

3.2.1   Study area

The MC basin is the primary river basin system in Colombia. It occupies a major portion of the country in the tropical Andes, draining an area of $\sim$ 276,000 km^2 which is about 25% of the total territory of Colombia (Fig. 3.1). The river begins at the height of about 3,700 m above sea level in the Colombian Andes and runs for some 1,612 km before flowing into the Western Caribbean, in the Atlantic Ocean (López López, Immerzeel, Rodríguez Sandoval, Sterk, & Schellekens, 2018; Restrepo & Kjerfve, 2000). The main tributary of
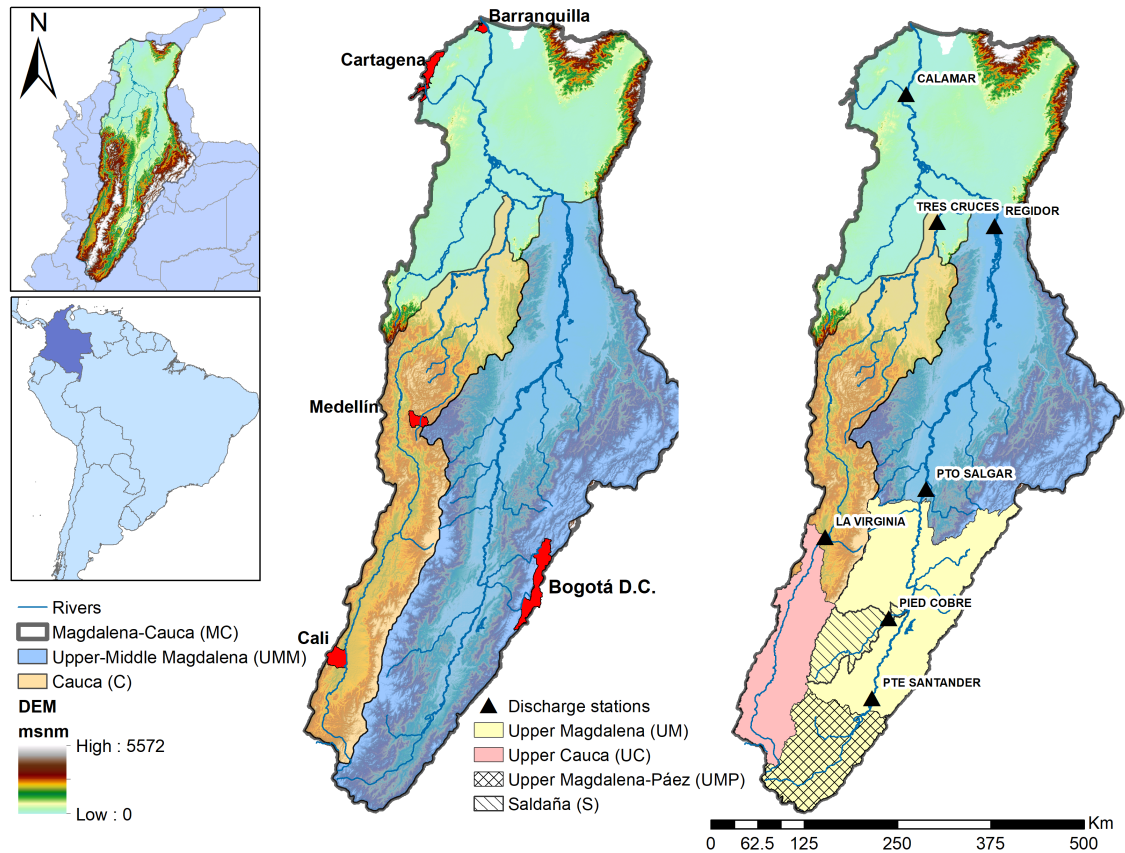
Figure 3.1: Location of the MC Basin in Colombia, as well as the sub-basins considered in this study. The triangles represent the locations of gauge stations measuring streamflow at the outlets of each (sub) basin.

the Magdalena River is the Cauca River, which flows along the western part of the basin and joins the main Magdalena River in a wetland area called La Mojana, which is found in the Mompós Depression region. The mean annual river discharge at the gauge station closest to the mouth (Calamar) is approximately 7,200 m^3 s^{-1} with mean maximum discharges occurring in November (10,200 m^3 s^{-1}), and minimum average flows in March (4,050 m^3 s^{-1}) (Camacho, Rodríguez, & Pinilla, 2008).

Due to the movement of the Intertropical Convergence Zone (ITCZ) around the Equator, the climate in the basin is characterised by two wet periods (March-May and October-November) interspersed by two dry periods. This bimodal climate dominates most of the basin, though the lower MC tends to a more unimodal behaviour, with a contiguous wet period from May to November (Fig. C.1 in Appendix C). The average annual precipitation in the basin is around 2,150 mm, while the annual average potential evapotranspiration is

estimated at 1,630 mm. The hydroclimatology of the basin is profoundly influenced by the El Niño - Southern Oscillation (ENSO) phenomenon (Poveda & Mesa, 1996). Widespread flood events caused by the La Niña event of 2010-2011 affected some four million Colombians and caused economic losses estimated at US 7.8 billion (Hoyos, Escobar, Restrepo, Arango, & Ortiz, 2013; Vargas, Hernández, & Pabón, 2018), while the severe droughts caused by the El Niño event of 2015-2016 had quite severe consequences, including water shortages in more than 25% of the towns, the highest temperatures on record and numerous fires that impacted several regions in the country (Hoyos et al., 2017).

To analyse the effect of basin size on model performance and GRACE data, we subdivide the macro-basin into several sub-basins (Fig. 3.1). While the overall basin at Calamar station has an area of $\sim 276,000$ km^2, the Upper-Middle Magdalena (UMM) has an area of $\sim 140,754$ km^2; the Cauca (C) $\sim 60,657$ km^2; the Upper Magdalena (UM) $\sim 56,992$ km^2; and the Upper Cauca (UC) $\sim 17,930$ km^2. The smaller basins of Upper Magdalena-Páez (UMP) has an area of $\sim 14,450$ km2 and Saldaña (S) $\sim 6,645$ km^2. It is important to highlight that the pixel size of GRACE data and models varies between $\sim 3,025$ km^2 (0.5x0.5) and ~ 730 km^2 (0.25x0.25).

3.2.2   GRACE data

TWS anomalies from GRACE satellites are processed by three centers, the Center for Space Research at University of Texas (CSR), the Jet Propulsion Laboratory (JPL), and Geoforschungs Zentrum Potsdam (GFZ), using two different schemes, Spherical Harmonic (SH) and Mass Concentration (mascon) solutions. The similarities and differences between the SH and the mascon data are well explained by Scanlon et al. (2016) and Shamsudduha et al. (2017). In a previous study, the GRACE products both harmonic solutions and mascon solutions, were assessed for the MC river basin (see Chapter 2 Sec. 2.3.1). Bolaños et al., 2020, evaluate the different products of GRACE through the comparison with water balances based on observed data. They found that the best representation of TWS is the GRACE TWS product derived from JPL mascon. So, in this analysis we use the TWS anomalies data available from April 2002 through December 2014 from GRACE RL05 level-3 land JPL mascon solution gridded at 0.5 (~ 55 km), based on an alternative processing approach which involves parameterizing the gravity field with regional mass concentration functions. This product has only recently become operational (Save, Bettadpur, & Tapley, 2016; Watkins, Wiese, Yuan, Boening, & Landerer, 2015; Wiese, Landerer, & Watkins, 2016).

All reported data are anomalies relative to the 2004–2009 time-averaged baseline. For consistency, all other data series used in this study are calculated as anomalies over their average values for the same period. The missing data due to battery management in GRACE were directly remedied by linear interpolation (Liesch & Ohmer, 2016; Ouma, Aballa, Marinda, Tateishi, & Hahn, 2015; Shamsudduha, Taylor, & Longuevergne, 2012; Xiao, He, Zhang, Ferreira, & Chang, 2015). Variations in water mass or storage are expressed as an equivalent water thickness (EWT; cm water). JPL mascon data were retrieved from the Tellus website `https://grace.jpl.nasa.gov/data/get-data/jpl_global_mascons/`.

3.2.3   Earth2Observe global water resources reanalysis data

In the analysis, input data were provided by the E2O project, which takes advantage of various global reanalyses and derived datasets to develop a global water resources reanalysis (WRR) (Arduini et al., 2017; Dutra et al., 2015; Dutra et al., 2017; Schellekens et al., 2017). This dataset includes the outputs of 10 different Global Hydrological and Land Surface Models (GHM and LSM), that are available at two resolutions and time ranges, denoted WRR1 and WRR2. In WRR1, models were forced by the WATCH Forcing Data applied to the ERA Interim data (WFDEI) meteorological reanalysis dataset (Weedon et al., 2014) at a resolution of 0.5 ($\sim$ 55 km at the equator) from 1979 to 2012. The WRR2 model runs were forced by the Multi Source Weighted Ensemble Precipitation (MSWEP) dataset (Beck et al., 2017) at a resolution of 0.25 ($\sim$ 27 km at the equator) from 1980 to 2014. Model algorithms were also improved between WRR1 and WRR2, such as by a better representation of hydrological processes, incorporation of anthropogenic influence, and by integrating earth observation data (Gründemann, Werner, & Veldkamp, 2018). Arduini et al. (2017), Dutra et al. (2015), Dutra et al. (2017), and Schellekens et al. (2017) provide a detailed of the two datasets and the model improvements. Table 3.1 provides an overview of models considered in this study, as well the main changes in the models between WRR1 and WRR2 for those models that have been run using both forcing datasets and at both resolutions. The performance of several of these models has been compared over the MC basin, finding that key water resources management indicators derived using these models compare well against those derived using in-situ data (Rodríguez et al., 2019).

In order to compare the different models and the WRR with TWS obtained from GRACE JPL mascon, data for the period from 2002 to 2012 were used in this study as a common period for WRR1 and GRACE, and 2002 to 2014 for WRR2 and GRACE. Data were downloaded from the E2O Water Cycle Integrator portal for the required period and for

the required spatial domain (`https://wci.earth2observe.eu/`, last access: 20 November 2018).

Table 3.1: Overview of models and main changes from WRR1 to WRR2. Note that not all models included in WRR1 were run for WRR2, in which case no changes are noted in the table.

Model	Provider Organisation	Model type	Model changes in WRR2	Reference
HBV–SIMREG	Joint Research Centre (JRC)	GHM	n/a	Lindström et al. (1997)
LISFLOOD	Joint Research Centre (JRC)	GHM	Increased number of soil layers, groundwater abstraction.	Van Der Knijff et al. (2010)
PCR–GLOBWB	Universiteit Utrecht (UU)	GHM	Water use included. Improvements to river routing reservoir schemes and water withdrawal and consumption.	van Beek and Bierkens (2009)
SWBM	Eidgenössische Technische Hochschule (ETH)	GHM	n/a	Orth and Seneviratne (2013)
W3RA	Eidgenössische Technische Hochschule (ETH)	GHM	Modified soil and groundwater hydrology equations, improved parameter estimates, dynamic data assimilation, evaporation of water not derived from rainfall.	Van van Dijk et al. (2014)

Table 3.1 – continued from previous page

Model	Provider Organisation	Model type	Model changes in WRR2	Reference
WaterGAP3	Universitat Kassel	GHM	Assimilation of soil water estimates, reservoir management.	Flörke et al. (2013)
HTESSEL	European Centre for Medium-Range Weather Forecasts (ECMWF)	LSM	Multi-layer snow scheme, increased number of soil layers.	Balsamo et al., (2009)
JULES	Centre for Ecology and Hydrology (CEH)	LSM	Rainfal-runoff processes, inclusion of a terrain slope dependency in the saturation excess runoff scheme.	Best et al. (2011) Clark et al. (2011)
ORCHIDEE	Centre National de la Recherche Scientifique (CNRS)	LSM	Revision of the ancillary data, surface roughness, snow scheme, soil freezing and routing.	Krinner et al. (2005)
SURFEX-Trip	Meteo France	LSM	Improvements in ground water, flood plains, land use, plant growth, surface energy and snow.	Decharme et al. (2010)

Source: (Dutra et al., 2017; Schellekens et al., 2017)

n/a: not applicable.

3.2.4 Assessment of model performance

Monthly change in TWS can be calculated as the result of water balance estimates as presented in Equation 3.1, where S is the terrestrial water storage, P and ET are the basin-wide totals of precipitation and actual evapotranspiration and R represents total basin outflow, or the net surface and groundwater outflow. Changes in TWS can also computed as the sum of the monthly changes in component storages, presented in Equation 3.2; where ΔGWS is the changes in groundwater storage, ΔSMS the changes in soil moisture storage, and ΔSWS the changes in surface water storage. ΔCWS is the changes in canopy water storage and ΔSWE represents the change in snow water equivalent, which as the area under snow influence represents less than 0.1% of the total area of the watershed is not considered in this study.

$$\Delta TWS = \frac{dS}{dt} = P - E - Q, \tag{3.1}$$

$$\Delta TWS = \Delta GWS + \Delta SMS + \Delta SWS + \Delta CWS + \Delta SWE, \tag{3.2}$$

Not all of the models considered explicitly represent groundwater storage. For those models that do represent groundwater storage as well as surface and soil moisture components we apply both equations for evaluating simulated TWS. For those models that include only surface water and soil moisture components we do not apply the second equation (Eq. 3.2). This with the objective of evaluating a more representative TWS in the models as GWS is the largest water component of TWS on land.

Table 3.2 shows the variables for each model available in the E2O Water Cycle Integrator portal. The table also provides an overview of which of the above equations to derive compute simulated TWS changes are applied in the two available model resolutions (WRR1 and WRR2).

Table 3.2: Components used in TWS change estimation for each model.

Model	Evaporation*	Runoff*	Variables		WRR1		WRR2	
			WRR1	WRR2	Eq.1	Eq.2	Eq.1	Eq.2
HBV-SIMREG	Penman 1948	Beta function	P, ET, R, SMS, GWS, CWS		X	X		
LISFLOOD	Penman–Monteith	Saturation and infiltration excess	P, ET, R, SMS, GWS		X	X		
PCR-GLOBWB	Hamon (tier 1) or imposed as forcing	Saturation and infiltration excess	P, ET, R, SMS, GWS, CWS, SWS	P, ET, R, SMS, GWS, SWS	X	X	X	X
SWBM	Inferred from net radiation	Inferred from precipitation and soil moisture	P, ET, R, SMS		X			
W3RA	Penman–Monteith	Saturation and infiltration excess	P, ET, R, SMS, GWS	ET, R, SMS, GWS	X	X		X
WaterGAP3	Priestley–Taylor	Beta function	P, ET, R, CWS, SWS	P, ET, R, CWS, SWS	X		X	
HTESSEL	Penman–Monteith	Saturation excess	P, ET, R, SMS, CWS	P, ET, R, SMS	X		X	

Continued on next page

Table 3.2 – continued from previous page

Model	Evaporation*	Runoff*	Variables		WRR1		WRR2	
			WRR1	WRR2	Eq.1	Eq.2	Eq.1	Eq.2
JULES	Penman–Monteith	Saturation and infiltration excess	P, ET, R, SMS, CWS	P, ET, R,	X		X	
ORCHIDEE	Bulk PET	Green-Ampt infiltration	P, ET, R, SMS, SWS		X			
SURFEX-Trip	Penman–Monteith	Saturation and infiltration excess	P, ET, R, SMS, GWS, CWS, SWS	P, ET, R, SMS, CWS, SWS	X	X	X	

* (Schellekens et al., 2017)

In order to understand the variation between TWS change from GRACE JPL mascon and simulated TWS from models at the basin scale, both model and GRACE time series were disaggregated using the Seasonal Trend decomposition by Loess (STL) proposed by Cleveland, Cleveland, McRae, and Terpenning (1990) to estimate the relative magnitudes of water storage variance of different time series components (Eq. 3.3):

$$\Delta TWS = \Delta TWS_{long-term} + \Delta TWS_{seasonal} + \Delta TWS_{residuals}, \qquad (3.3)$$

Hydrological performance of the monthly simulated TWS changes from all models was assessed using commonly used model evaluation statistics. We consider Pearson's correlation coefficient (r), Root Square Mean Error (RSME), Ratio of RMSE to the standard deviation of the observations (RSR), and the Kling-Gupta efficiency (KGE; Gupta, Kling, Yilmaz, and Martinez, 2009). Pearson's correlation coefficient (r) provides an indication of the linear relationship between simulated TWS and the benchmark TWS derived from GRACE. Correlation coefficients are widely used to describe the proportional decrease or increase of two variables. RSME indicates how close model predicted values are to ob-

served data, estimating the square root of the variance of the residuals. Lower values of RMSE indicate better fit. RSR standardizes RMSE using the standard deviation of the observations. It is calculated as the ratio of the RMSE and standard deviation of measured data. RSR varies from the optimal value of 0, which indicates zero RMSE or residual variation and therefore perfect model simulation, to an infinitely large positive value. The lower RSR, the lower the RMSE, and the better model performance (Moriasi et al., 2007). Finally, the KGE index facilitates analysis of the relative importance of different components in the context of hydrological modelling. In the computation of this index, there are three main components involved: the Pearson's correlation, the ratio between the standard deviation of the simulated values and the standard deviation of the observed ones, and the ratio between the mean of the simulated values and the mean of the observed ones. KGE ranges between $-\infty$ and 1, where 1 indicates a perfect representation of TWS.

3.3 Results

3.3.1 TWS evaluation for the whole MC basin

In order to evaluate how well the models represent TWS for the whole basin, we apply Eq. 3.3 and analyse the monthly series, seasonality and long-term trends of TWS for each data sets against GRACE data. One way to see graphically and statistically the representation of TWS change respect GRACE data, is through Taylor Diagrams. This diagram provides a way of three statistics plotting on a 2D graph that indicate how closely a pattern matches observation. The similarity between two patterns is quantified in terms of their correlation(s), the ratio(s) of the normalized root–mean–square (SMS) differences between 'test' dataset(s) and 'reference' dataset(s), and the amplitude of their variations (represented by their standard deviations) (Taylor, 2001). Figure 3.2 shows Taylor Diagrams for the complete monthly series, as well as the seasonal and long-term trends. In all cases the corresponding constituents of the GRACE JPL mascon dataset are used as reference. Best performances indicate values of correlation close to 1 with low RMS error, and a ratio of standard deviations close to 1. In this figure, as in all further figures, a blue colour is used to represent the GHM in WRR1 and yellow is used for the GHM in WRR2. The LSM in WRR1 are represented with a red colour, while LSM in WRR2 are shown in green.

From Figure 3.2 it is not possible to distinguish clearly which of the in total 23 data sets from GHM WRR1, GHM WRR2, LSM WRR1 and LSM WRR2 better represents TWS when compared to GRACE. Model runs derived from WRR1 are denoted as R1 for brevity, while those derived from WRR2 are denoted as R2. It is noteworthy that correlations are
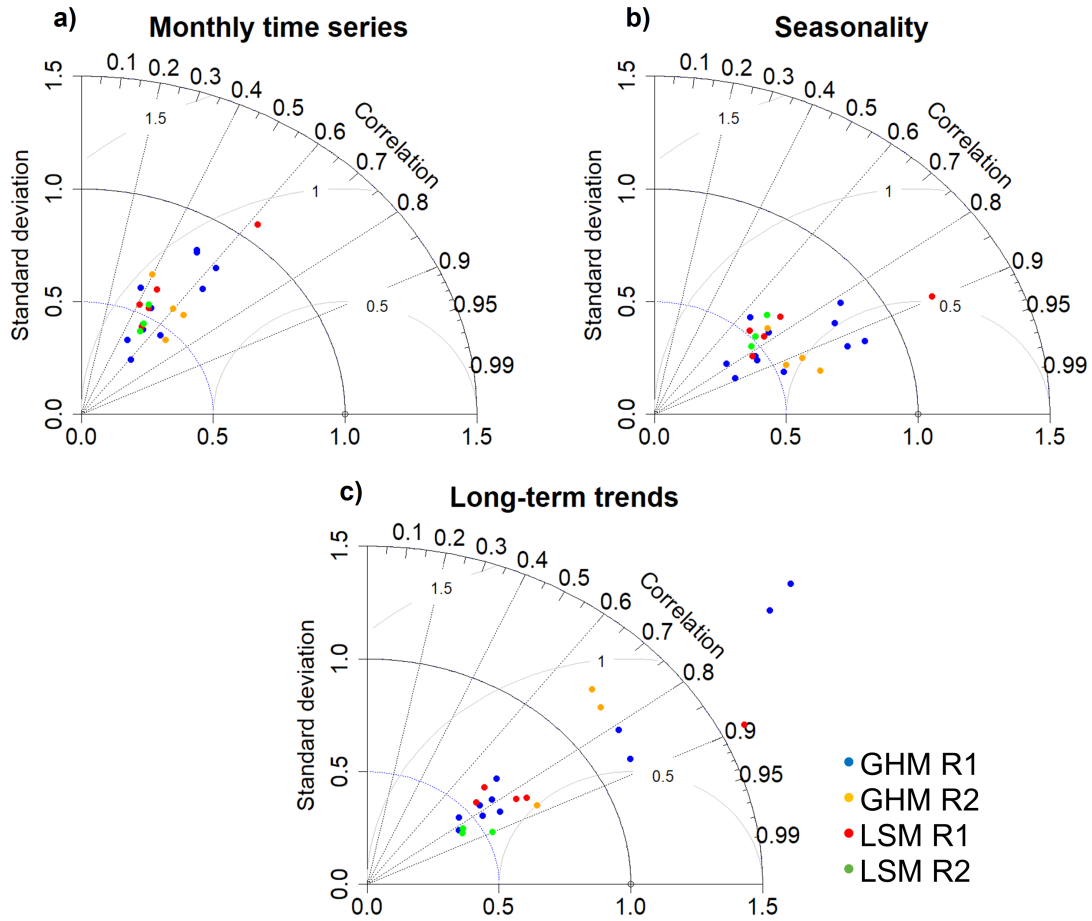
Figure 3.2: Taylor diagrams between the time series of each model and GRACE for the Magdalena river basin for a) monthly time series, b) annual cycle, c) long-term trends. R1 indicates the models with the first reanalysis WRR, and R2 the second WRR.

better for almost all models when considering seasonality and long-term trends. For the monthly series, the correlations of the models range between 0.36 and 0.68, with the highest correlation corresponding to the W3RA R2Eq2 and the lowest to LISFLOOD R1Eq1. However, for almost all models (except Surfex-Trip R1Eq2) is observed smaller standard deviations than those observed by GRACE.

For the representation of seasonality, we observe that correlations increase in all models, with the highest correlation found for PCR-GLOBWB R2Eq2 (r = 0.96) and the lowest for LISFLOOD R1Eq1 model (r = 0.65). We also observed that the models with good correlation and whose standard deviations are closer to those observed are for the GHM, particularly PCR-GLOBWB R1Eq1, PCR-GLOBWB R1Eq2, W3ERA R1Eq1 and W3RA

R1Eq2 models. For long-term trends, an increase in correlations is also observed. The highest correlation is now presented by HTESSEL R2Eq1 model (r = 0.91) and the lowest by WaterGAP3 R2Eq1 (r = 0.23). Standard deviations for most models are lower than those observed, indicating little variability, while for WaterGAP3 R2Eq1, PCR-GLOBWB R1Eq1 and Eq2, and SurfexTrip R1Eq2 show very high standard deviations to those observed in GRACE.

3.3.2   TWS monthly values evaluation

To provide an overview of the range in performance metrics comparing TWS at the sub-basin scale to GRACE derived TWS, Figure 3.3, groups the correlation, RMSE and RSR by model type (GHM and LSM) and reanalysis (WRR1 and WRR2). We observe an improvement in the performance of the WRR2 models over the WRR1. In general, correlation values increase and both the RMSE and the RSR decrease, with the exception of the WaterGAP3 model as we can observe in the Figure 3.4 that shows the boxplots for each model individually for WRR1 and WRR2. The model with the highest correlation in all basins is W3RA R2Eq2. Models with the lowest RMSE alternate between W3RA R2Eq2, WaterGAP3 R1Eq1 and JULES R2Eq1. Models with smaller RSR alternate between W3RA R2Eq2, PCR-GLOBWB R2Eq2 and WaterGAP3 R1Eq1.

The relationship between TWS of the sub-basins area of the MC basin and the error statistics for the models in WRR1 and WRR2 is illustrated in Figure 3.5. To allow comparison, error statistics are normalised and standardized. As RSME and RSR then have similar behaviour, we present the figure for RSR in Figure C.2 in Appendix C. These results clearly demonstrate the detriment in model performance as basin size decreases. This can be best observed by looking at the KGE statistic (Fig. 3.5a). It is evident that the models are generally able to better capture the hydrology for the main basins in both WRR1 and WRR2, but from the UM sub-basin (56,992 km^2) the models begin to decrease in performance, although the only slightly larger Cauca basin (60,657 km^2) shows much better performance. This provides an indication of the basin size at which the models are capable of capturing TWS and also illustrates the difference in forcing, resolution and the model's improvements made in WRR2 over WRR1. For WRR1 the best performance for the MC and UM basins is found for HBV-SIMREG R1Eq2 model, the W3RA R1Eq2 model performs reasonably well for the UMM and Cauca basins, and the SWBMExp1 R1Eq1 model has the best performance for UC, UMP and Saldaña basins. All three of these models are GHM. For WRR2, the best performance in almost all basins is found for the W3RA R2Eq2 model, though for the smaller basins (UMP and Saldaña) it is found to be the JULES R2Eq1

47
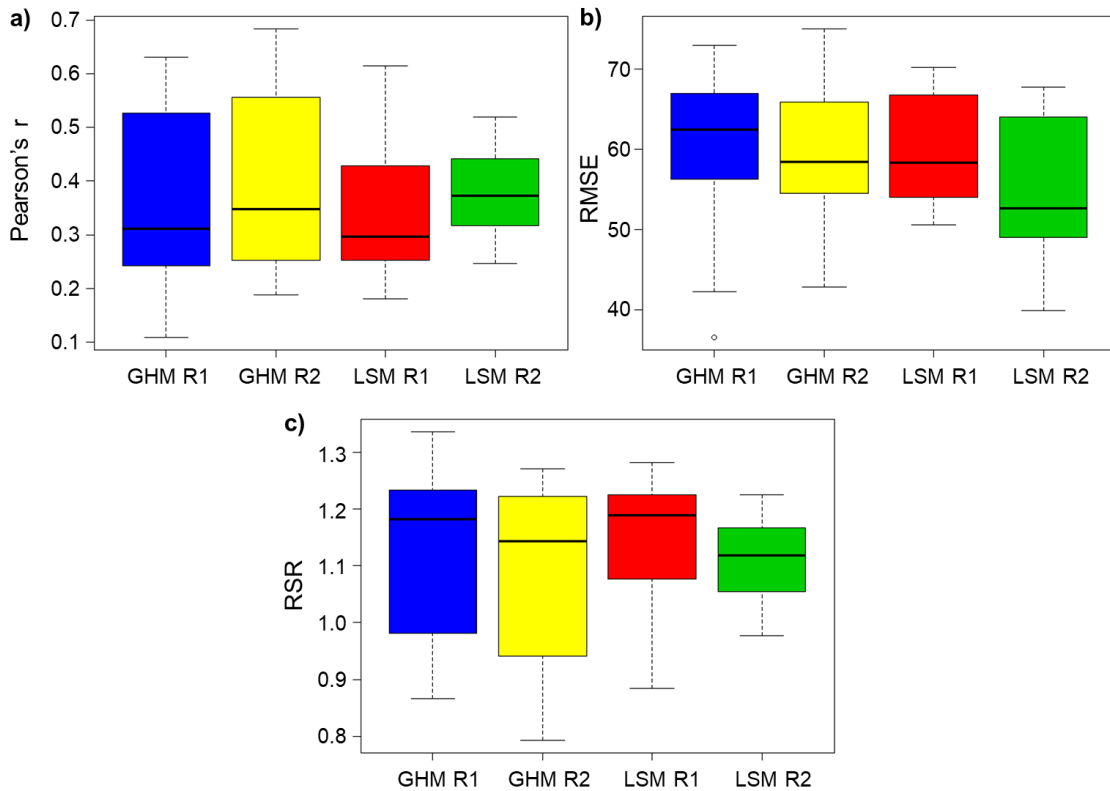
Figure 3.3: Distribution of model performance for the three metrics considered, grouped by model type (GHM or LSM) and forcing/resolution (WRR1 and WRR2). Three performance metrics are shown; (a) Pearson's r, (b) RMSE, and (c) RSR.

model. The first of these is a GHM and the second an LSM. The models with the lowest KGE values are LISFLOOD R1Eq1 for MC, UMM and UM basins, WaterGAP3 R2Eq1 for Cauca, and PCR-GLOBWB R1Eq2 for the last three basins. For models that have been run both for WRR1 and WRR2, it is not consistently found that the WRR2 runs have improved performance for all basins. PCR-GLOBWB WRR1 is found to be better than WRR2 for only the Cauca basin, while for HTESSEL WRR1 is better for the Cauca and UC basins. WaterGAP3 presents better performance for WRR1 in all basins, while Surfex-Trip has highest values for WRR1 than for WRR2 for all basins except the two smaller basins. For W3RA the best performance is consistently found for WRR2 across all basins.

The Pearson's correlation coefficient, r, displayed in Figure 3.5b shows relatively consistent correlations for each model. For both WRR1 and WRR2, the best performances are consistent with the KGE index. With some exceptions, in general the WRR2 models presents an improvement performance over WRR1. WaterGAP3 is the opposite case, and SURFEX-Trip has an improvement in WRR2 over WRR1 only in the UMP and Saldaña

48

basins. The RMSE in Figure 3.5c shows consistency with the other statistics. The lowest values correspond again to W3RA R2Eq2 and JULES R2Eq1 showing the best performance.

Even though some models perform relatively well, the overall performance of the mod-
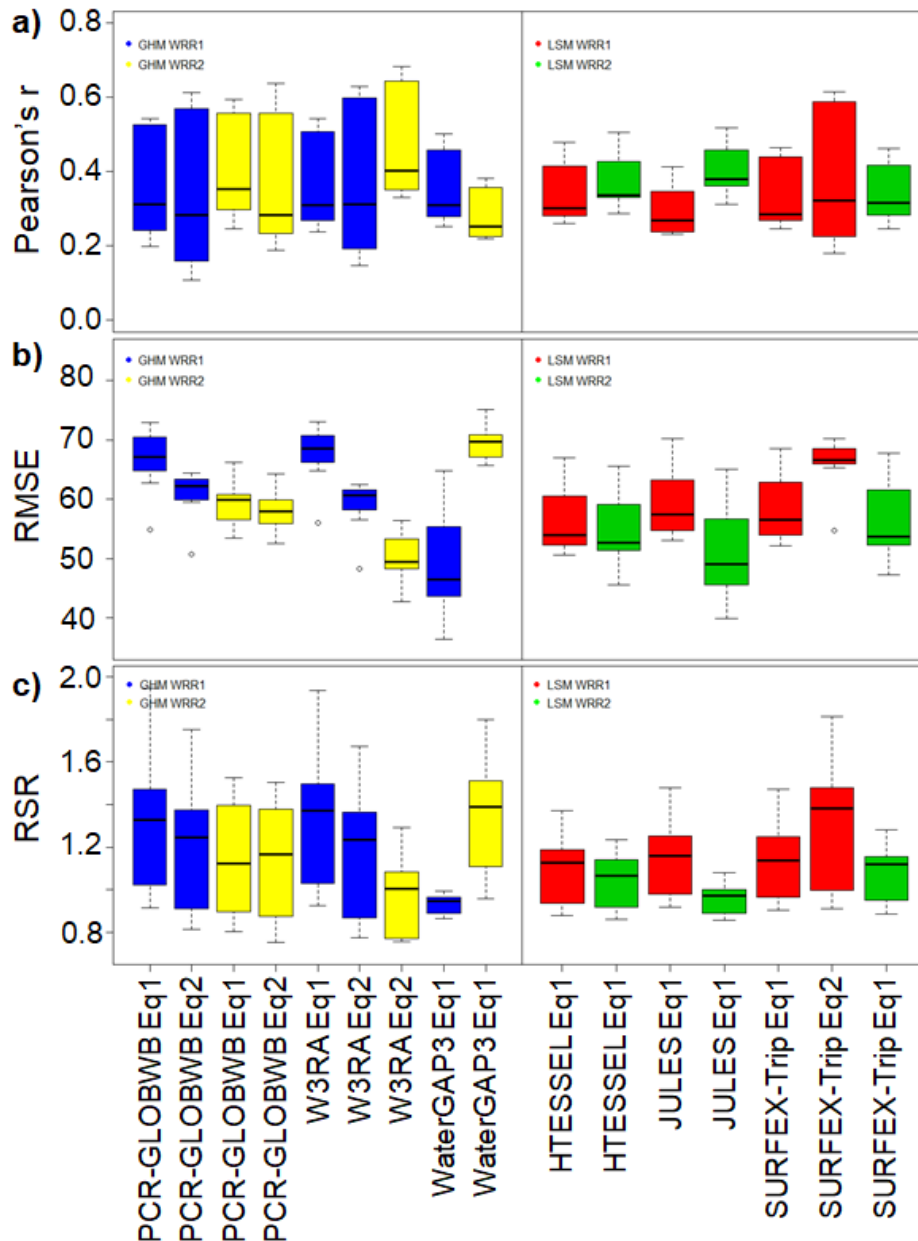
Figure 3.4: Distribution of model performance for the three metrics considered for each GHM and LSM with both WRR1 and WRR2 version. (a) is the Pearson's r, (b) RMSE, and (c) RSR.
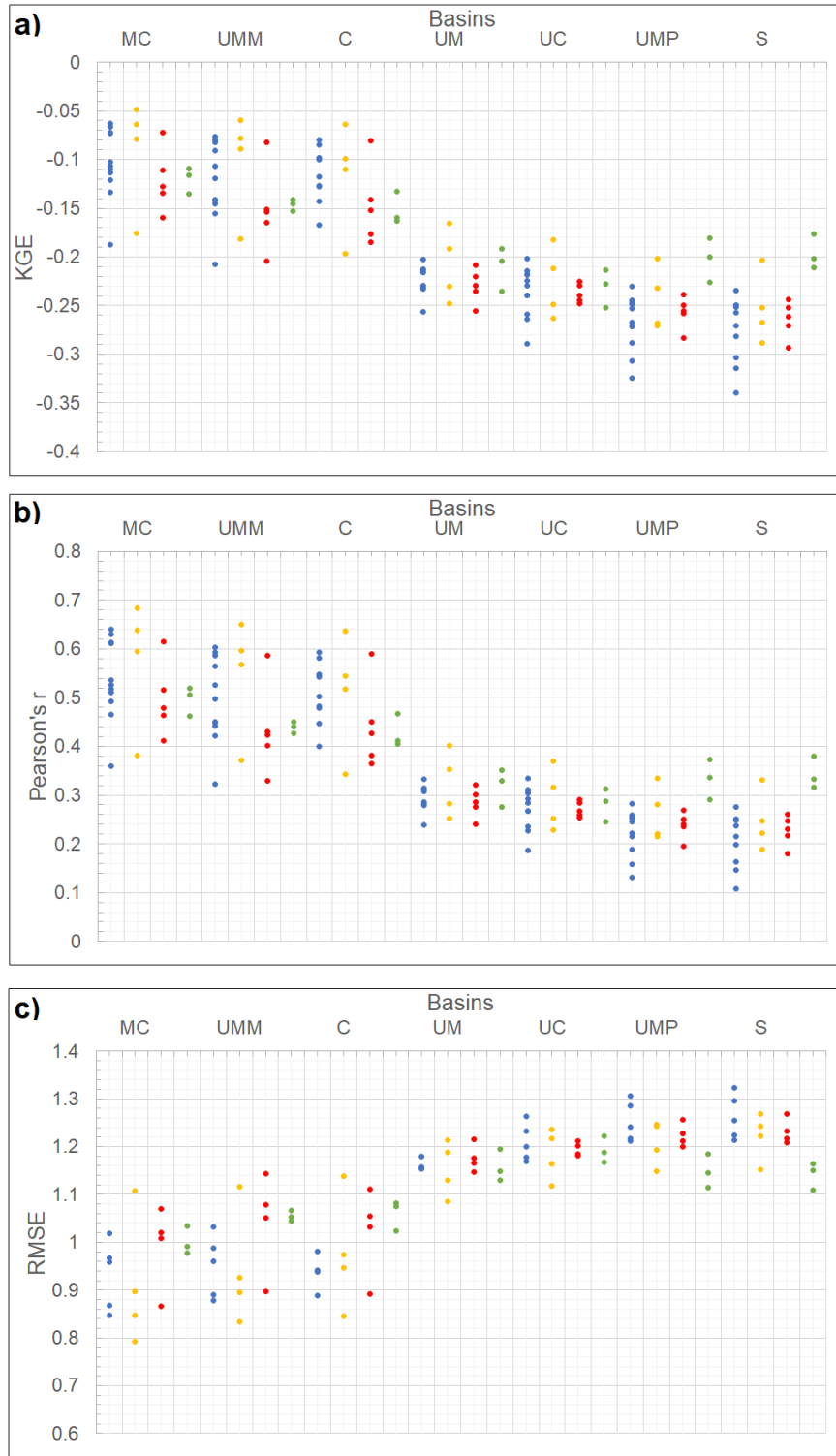
Figure 3.5: Performance statistics between GRACE and the GHM (blue and yellow points for WRR1 and WRR2 respectively) and LSM (yellow and green points for WRR1 and WRR2) at different scales. In a) the KGE index, b) Pearson's r, and c) the RMSE. The basins are organized from major to minor area, and the data is standardized and normalized.

els is in general, poor. Average KGE remains negative for all models and sub-basins, and the average Pearson's r value does not exceed 0.5 in most cases. We highlight the decrease in the performance of all models towards the smaller basins. The shift between the Cauca and UM basins, with areas of $\sim$ 60,657 km^2 and $\sim$ 56,992 km^2 respectively is interesting, although the specific catchment conditions in these two basins may lead to what appears a step change. It is worth noting that GRACE resolution begins to have more limitations in these smaller basins.

Figures 3.6 and 3.7 show the spatial relationship between the TWS monthly values of GRACE and the models with both reanalysis version WRR1 and WRR2, and the models with only WRR1 respectively. For this, we rescale the GRACE and the models from 0.5°to 0.25°using bilinear interpolation to interpolate from one rectilinear grid to another, to be consistent with the finest resolution WRR2 models. The W3RA Eq2 WRR2 is the model with the highest correlation values. The maximum values presented in the maps are close to 0.8 and are located mainly towards the North of the macro-basin, with the minimum values towards the South. This is coherent with Figure 3.5, in which we observe a reduction in performance of all models upstream of the UM basin. This suggests that is not only basin size that is relevant to the performance of each model. The prevailing pattern could suggest it is related to hydrological process, or more likely to the presence of storages in these areas that the models are not properly simulating. In Figure 3.6 it is also clear that there is an improvement in the spatial correlations of models with when forced with WRR2 rather than WRR1, except for WaterGAP3.

3.3.3   TWS seasonality and evaluation of long-term trends

To assess the seasonal signals and long-term trends of the models against GRACE TWS we show in Figure 3.8 the Pearson's r coefficient and RMSE statistic for all sub-basins. We observe a similar pattern as in the Taylor Diagrams presented in Figure 3.2 for the macro basin, but now highlighting model performance with decreasing basin size. We observe the same shift in the performance of models for basins of the size of the UM basin and smaller both for seasonality (Fig. 3.8a,b) and long-term trend (Fig. 3.8c,d). The Pearson's r values for both is better than in the monthly values analysis (Fig. 3.8a,c). For seasonality, the highest r coefficient is found for PCR-GLOBWB R2Eq2 for the MC and UMM basins, and for W3RA R2Eq2 for the remaining sub-basins, which coincides with the lowest RMSE in Figure 3.8b. For long-term trends, the highest r coefficient is presented in HTESSEL R2Eq1 for MC, JULES R2Eq1 for UMP, and W3RA R2Eq2 for remaining sub-basins,
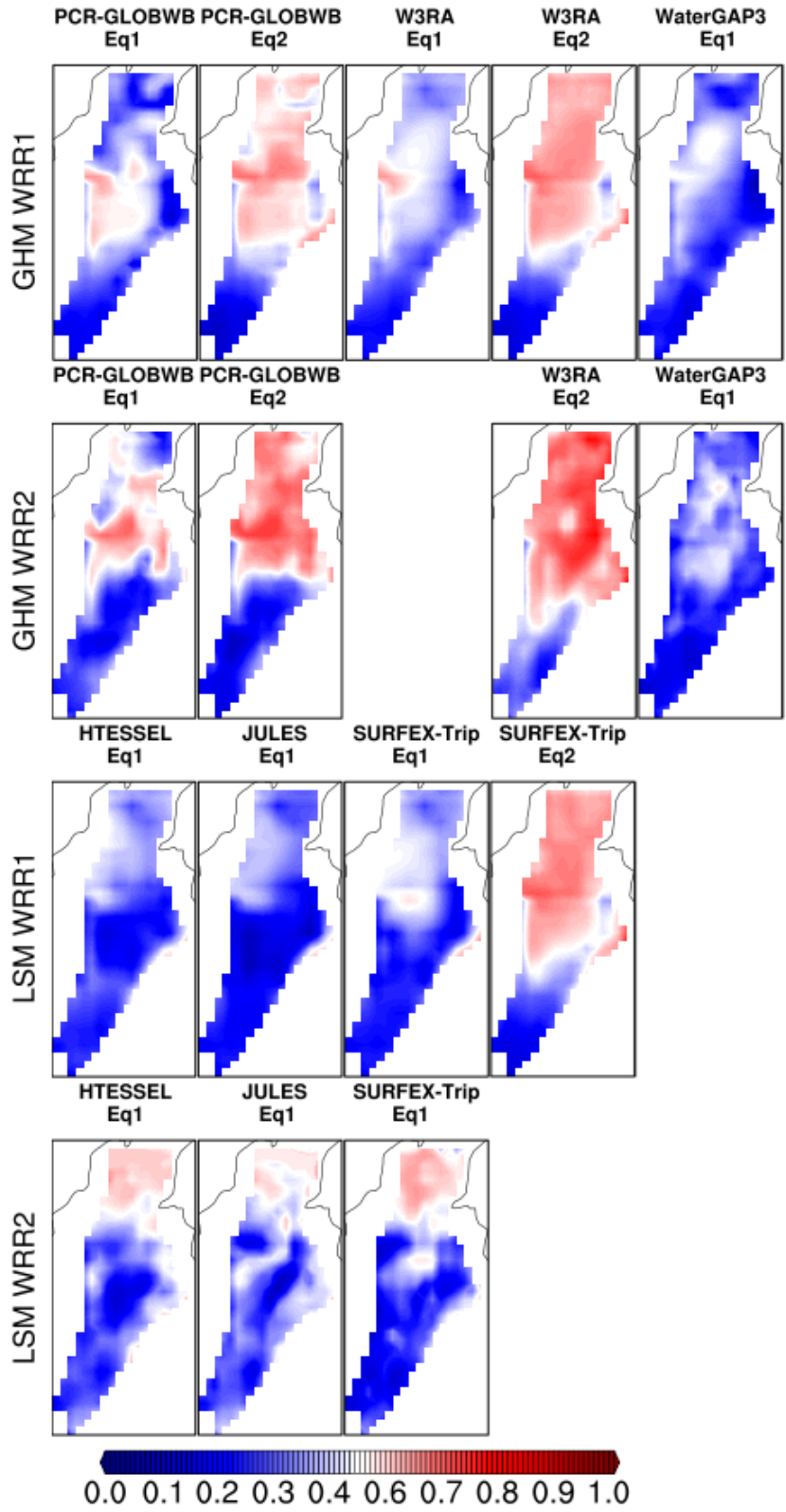
Figure 3.6: GRACE JPL vs Models correlation maps for whose that are available both in WRR1 and WRR2 for Eq1 and Eq2.
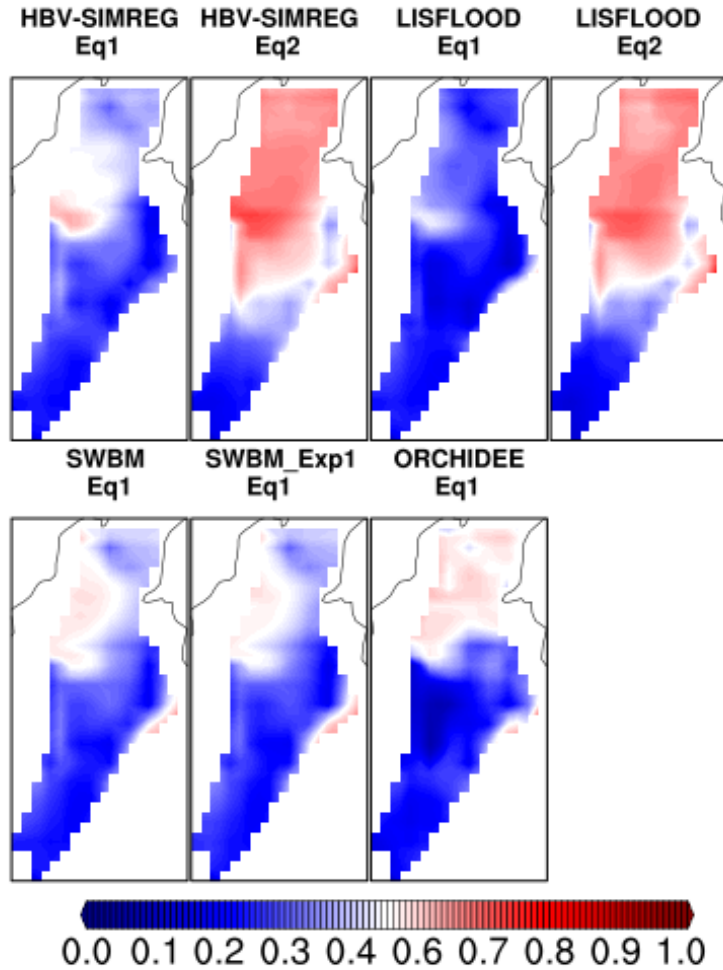
Figure 3.7: GRACE JPL vs Models correlation maps for whose that are available only in WRR1 for Eq1 and Eq2.

which coincides with the lowest RMSE in Figure 3.8d. WaterGAP3 R2Eq1 presents the lowest performance for all sub-basins in the long-term trends.

The seasonality found for the GRACE data, as well as for each group of models and for each sub-basin is presented in Figure 3.9. In general, we observe good agreement between TWS from the models and GRACE for the main basins. The bimodal behaviour in all models and in the GRACE data is consistently represented, as a consequence of the dominant bimodality of precipitation in the macro-basin ((Poveda, 2004)). However, for the UM basin and the smaller basins, the models tend to overestimate the second peak in the SON (September–October–November) season. The maximum peak in GRACE for all sub-basins occurs in the month of May, while in the models it varies.
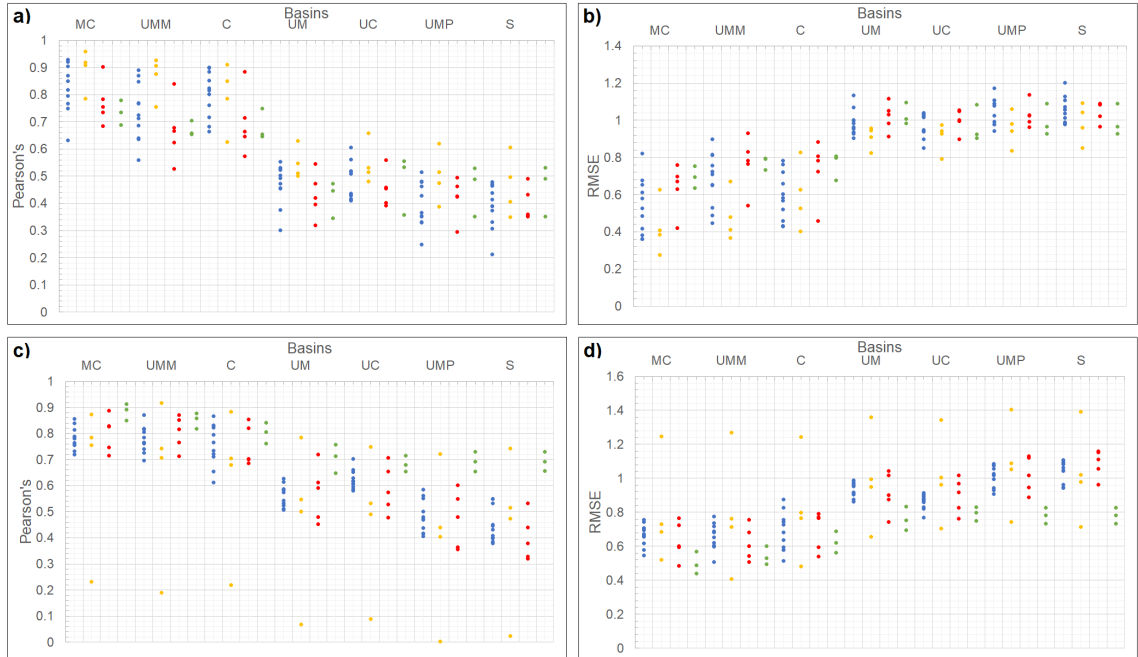
Figure 3.8: Performance statistics for the seasonality (a–b) and long-term trends (c–d) of GRACE and the GHM (blue and yellow points for WRR1 and WRR2 respectively) and LSM (yellow and green points for WRR1 and WRR2) at different scales. In a) and c) the Pearson's r coefficient and in b) and d) the RMSE.

Figure 3.10 compares the seasonal maps of TWS estimated for GRACE and the models with the highest correlations following the Figures 3.6 and 3.7 and models that perform similar. The seasonal maps of TWS for the other models are shown in the supplementary material (Figs. C.3 and C.4). Here, we observe that the amplitudes for most models is smaller than for the GRACE data. This implies that the models tend to underestimate seasonal variation. For DJF (dry season) the models tend to be consistent with GRACE, with the lowest biases found in the North. In general, for the basin the values of TWS are negative or near zero. On the other hand, MAM (the first wet season), shows the opposite case with positive values throughout the macro basin, with some exceptions towards the North like the W3RA R2Eq2. In JJA (dry period) we again observe consistency. There is a transition between the two rain periods, with positive bias in the North and negative bias in the South of the basin. In SON the models differ spatially with GRACE. The highest values of TWS from GRACE are found in the North of the basin in SON. This part of the basin is dominated by La Mojana wetlands. On the contrary, the models mostly present biases in the area of La Mojana close to 0, and higher TWS values towards the South of the basin. These higher values in the South correspond with the peaks observed in Figure 3.9. This behaviour is likely due to the poor representation of the wetlands in the models.
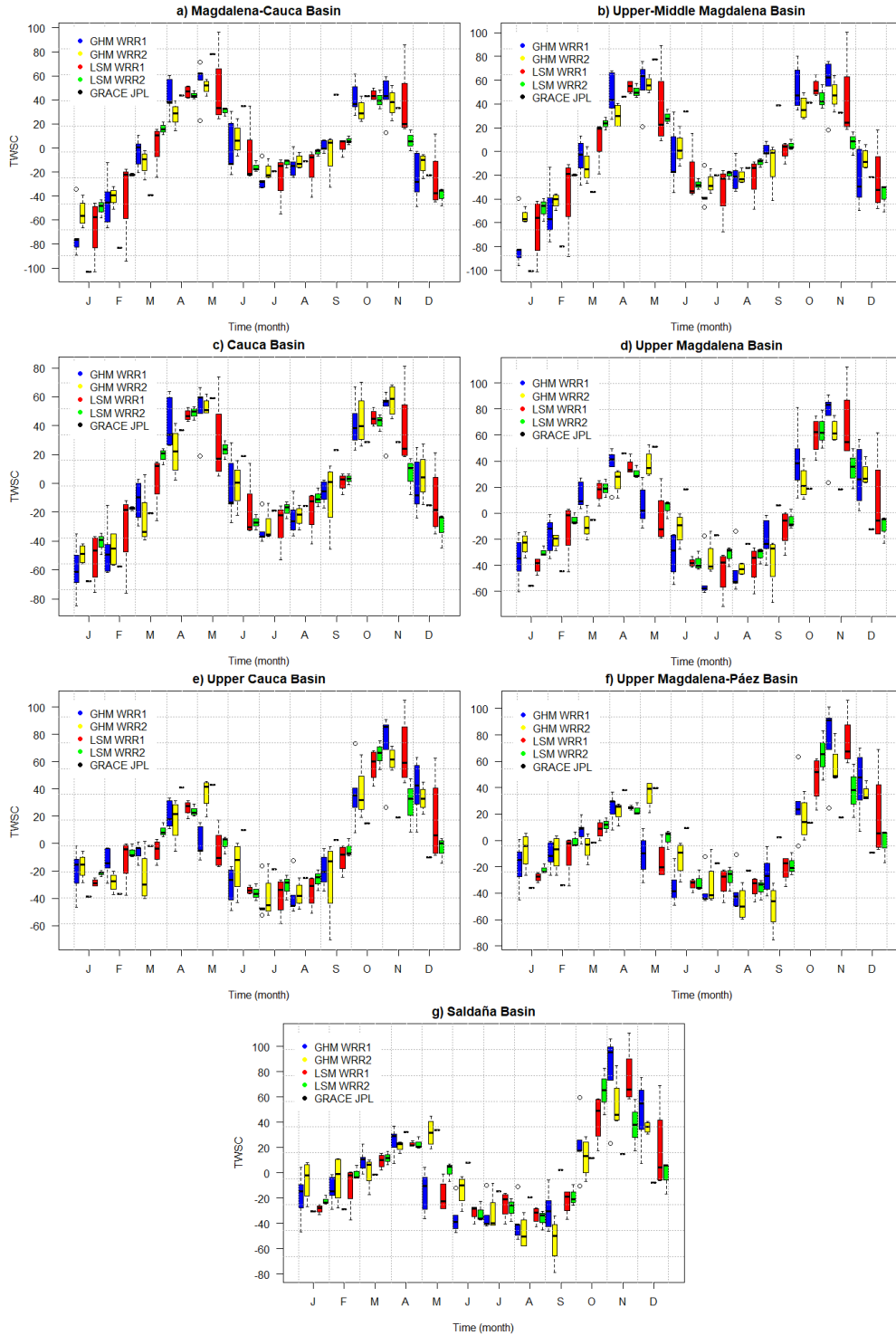
Figure 3.9: Comparative boxplots between the climatology of GHM and LSM, and GRACE JPL for each subbasin.
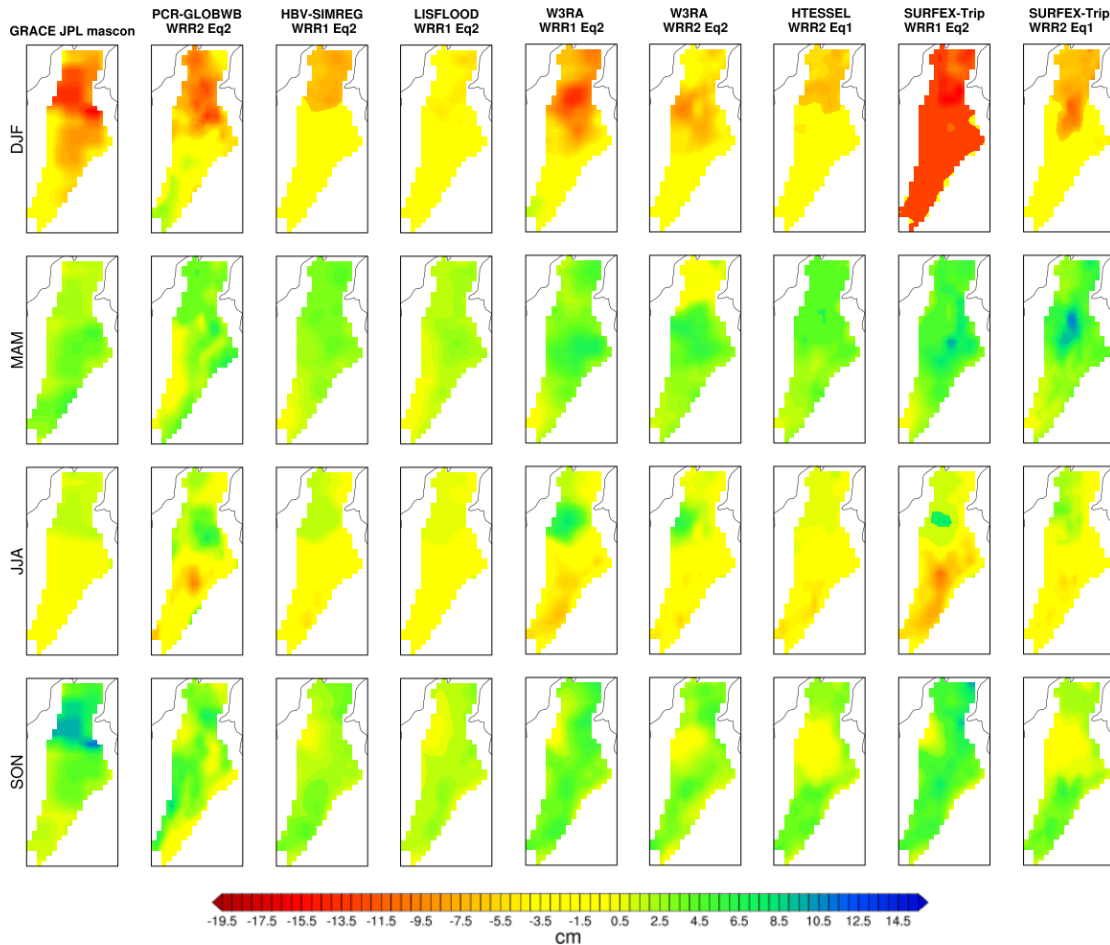
Figure 3.10: Seasonal maps for GRACE JPL, GHM, and LSM.

The buffering capacity in the models is poorly represented, which means that these dry out too much in the drier DJF period and cannot represent the wet period in SON in La Mojana area, which on can be observed by GRACE. For the second dry season, the fact that the climate becomes more unimodal to the North (see Fig. C.1) may also contribute. Both drying and wetting may also be overestimated by the models as observed in the South, specially, during JJA and SON, and SURFEX-Trip R1Eq2 during DJF.

Finally, we explore the agreement between the models and GRACE for the long-term component. Figure 3.11 shows the series for GRACE JPL (black line) as well as for each model group GHM WRR1, GHM WRR2, LSM WRR1 and LSM WRR2 (blue, yellow, red and green lines respectively). We present the graphs for MC, Cauca, UM, and Saldaña basins, as the other sub-basins are similar to these and are shown in the supplementary material (Fig. C.5). The MC and Saldaña basins are the largest and smallest basins re-

56

spectively, while the change in model performance occurs between Cauca and UM basins. Large discrepancies between models and GRACE can be seen, with these increasing as basin size decreases. We observe that WaterGAP3 R2Eq1, PCR-GLOBWB R1Eq1 and Eq2, and SURFEX-Trip R1Eq2 (the first two are GHM and the last is an LSM), overestimate both highs and low peaks. By contrast, LISFLOOD R1Eq1 and SWBM R1Eq1 outputs are relatively flat, underestimating both the highs and the lows. However, all models are able to capture the increase in TWS during the 2010-2011 ENSO event (La Niña), likely due to the (common) precipitation forcing. Better performance is shown for the LSM than for GHM in general, although the results for W3RA R2Eq2 are closest to observations.

3.4   Discussion

3.4.1   Evaluation of the performance of the models

To summarize the results of the performance of the models with respect to GRACE, we present the performance metrics for each model and WRR in Figure 3.12. Higher score values (blue boxes) correspond to better performance in representing TWS, while lower score values (red boxes) indicate poor representation for monthly time series, seasonality and long-term trends. As we observe in the results and in Figure 3.12, in general terms the WRR2 models exhibit better performance than for the lower resolution WRR1. This is coherent with results of (Gründemann, Werner, & Veldkamp, 2018), who assessed simulated discharges from seven of the ten models studied here, as well as the ensemble mean of those models, focussing on the occurrence of floods in the Limpopo Basin in Southern Africa. The exception of this improved performance is found for WaterGAP3, contrary to Rodríguez et al. (2019) where streamflow is evaluated and WaterGAP3 presents an improvement. Since the models have the same input/forcing for each WRR, differences in simulation results must be due to the model structure and internal dynamics. There are a number of factors that could contribute to this notable exception of WaterGAP3 for the study area, these include model modifications and how reservoir management is represented. The model improvements that have been made primarily affect the water stored in the reservoirs and not the surface runoff, evapotranspiration, or other surface fluxes (Dutra et al., 2017).

Figure 3.12 shows that over the macro basin as a whole, the TWS change computed from W3RA WRR2 using Eq2 (Eq. 3.2), is the model that best captures the signals found in the GRACE data; including the monthly series, seasonality and long-term trend. The
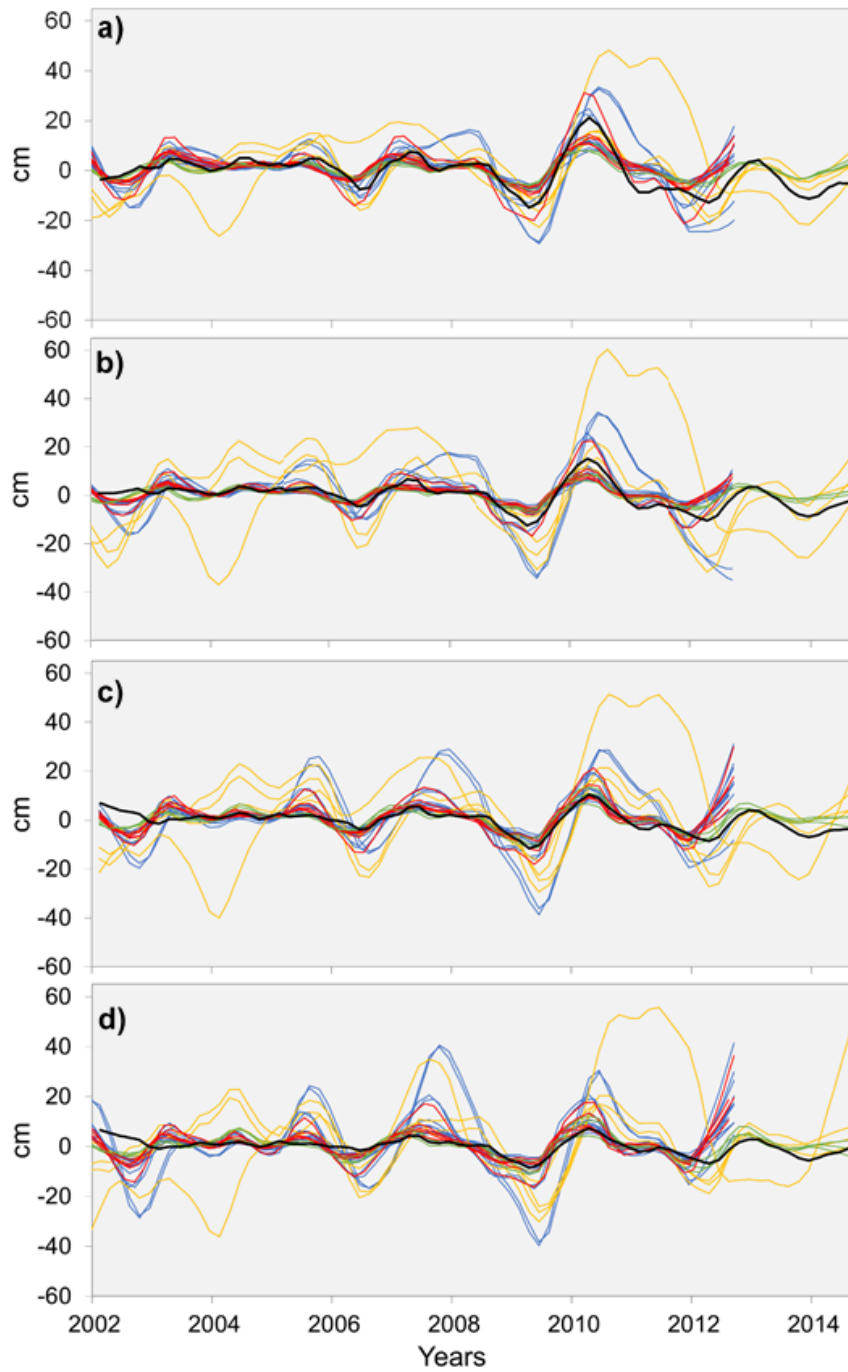
Figure 3.11: Long-term trends time series for the models and GRACE for a) MC, b) Cauca, c) UM, and d) Saldaña basins. The black line indicates the GRACE JPL, the blue and red lines the GHM WRR1 and WRR2 respectively, the yellow lines the LSM WRR1 and the green lines LSM WRR2.
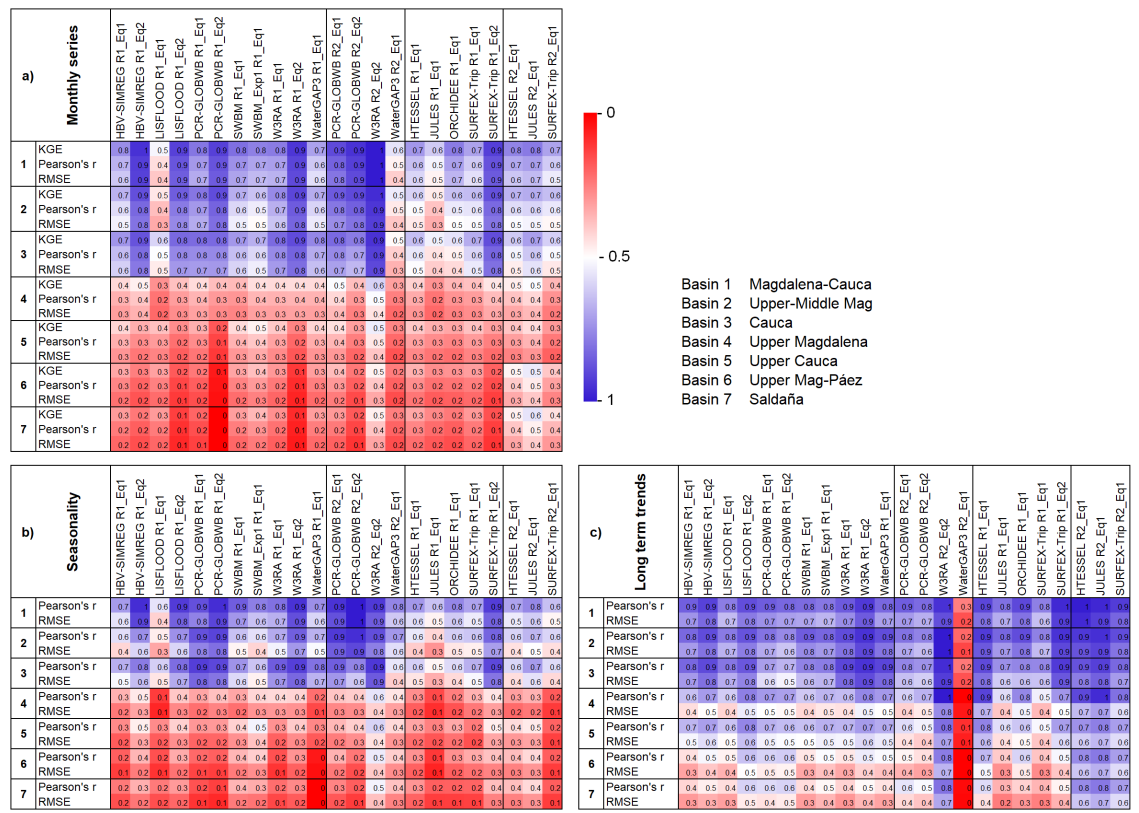
Figure 3.12: Summary figure of the models performance respect to GRACE data. Statisticians of KGE, Pearson's r, and RMSE were rescaled between 0 and 1, with 0 being the worst performance among the models and 1 being the best performance. The evaluation for the monthly time series is presented in a), in b) the evaluation for the seasonality, and in c) for the long-term trends.

performance metrics evaluated demonstrate that for the different sub-basins, the best performing models include both GHM and LSM. In addition to W3RA, for the monthly series JULES R2Eq1 performs best in the smaller basins. Besides W3RA, for seasonality signal, PCR-GLOBWB R2Eq2 performs relatively well, while for long-term trends, two LSM; HTESSEL R2Eq1, and JULES R2Eq1 also have good agreements. Each of these models performed well with roughly similar statistics through the basin, despite differences in structure of these models.

Zhang et al. (2017) evaluate the TWS estimates of four available hydrological models (two GHM and two LSM) and GRACE in 31 of the world's largest river basins. Although the Magdalena-Cauca basin is not included in their study, they find that the performance of the models varies from basin to basin, even within the same climate zone. They conclude that the variation in performance of models could be due to model structure, as we

59

mentioned, parameterization, different water storage components included in TWS, as well as being connected to the differences in simulating runoff and evaporation scheme (Ramillien et al., 2006; Zhang et al., 2017). In our case, the best performing models, W3RA, HTESSEL and JULES calculate the evapotranspiration using Penman–Monteith method, and Saturation and infiltration excess for calculate runoff. However, the worst performing models, LISFLOOD and SURFEX-Trip also use these same schemes, while WaterGAP3 uses the Priestley–Taylor method for evapotranspiration and Beta function for runoff. This would imply that the relationship between model performance and structure is yet inconclusive.

However, checking Schellekens et al. (2017) we note that the interception processes for W3RA model follows a Gash event-based model, while most of the models follow a single reservoir and potential evaporation process to compute interception. Other models do not use an interception scheme, which may be important in a tropical basin such as the Magdalena. The routing scheme, whether human water use is incorporated, and time step can also cause significant differences between the models. Also, how the models simulate each component of the hydrological cycle does, make a difference in the performance of the TWS change calculation. For example, models with groundwater component used in Equation 3.2 show better performance over the same models that use Equation 3.1 to compute TWS (Fig. 3.12). Notwithstanding, future analysis is still needed in which internal process, evapotranspiration, and runoff approaches are evaluated in depth.

It is also important to note that, if similar research were to be applied elsewhere, the ranking of model performance may be quite different and depends on the aim of the research. For example, WaterGAP3 performed poorly with respect to other global hydrological models in research focussing on a snowmelt-driven catchment (Casson, Werner, Weerts, & Solomatine, 2018). Conversely, for the Limpopo River basin WaterGAP3 in WRR2 demonstrated the best performance for the identification of flood events in Southern Africa (Gründemann, Werner, & Veldkamp, 2018).

3.4.2   Seasonality and long-term trends performance

The differences in TWS change seasonality and long-term trends may be due to different reasons. Following the Scanlon et al. (2019), differences in seasonal amplitudes of TWS between models and GRACE can result from uncertainties in models or GRACE or both. These uncertainties may come from the scheme of modelled storage capacity and storage compartments included in each model (Table 3.2), uncertainties in modelled in-

flows/outflows, and uncertainties in modelled human interventions in the case of GHM, or lack of these in LSM. Storage capacity and compartments such SWS and GWS are critical in tropical basins, where the magnitudes of TWS seasonal amplitudes are high, driven by seasonal precipitation (Scanlon et al., 2019). The bimodal behaviour is evident in the seasonal signal of TWS from GRACE and models, but the peak in the SON season in the models is greater when observing smaller basins. The peak in the SON season follows mainly the precipitation used to force the models, but in GRACE this peak is lower. The overestimation or underestimation of modelled seasonality of TWS change relative to GRACE in the study area could result from overestimation or underestimation respectively of the storage capacity. A possible explanation about peaks observed in GRACE is that the first rainy season is preceded by a strong dry season. As the soil receives a large amount of water, this infiltrates and recharges groundwater storages; the soil becomes saturated; and the remainder becomes surface runoff. For the second rainy season, which is generally stronger and of greater quantity, the soil is not as dry as the first wet season, and therefore soils saturate more rapidly generating more runoff that quickly leaves the basins. Due to the poor representation of the storage capacity in the models, these may be overestimating the changes of TWS in SON especially in the South, where the topography is more complex.

Similarly, discrepancies in long-term trends in TWS may be related to uncertainties in models and/or GRACE. Scanlon et al. (2018) evaluate seven different global models against GRACE. Considering initial conditions, water storage compartments and capacity related to model structure, precipitation uncertainty, and model calibration, they conclude that the models considered underestimate large decadal water storage trends relative to GRACE data. In this study, the models have the same input/forcing for each WRR and are not calibrated, so the differences must be due to model structure (e.g. representation of water storage compartments) and parameterization (e.g. capacity of compartments) (Dutra et al., 2017). The way each model computes the storage capacity could be related to the lack of storage compartments, soil profiles (thin and number of layers), or exclusion of processes, such as river flooding (Scanlon et al., 2018). One of the clear factors is that most LSM do not model SWS and GWS compartments, with the exception of Surfex-Trip. However, the inclusion of SWS and GWS is not conclusive for a good agreement with GRACE in our study due to Surfex-Trip overestimating long-term trends and the LSM in general having better performance over most GHM (Fig. 3.8c,d and Fig. 3.12c). Models also differ in how storage compartments such as the soil layer are discretised (Schellekens et al., 2017). While W3RA has three soil layers and shows good agreement, WaterGAP just has one, and SurfexTrip 14 soil layers. More than the number of soil layers, the thickness and

depth could result in an important variable for storage capacity calculation. Swenson and Lawrence (2015) report that the thickness of the profile required to replicate the GRACE TWS variability is up to 8-10 m in tropical regions (e.g., Amazon, Congo) and in South Africa, while most models have a floor thickness of 1 to 4 m (Dutra et al., 2017; Schellekens et al., 2017).

3.4.3   Basin scale analysis

As basin area reduces, the performance of models is found to decrease. Here it is important to highlight that GRACE measurements and leakage uncertainties increase with decreasing basin size (Scanlon et al., 2016). In the Figures 3.5 and 3.8, the shift occurs between the Cauca ($\sim$ 60,657 km^2) and UM ($\sim$ 56,992 km^2). Currently, basins with a size of $\sim$ 63,000 km^2 can be resolved to an error level of 2 cm in terms of equivalent water height (Vishwakarma, Devaraju, & Sneeuw, 2018), which would agree to the size smaller than which we find a marked decrease of performance. Notwithstanding, when we analyse the spatial correlation maps (Figs. 3.6 and 3.7) and the seasonal maps (Fig. 3.10), we observe that there are large discrepancies for the South of the macro-basin. The Southern part of the basin corresponds to an area with a more complex topography. In addition, the basin is highly intervened by anthropic activities, which is a challenge for the models to simulate flows and water storage compartments. While the global models in general, cannot represent well the wetlands in the North of MC, in the mountainous area the precipitation not only depends on the macroclimatic phenomena of ENSO and the movement of the ITCZ, but it is influenced by other atmospheric circulation mechanisms such as Mesoscale Convective Systems, soil-atmosphere interaction processes, and local wind circulation (Poveda, 2004). Also, is important to highlight the presence of high-altitude montane wetlands (Paramo), which is one of the most important ecosystems in Colombia as they are an important source of water supply for many big cities (Rodríguez & Armenteras, 2005). This means there are significant challenges to how well models represent the full spectrum of hydrologic fluxes and stores.

Gründemann, Werner, and Veldkamp (2018) point out that models that capture only natural flow conditions, and do not take artificial reservoirs and water usage into account, may be able to reasonably estimate runoff volumes, though they do tend to overestimate the actual magnitude of discharges. This suggests that GHM would have better performance due to the inclusion of human interventions over the LSM. While we do observe this to be the case for the general MC as well as selected sub-basins (UMM and Cauca), but when comparing monthly time scale of TWS for smaller basins, we find that the LSM WRR2

62

have a better agreement over GHM (Fig. 3.12).

3.5 Conclusions

With the availability of measured hydrological data in the Magdalena-Cauca (MC) decreasing, there is an increasing interest in the use of remote sensing data and models to study water resources. The recently developed Earth2Observe (E2O) reanalysis dataset provides hydro-meteorological data of sufficient length and coverage to help in the study of hydrological variables in basins with insufficient or poorly spatially data. GRACE on the other hand, is a recent and powerful tool that provides independent and distributed observations of Total Water Storage (TWS) that would be not possible with conventional methods. This raises the question about how representative the TWS is represented in the models, when validated against the GRACE database in a medium-size tropical basin. Here, we evaluate the representation of TWS change from ten models, six Global Hydrological Models (GHM) and four Land-Surface Models (LSM) in the MC river basin. Also, we assess the potential of the two global Water Resources Reanalysis (WRR1 and WRR2) available from the E2O dataset by studying the TWS change performance through commonly used statistics.

Error statistics reveal that the variability of GRACE TWS is better captured by the models of the larger watershed areas compared to the smaller watersheds. Watershed areas at which WRR1 and WRR2 models are able to provide better representation of the hydrological behavior are observed for areas above around 60,000 km^2, with a significantly poorer performance for smaller catchment sizes. However, we observe that spatially, the models do not adequately capture the hydrological process in the South of the basin, which corresponds to the area with more complex topography, high level of anthropogenic intervention, as well as the the presence of high montane wetlands that have an important water regulating function. In general, models in the WRR2 dataset have performance better than WRR1. This shows that the continuous improvements in the global models, either due to improved higher-resolution forcing or due to improved model structures and parameterization, can lead to a better representation of the observed TWS variability.

This comparison highlights the relevance of the use of new, independent, remote sensing data to validate these large scale models, as well as for prioritising future model development, particularly in the simulation of water storage. The inability of models to adequately capture water storage based on GRACE, may results in underestimating / overes-

63

timating hydrological variability in water resources studies and climate projections. The disparity between GRACE and the models is, however, subject to uncertainties in both GRACE and the models. However, it should be noted that GRACE processing is continually improving, so the associated uncertainties are reducing. In this study we use the last GRACE release (RL5) before the satellites were down. Currently, GRACE Follow-On mission is a successor to the original GRACE mission and was launched on May 22 of 2018. The RL6 will shortly become available for future research. The continued advances in GRACE data, may improve our understanding of water resources in the different basins around the world. Future modelling should consider the integration of remote sensing as GRACE, in addition to in situ data for calibration, resulting in less uncertainties in the results of models for future projections under climatic and anthropic change.

CHAPTER 4
OUTLOOK AND CONCLUSIONS

Colombia is a country of great geographical diversity (Rangel, 2005) with abundant water resources (IDEAM, 2019). It is estimated that within its territory 60% of the world's Páramos can be found, a high montane neotropical grassland ecosystem unique to the Andes, well as some 31,702 wetlands. These are strategic ecosystems and water sources to supply and meet the demands of the population, environment, and economic sectors. The main services that wetlands present are related to the regulation of the water cycle and the conservation of biodiversity (Jaramillo Villa et al., 2016). On the other hand, although still less studied, in Colombia groundwater is considered a strategic source to ensure water security in the face of climate variability and climate change. Groundwater is widely used for agriculture, as a source of domestic water supply and in the industrial sector, and plays a very important role in the sustainability of many ecosystems (IDEAM, 2019). The interaction between wetlands and aquifers, especially in the aquifer discharge areas, has led to the consideration of shallow aquifers as wetlands (García-Giraldo, Betancur-Vargas, & Villegas, 2018).

In the Magdalena-Cauca basin (MC), 8 hydrogeological provinces have been identified, within which preliminary studies have been carried out for 34 aquifer systems (Fig. A.7 and Appendix A)). These aquifers are primarily exploited through artisanal wells with average depths that do not exceed 40 m and capture only the shallow aquifers. Though of smaller quantity, there are also larger wells that reach depths of more than 100 m (IDEAM, 2019). Despite the widespread use of groundwater, most of the aquifer systems across the country are poorly monitored and their dynamics at the regional and national level is not well understood. Coupled with the decrease in hydro-meteorological stations (Rodríguez et al., 2019), the use of remote sensing and global models to support hydrological studies in the country has increasingly been gaining attention.

In this thesis, we use GRACE to evaluate the dynamics of total water storage (TWS) for the MC basin. The results presented in Chapter 2 show that there are two distinct trends in TWS within the study period. An increase in TWS between 2002 and the end of 2010 is identified, followed by a decrease between 2011 and 2016 (Fig. 2.3). These variations coincide with the dynamics of climatic variability regulated by the El Niño and La Niña phenomena (Fig. 2.6). These trends are also found when we calculate trends in

groundwater storage (GWS) established through a combining GRACE with data from the GLDAS land-surface model (Fig. 2.4).

Clifton et al. (2010) identify groundwater as a crucial resource for climate change adaptation because confined aquifers respond more slowly to climatic variation than do surface waters. However, in Figure 2.6 we observe that the maximum correlation between the storage data derived from GRACE and key ENSO indicators is found at a lag of 2-months, which in hydrogeological terms represents a rapid response. Bastidas, Betancur, and Martinez (2019) evaluate variations at the hourly time scale of the phreatic level in a shallow aquifer in the tropical region of the Gulf of Urabá in Northern Colombia and how these relate to precipitation, finding that the lag time with which the groundwater levels respond rarely exceeds 3 days. Their conclusions, along with our current results, suggest that the change in GWS from the analysis with GRACE (Fig 2.4), represents the variations that occur in unconfined or shallow aquifers, in the basin.

In the MC basin, the hydro-stratigraphic units associated with alluvial deposits and geological formations of primary porosity are located in the valleys of both the Magdalena and Cauca and in the Eastern Cordillera of Colombia. In 2016, the Alexander von Humboldt Biological Research Institute (Jaramillo Villa et al., 2016), delimited the continental wetlands of Colombia. Betancur-Vargas et al. (2017) established the relationship between wetlands and groundwater, and identified 14 wetlands connected with aquifer systems within the MC basin. It is clear that the difference in the resolution of the spatial representation of the mapping of aquifers and wetlands in Colombia and the results of GRACE is considerable. However, our results related to the changes in terrestrial storage can be, preliminarily, taken as indicators of the implications that this could have on the coupled shallow aquifer–wetland system, if this is considered to be a single system (García-Giraldo, Betancur-Vargas, & Villegas, 2018). In Figure 4.1 we present a superposition of the estimated GWS with the aquifer systems identified in the MC basin (Fig. A.7), for the months of December 2010 and March 2016, the months with the largest and smallest change in storage respectively. The spatial extent of these largest changes is similar to the extent of the wetlands as shown in Figure 2.7.

Considering that the estimated volumes of the change of GWS in the MC basin during the 2002-–2010 and 2011–2017 periods (Fig. 2.4) is of the order of 32.71 km^3 and -56.39 km^3, and evenly distributing these over the total surface of the basin, a net recharge of 118.34 mm would be found for the first period and a net discharge of 203.98 mm for the
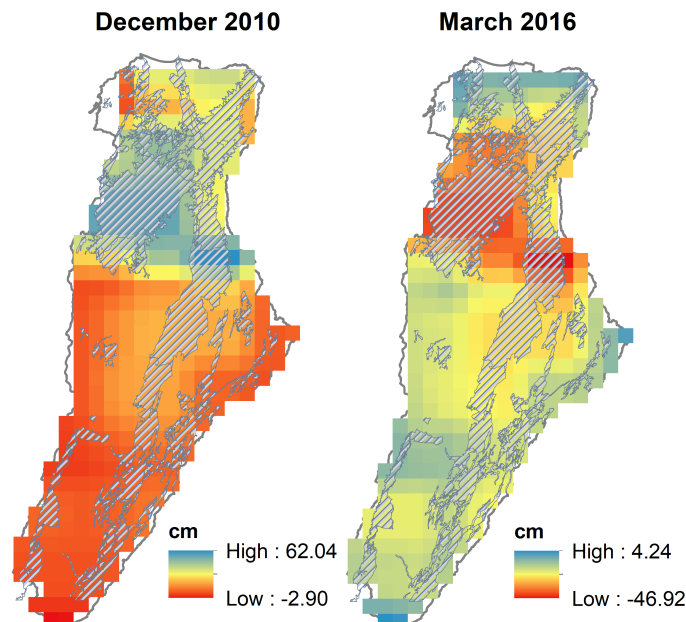
Figure 4.1: Superposition of the spatial extent of aquifer systems and the maps of TWS for December 2010 and March 2016. The hatched areas correspond to aquifer systems as identified in ENA 2018.

second. Given the hydro-stratigraphic conditions, we distribute the recharge and discharge volumes only over the surface of the aquifer-wetland coupled systems that have been identified, resulting in a net recharge of 284.65 mm and net discharge of 490.68 mm, for the aforementioned periods. Further considerations can be taken into account in distributing the volumes of the basin given the characteristics of the system. For example: i) considering only the Upper-Medium Magdalena (UMM) basin for the period with a positive trend the net recharge over the surface of the aquifers of the Magdalena Valley and the Eastern Cordillera would be approximately 360.02 mm, and the discharge 637.39 mm; ii) on the aquifers of the Upper Cauca (UC) basin, where the period with a positive trend is between 2002 and January 2008 (Fig. 2.4), the net recharge would be 260.29 mm, and the discharge between 2008 and 2017 would be 229.70 mm; iii) for the wetlands of La Mojana area and the aquifer systems found in the lower part of the basin, between 2002 and 2010 an approximate net recharge of 461.15 mm is found, and a loss of 848.39 mm between 2010 and 2017 considering the quite significant changes in GWS in the north zone (Fig. 2.5).

Table 4.1 shows the estimated recharge and discharge in water depth according to the volumes calculated for TWS and GWS for different areas of the aquifer systems in the basin. It should be noted that the values shown here are to be considered as guidance

and are not intended to be precise predictions due to the uncertainty associated with the resolution of GRACE data and the GLDAS model used to calculate GWS. Since there is no continuous and sufficiently dense monitoring network of groundwater in Colombia, these GWS results should be validated in the future with continuous piezometric monitoring data. The recharge and discharge values presented in this discussion are preliminary values that invite us to think about how these results can be used, as well as how these can be refined as satellite data, evaluation methods and the availability of concurrent datasets are improved.

Table 4.1: Estimated depths of recharge and discharge to/from groundwater for the periods with positive respectively negative trends for the whole basin as well as for selected sub-basins, and considering the area where wetland and aquifer systems coincide.

	2002–2010		2011–2017	
	TWS	**GWS**	**TWS**	**GWS**
Volume for MC	41.04 km^3	32.71 km^3	-77.68 km^3	-56.39 km^3
MC basin (276,000 km^2)	148.45 mm	118.34 mm	-280.97 mm	-203.98 mm
Aquifers and wetlands within the basin (114,926 km^2)	357.11 mm	284.65 mm	-675.88 mm	-490.68 mm
Volume for UMM	18.97 km^3	15.61 km^3	-37.82 km^3	-27.64 km^3
UMM basin (140,754 km^2)	134.76 mm	110.90 mm	-268.73 mm	-196.34 mm
Magdalena Valley and the Eastern Cordillera aquifers (43,358 km^2)	437.46 mm	360.02 mm	-872.39 mm	-637.39 mm
Volume for C	8.27 km^3	7.63 km^3	-10.19 km^3	-6.30 km^3
C basin (60,657 km^2)	136.43 mm	125.79 mm	-177.97 mm	-103.8 mm
Cauca Valley and Central Andes aquifers (6,562.45 km^2)	1260.99 mm	1162.67	-1645 mm	-959.44 mm
Volume	26.14 km^3	20.60 km^3	-49.96 km^3	-37.89 km^3
Lower basin (105,954 km^2)	246.68 mm	194.40 mm	-471.54 mm	-357.65 mm

Table 4.1 – continued from previous page

	TWS	GWS	TWS	GWS
La Mojana wetlands and the lower basin aquifers (44,666 km^2)	585.18 mm	461.15 mm	-1118.56 mm	-848.39 mm
	2002–2008		**2008–2017**	
Volume for UM	4.92 km^3	4.41 km^3	-9.28 km^3	-4.17 km^3
UM basin (56.992 km^2)	86.39 mm	77.36 mm	-162.62 mm	-73.22 mm
Upper Magdalena valley aquifers (19,466 km^2)	252.95 mm	226.50 mm	-476.11 mm	-214.38 mm
Volume for UC	1.78 km^3	1.60 km^3	-2.91 km^3	-1.41 km^3
UC basin (17,930 km^2)	99.43 mm	89.33 mm	-162.30 mm	-78.83 mm
Cauca valley aquifers (5,259 km^2)	289.25 mm	260.29 mm	-472.87 mm	-229.70 mm

Reflecting on how these results relate to water availability, we should start from projections that can be made based on current data. In the most recent National Water Study (IDEAM, 2019), the demand for water in the whole country is 37.31 km^3, with the agricultural sector being the dominant user. For the MC basin, the demand for water is 25.77 km^3, of which 42.51% is used in agriculture, while only 7.56% is for domestic use. In contrast to the volumes recharged for the MC basin, we can observe that for the period for which a positive trend in TWS is found, the total water storage would support the estimated demand. However, for the period where there is a negative trend, we can see water scarcity may develop. According to the ENA 2018, spatially the highest demands are found in the lower part of the basin where the La Mojana area is located as well as towards the eastern party of the basin.

In Figures 4.2 we illustrate the change in TWS through two photographs in the La Mojana area for two periods of time; the first during the 2010 La Niña event that caused serious flooding, and the second during the 2016 El Niño event that brought severe droughts. These images are consistent with the trends found in TWS and their strong relationship with the ENSO phenomenon.

To conclude, this study evaluated data from GRACE satellites through a combination of global and in-situ hydro-meteorological information. We use GRACE data to evaluate the

Figure 4.2: Photographs of wetlands of the La Mojana. a) during La Niña in 2010–2011 (Source: https://www.elheraldo.co/politica/emergencia-en-la-mojana-por-fenomeno-de-la-nina-no-esta-siendo-bien-atendida-senadores-1236). b) during El Niño in 2016 (Source: https://www.semana.com/nacion/galeria/fenomeno-de-el-nino-seca-las-cienagas-de-sucre/465892)

spatio-temporal dynamics of total water storage in the MC river basin, in order to assess the variability of continental water storage in regions of hydrogeological interest in Colombia. These results can inform the formulation of better policies and improved management of water resources to ensure future water security. In addition, under the assumption that the data obtained from GRACE adequately represents the hydrological reality of the MC basin in terms of water storage (as shown through the evaluation made in Chapter 2), simulations of the continental water storage obtained from a large set of global hydrological models provided by the EartH2Observe (E2O) research project were compared and evaluated over the MC and selected sub-basins.

Based on the results obtained, the main conclusions of this thesis are the following:

1. This study contributes to the specification of GRACE level-3 products for hydrological applications in the study area. Our analysis indicates that the JPL-Mascon product is the best performing product for the MC basin, demonstrating the ability to use GRACE data to evaluate the dynamics of water storage for this basin. As GRACE can be considered as an independent observation it can serve as the basis for future applications.

2. Significant trends were found in total water storage, groundwater storage and soil moisture, which are mainly due to the ENSO effect. A positive trend was found between 2002 and the end of 2010 and a negative trend after 2010 for the entire basin, as well as for sub-basins such as the Upper Middle Magdalena and Cauca Basins. Due to the relatively short period of record of GRACE, it is, however, not possible to conclude if the negative trend continues and if this is a sign of the impact of climate change. Continuous monitoring of the hydrological and hydrogeological variables, both in situ and through remote sensing is required to determine longer-term trends and the possible measures to ensure the sustainable management of water sources and associated ecosystems in the basin.

3. Trends in water storage are not uniform throughout the MC basin. Spatial variations of trends exhibit a pronounced contrast between the higher and lower parts of the basin; i.e. between the mountainous (predominantly Andean) and flatter (near the Caribbean Sea) parts of the basin. The lower part includes the La Mojana area, which is an area with a large diversity of ecosystems and complex hydrodynamics. This area is characterized by the presence of important wetlands that act as a regulatory system, and serve to both contain floods and ameliorate droughts. The global models evaluated largely fail to capture the floodplains of this wetland system, and

71

therefore do not fully capture the spatial variation of total water storage across the basin. GRACE is shown to be able to identify this spatial variation.

4. The trends found for groundwater storage are probably largely related to shallow aquifers identified for the MC region. These are connected to several wetland systems. The dynamic response of these coupled wetland – aquifer systems to climatic variability is fast.

5. Through validating simulation results from the global hydrological models provided by the E2O project, the error statistics reveal that the variability of GRACE TWS is better captured by the models for the larger basin areas than for the smaller sub-basins. The basin area at which both the lower resolution 0.5 degree WRR1 model datasets and the higher resolution 0.25 degrees model datasets are able to provide better representation of the hydrological behavior is observed to be for areas above around 60,000 km^2, with a significantly poorer performance for smaller catchment sizes.

6. The validation of the global models against GRACE data as an observed dataset shows that the models do not adequately capture the hydrological process in the South of the basin, which corresponds to the area with more complex topography as well as the presence of high montane wetlands (Páramos) that have an important water regulating function.

7. In general, models in the WRR2 dataset exhibit better performance than the WRR1 dataset. The best performing model in this study was found to be the W3RA model at the higher WRR2 resolution. This shows that the continuous improvements in global models, either due to improved resolution of the forcing or due to improved model structure and parameterization, can lead to a better representation of the observed TWS variability.

It should be noted that the trends found in this study; the growing demand for water; and the possible impacts of climate change on alluvial aquifers in Colombia (Bolaños-Chavarría & Betancur-Vargas, 2018), underline the importance of more studies being carried out to support better monitoring of available water resources and development of management plans that ensure water security in the country. The next generation of gravitational field data, which will be at a finer resolution (GRACE-FO), will allow for an improved evaluation of water resources in river basins in the country, as well as a better spatial evaluation

of aquifers. This would otherwise not be possible due to the poor instrumentation of many of the water bodies at national level. In addition, the integration of these tools in (global) hydrological models will improve the understanding of the water cycle, which will lead to a decrease in the uncertainty in the results of these models, thus supporting improved projections of future water security under climate change and socio-economic scenarios.

Appendices

APPENDIX A
CARACTERÍSTICAS GENERALES DE LA MACROCUENCA MAGDALENA-CAUCA

Colombia está localizada en la esquina septentrional de Suramérica y tiene una extensión continental de 1.141.742 km². El territorio nacional está dividido en 5 macrocuencas (Fig. A.1): 1) Caribe, 2) Magdalena-Cauca, 3) Orinoco, 4) Amazonas y 5) Pacífico (IDEAM, 2013b).

La macrocuenca Magdalena-Cauca está enmarcada en el territorio andino que comprende tres Cordilleras: Oriental, Central y Occidental (Fig. A.2). Tiene una orientación Sur Norte y es surcada por los ríos Cauca (entre las Cordilleras Occidental y Central) y Magdalena (entre las Cordilleras Central y Oriental). El río Magdalena tiene una longitud de aproximadamente 1.240 Km, hasta su confluencia con el río Cauca, que recorre 1.350 Km. Desde allí, en la llamada depresión Momposina hasta la desembocadura en el Océano Atlántico hay aproximadamente 300 km más, para una longitud total del río Magdalena de 1.540 Km (IDEAM & CORMAGDALENA, 2001).

En esta macrocuenca habita alrededor del 80% de la población de Colombia (cerca de 35 millones de colombianos). En términos industriales y, específicamente de generación de energía, se encuentra que en esta cuenca y con destino a la interconexión eléctrica nacional, se genera el 95% de la producción termoeléctrica y el 70% de la hidroeléctrica (IDEAM & CORMAGDALENA, 2001).

Dado que la cuenca Magdalena-Cauca está situada en la parte interandina del territorio colombiano, tiene lugares a diferente altura y se presentan diferentes pisos climáticos (CORMAGDALENA, 2007; IDEAM & CORMAGDALENA, 2001). En el norte de la cuenca, los valores mas altos de temperatura media del aire oscilan entre 28 y 32°C. Los valles de los principales ríos, como el Magdalena, el Cauca y el Sogamoso, registran los más altos valores, entre 24 y 28°C, mientras que, en la zona montañosa se presentan valores bajos, entre 12 y 16°C. En las áreas de los nevados y en las regiones de páramo presentan los valores mínimos, inferiores a 4°C. El desplazamiento anual de la Zona de Convergencia Intertropical (ZCTI), que es consecuencia de la traslación de la Tierra alrededor del Sol, marca la distribución de las lluvias sobre el territorio nacional y, naturalmente, sobre la cuenca. Dado que su presencia asegura la lluviosidad en las regiones que cubre, en la
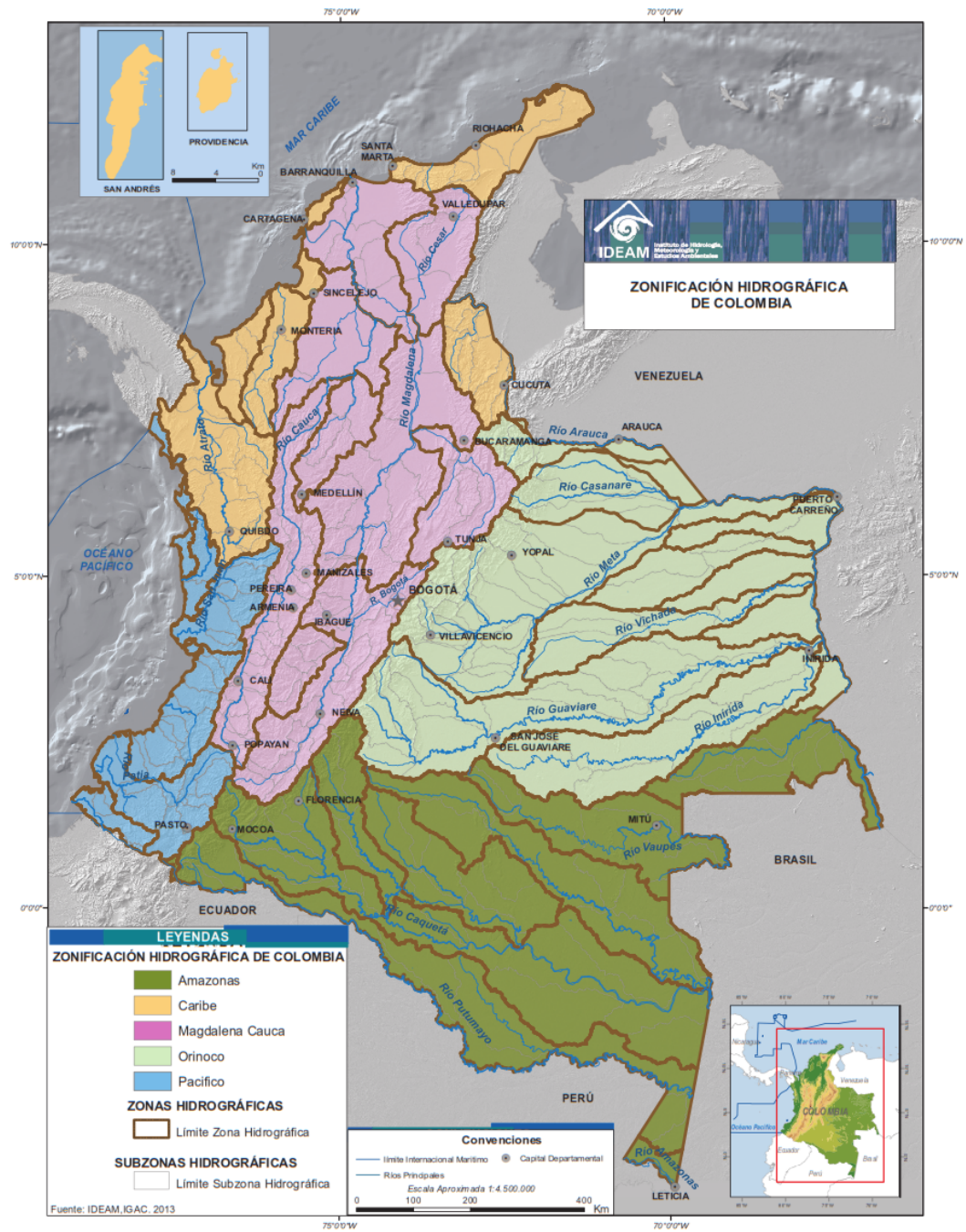
Figure A.1: Mapa con las 5 macrocuencias de Colombia. Tomado de: IDEAM (2013b).
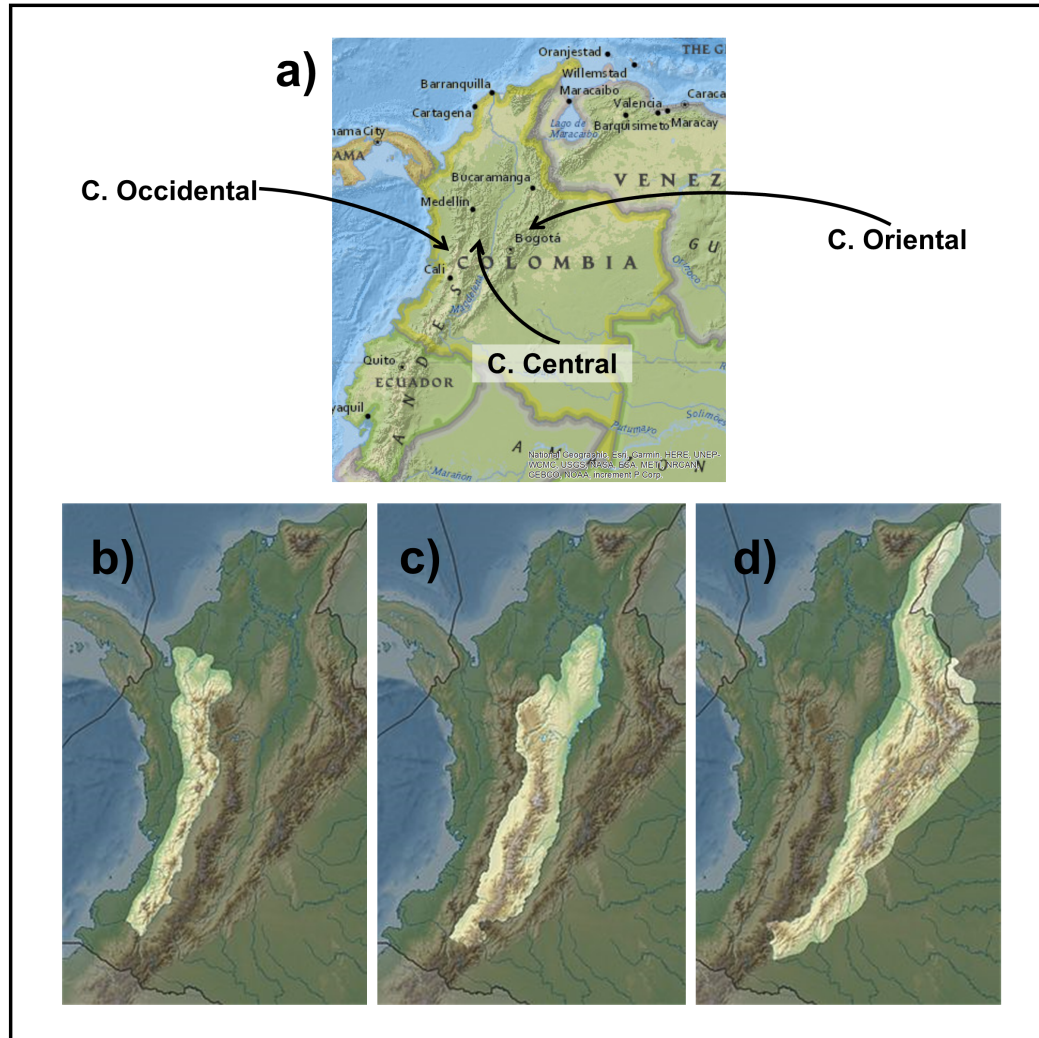
Figure A.2: Mapa físico de Colombia en a), con la cordillera Occidental resaltada en b), cordillera Central resaltada en c) y cordillera Oriental resaltada en d).

cuenca conforma un patrón general anual de precipitaciones caracterizado por dos períodos secos y dos lluviosos. Algunas áreas de la cuenca presentan distribuciones monomodales debido a condiciones locales. La diversidad climática de la cuenca condiciona aspectos de cobertura natural, y junto con la geomorfología y geología condicionan las características de los suelos.

Tres condiciones físicas de la cuenca Magdalena-Cauca, de interes especial para el propósito de la investigación, se resumen a continuación: Suelos, Geología, Hidrogeología.

A.1 Suelos

Sobre las formaciones superficiales se destaca la parte más externa de la corteza terrestre que son los suelos, conformando la base del sustento de la cobertura vegetal, base de los ecosistemas bióticos. Los suelos ofrecen bienes y servicios, donde se producen intercambios y flujos de materia y energía entre los elementos integrantes del ecosistema, y que de la disponibilidad de estos elementos garantiza la sostenibilidad del medio (IDEAM & CORMAGDALENA, 2001).

En relación con la oferta de los suelos, en el Estudio Ambiental de la cuenca Magdalena-Cauca y orientaciones para su ordenamiento territorial (IDEAM & CORMAGDALENA, 2001), se presentan dos aportes (Fig. A.3 y A.4): una aproximación de los suelos de las macrounidades morfogénicas con una evaluación desde lo ecosistémico, lo cual nos da apreciaciones necesarias para evaluar usos alternativos sostenibles de los suelos que deben evaluarse a niveles más detallados. Lo segundo se refiere al ciclo hídrico en el suelo; dentro del ciclo hidrológico, el agua que pasa por los suelos puede infiltrarse, escurrirse, ascender y almacenarse, de acuerdo con las características fisicoquímicas y biológicas; un suelo ofrece capacidades de almacenamiento y regulación del agua.

El conocimiento de esta información es básica para entender la incidencia de la dinámica del agua en la evolución de los suelos y de los ecosistemas, incluyendo los agrosistemas; en la oferta de agua para el hombre y en el desarrollo de sus proyectos, en la determinación del balance hídrico, en la capacidad edáfica como filtro y captador de alterógenos, en la estimación de procesos erosivos y remoción en masa y en la evaluación de los efectos sobre las calidades de los suelos por el incremento de la temperatura y variación de la precipitación, como manifestación del cambio climático o efectos climáticos regionales como el fenómeno Cálido del Pacífico (El Niño) o Frío del Pacífico (La Niña).

También los suelos se presentan como elemento de soporte y de estabilidad de los ecosistemas, y su deterioro afecta el normal funcionamiento de éstos en la cuenca. Por tal razón, el estudio de la degradación de los suelos ofrece unos indicadores de estabilidad del sistema en donde procesos como la erosión, desertificación, compactación suelos y degradación física pueden conducir a un deterioro de los ecosistemas y, por consiguiente, de la cuenca misma.

Dentro de estos procesos, las variaciones dentro de la composición química de los
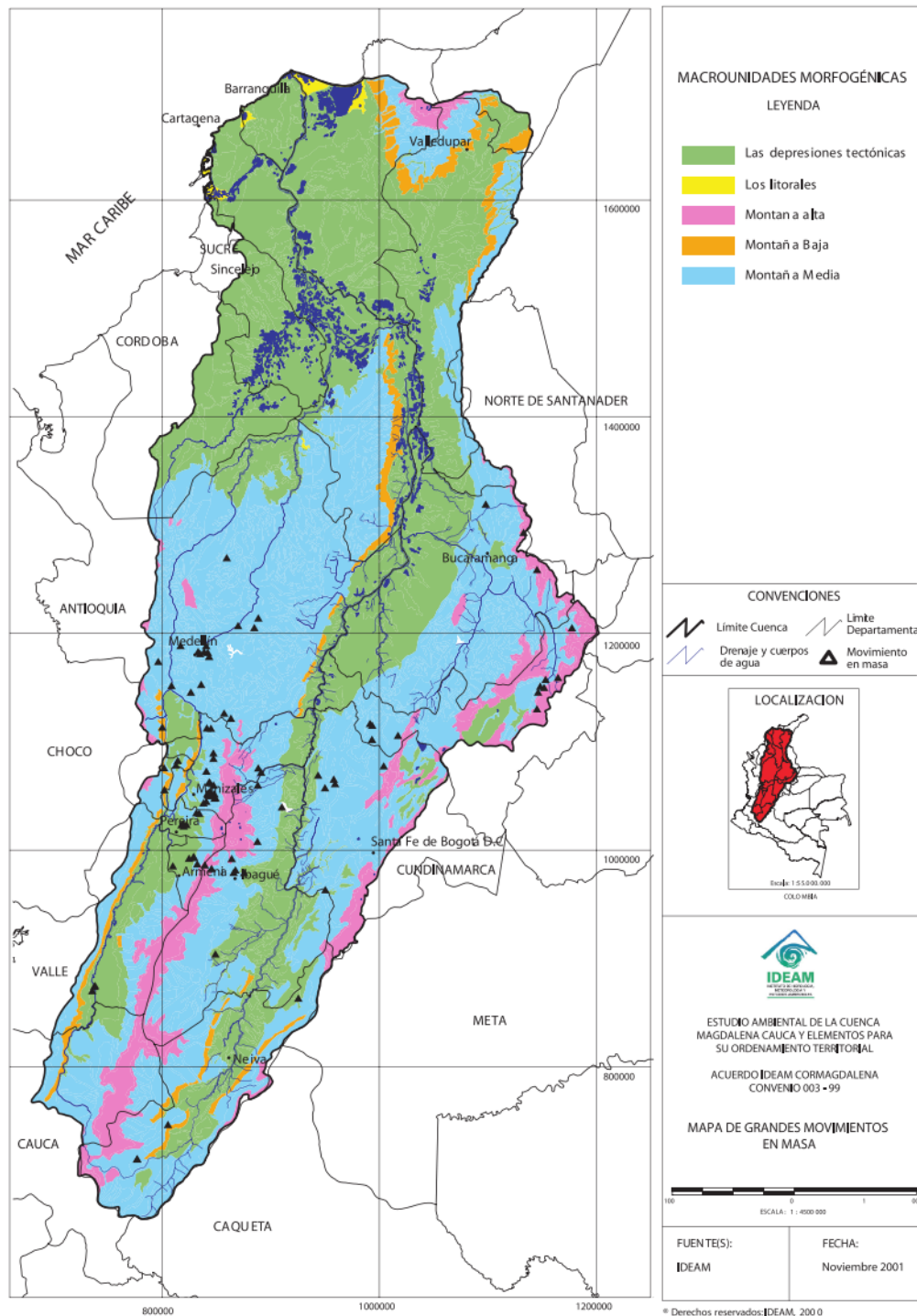
Figure A.3: Macrounidades morfogénicas de la cuenca del río Magdalena-Cauca. Tomado de: (IDEAM & CORMAGDALENA, 2001).
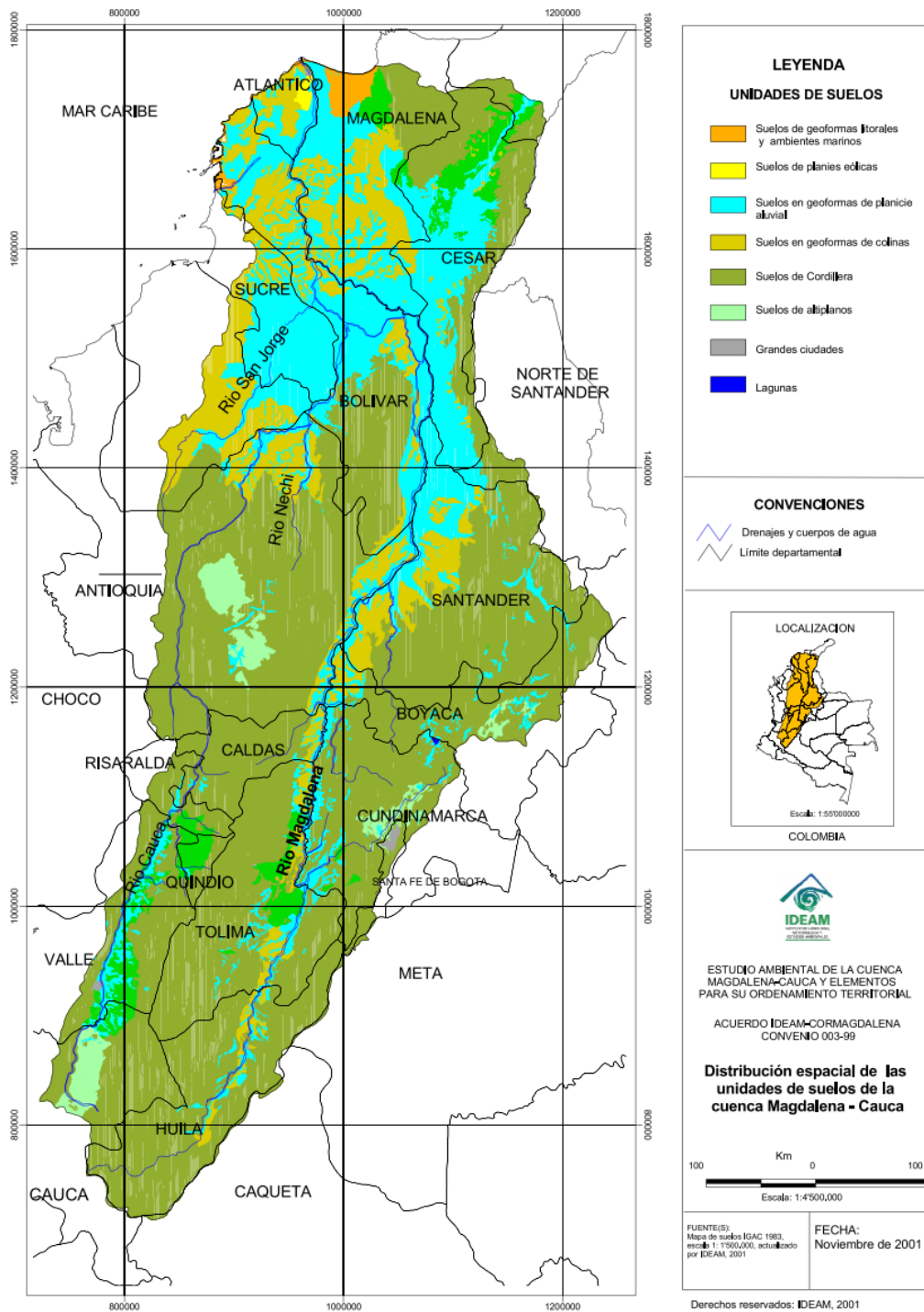
Figure A.4: Unidades de suelos de la cuenca del río Magdalena-Cauca. Tomado de: (IDEAM & CORMAGDALENA, 2001).

suelos, como la contaminación por algunos elementos aplicados como insumos de mejoramiento agrícola, o malos manejos con residuos de metales pesados, se constituyen en una amenaza para la estabilidad química del suelo. En la cuenca, los procesos hidrológicos actúan como catalizadores o aceleradores de la degradación de los suelos, y su estudio genera un entendimiento para la toma de medidas de control de tal degradación (IDEAM & CORMAGDALENA, 2001).

De los resultados de erosión, se puede establecer que el 72% de la cuenca Magdalena-Cauca muestra algún grado de erosión establecido así: 7% erosión muy baja, 20% erosión baja, 16% erosión moderada, 8% erosión alta y 20% erosión muy alta. En general, se puede estimar que la cuenca presenta un grado de degradación moderada por erosión y que se presentan en todos los ecosistemas terrestres. En relación con la desertificación se estableció que en la cuenca 3.145.056 hectáreas, correspondientes al 11.47% del área total, presentan desertificación actual y se encuentra en ecosistemas secos. El 58% del área de la cuenca presenta susceptibilidad muy alta a la compactación y el 27% es de categoría alta y se encuentra en todos los ecosistemas terrestres. La evaluación de la salinización arroja el siguiente resultado: el 21% de la cuenca correspondiente a 5.722.676 hectáreas presentan propensión a la salinización y /o sodificación, en sectores localizados en las llanuras de la región Caribe, en los valles interandinos y en algunos altiplanos Andinos. Es de resaltar su presencia en ecosistemas secos en climas cálidos y fríos, muy relacionados con áreas en desertificación y erosión (IDEAM & CORMAGDALENA, 2001).

A.2 Geología

La cuenca de los ríos Magdalena y Cauca está formada por rocas con edades desde el Precámbrico hasta el Terciario. Estas rocas se presentan cubiertas parcialmente por depósitos no consolidados del Cuaternario. Litológicamente el territorio presenta rocas ígneas, sedimentarias y metamórficas, con una gran variedad de tipos y texturas. En cuanto a la extensión de las unidades geológicas los depósitos no consolidados o formaciones superficiales del Cuaternario cubren un 26% del área de la cuenca; las rocas del Terciario, predominantemente sedimentarias, comprenden el 24%; los cuerpos intrusivos y metamórficos del Cretáceo y el Jurásico tienen una extensión de 18%, cada una; las rocas del Paleozoico cubren un 9% de la extensión de la cuenca y el 5% restante corresponde a rocas más antiguas (Fig. A.5).

A continuación, se presenta una breve descripción de las unidades cronoestratigráficas

por unidades de roca y depósitos no consolidados o formaciones superficiales que se destacan en la cuenca Magdalena - Cauca. También se incluyen los principales rasgos estructurales y la evolución de la cuenca.

A.2.1   Litología

Estudios sobre la geología y evolución del sistema andino en torno a la cuenca Magdalena-Cauca, ha sido abordado por muchos autores, entre ellos se destacan Álvarez (1983), Toussaint and Restrepo (1982), Álvarez, Ordóñez, Martens, and Correa (2009); en relación con las características de la Cordillera Oriental se destacan los estudios de Mojica and Macía (1983).

Cordillera Central

La Cordillera Central que representa un espesor cortical aproximado de 35 km, está compuesta por un núcleo de neises y anfibolitas precámbricas que forman parte del Escudo de Guayana, y una faja geosinclinal pericratónica adosada al mismo, compuesta por metasedimentitas del Paleozoico con facies de esquistos verdes y anfibolita. Secuencias sedimentarias, sedimentario-volcánicas de ambientes marinos neríticos y asociaciones de rocas ofiolíticas del Cretácico, se presentan dispersas principalmente en el sector norte de la Cordillera Central. En este mismo sector aflora un pequeño remanente de sedimentitas marinas neríticas Jurásicas. Asimismo, depósitos marinos de aguas someras intercalados con material volcánico y capas rojas continentales de edad Jura-Triásica, se presentan en el pie oriental de la misma.

Los cuerpos cretáceos carecen de vestigios claros de actividad volcánica asociada. Sin embargo el Cauternario esta marcado por intensa actividad volcánica en esta cordillera.

Cordillera Occidental

En la Cordillera Occidental, toleitas cretácicas con afinidades a las generadas en arcos volcánicos inmaduros se extienden al oeste de la zona de fallas de Romeral, paleozona de sutura a lo largo de la cual se emplazaron durante el Cretáceo ofiolitas no secuenciales y rocas metemórficas. Las rocas de la Cordillera Occidental fueron probablemente deformadas durante el Cretáceo temprano y metamorfizadas y nuevamente deformadas en el Cretáceo tardío, época en la cual la Cordillera emergió definitivamente y fue acrecionada al continente.
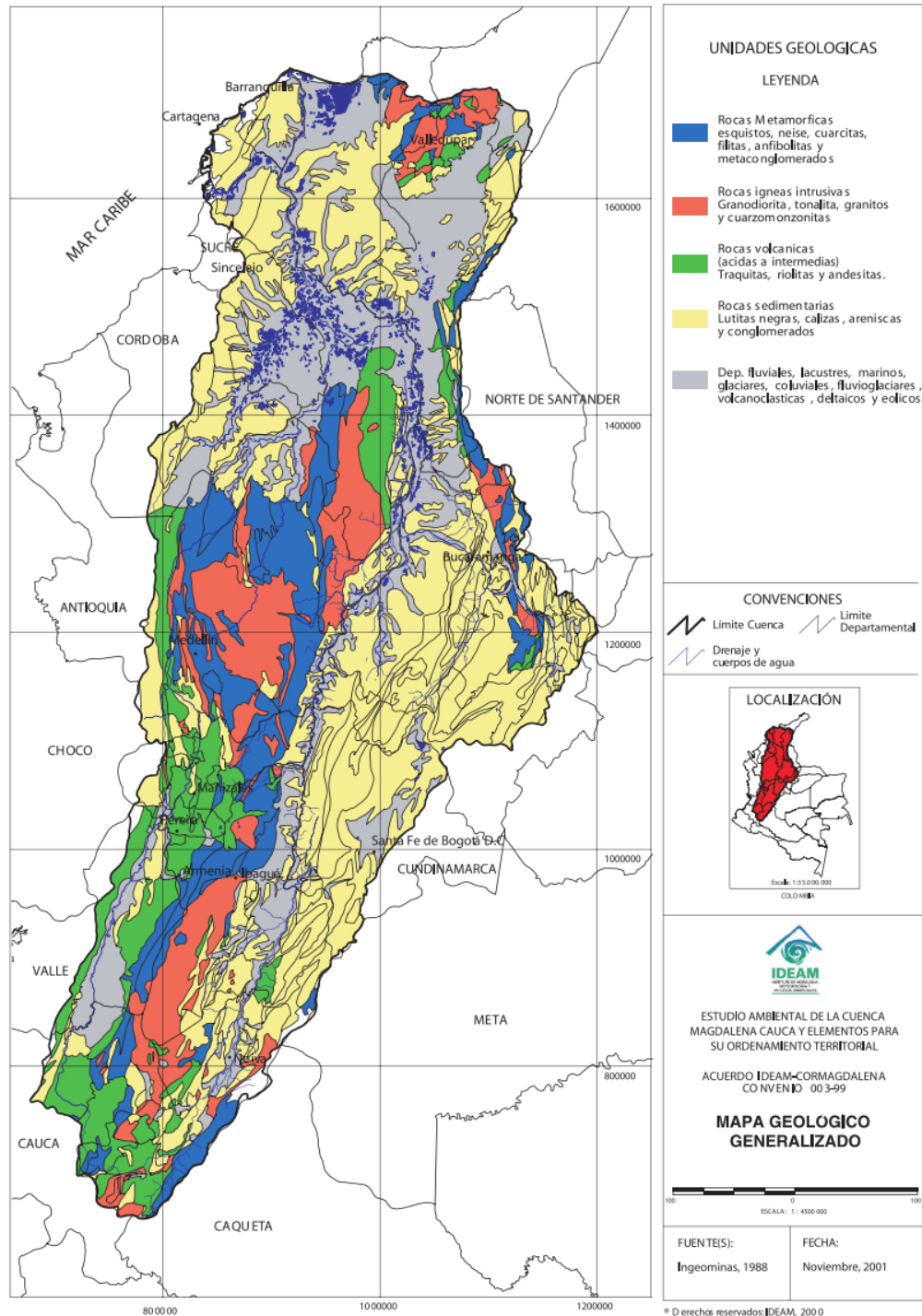
Figure A.5: Unidades geológicas de la cuenca del río Magdalena-Cauca. Tomado de: (IDEAM & CORMAGDALENA, 2001).

Cordillera Oriental

De acuerdo con Mojica and Macía (1983), al Sur del país, antes de que el sistema andino se trifurque dando lugar a la configuración de Los Andes en Colombia, la Cordillera Oriental está constituida sobre un basamento del Precámbrico por rocas ígneas, metamórficas y sedimentarias del Mesozoico y sedimentarias del Terciario. Dentro del domino sedimentario, predominante en la Cordillera Oriental, se intercalan estratos asociados a eventos de transgreción marina con rocas sedimentarias continentales procedentes de la antigua vertiente central. La cordillera Oriental es la cordillera más ancha, sobre ella se emplazan extensas planillanuras. Al norte, en el Páramo de Santurban (departamento de Santander) se bifurca en la Cordillera de Mérida (Venezuela) y la Serránia de Perijá (Colombia).

Depósitos y formaciones superficiales

En la cuenca Magdalena-Cauca los depósitos no consolidados o formaciones superficiales del Cuaternario son las unidades litológicas de mayor extensión y se presentan cubriendo parcialmente rocas más antiguas que se distribuyen como masas discordantes sobre toda la cuenca, particularmente en el valle del río Magdalena y en la parte norte de la cuenca. Los predominantes son los de origen aluvial que se manifiestan en forma de lechos activos, llanuras, deltas, abanicos, terrazas y planicies aluviales. Otros depósitos de origen coluvial, no representativos a escalas regionales por su pequeña dimensión, se presentan sobre las zonas montañosas y de piedemonte de las tres cordilleras. Depósitos de origen glaciar y fluvioglaciar se presentan sobre las laderas altas, generalmente por encima de los 2.500 metros de altura sobre el nivel del mar.

A.2.2   Estructuras

La cuenca Magdalena-Cauca, por constituir gran parte de las cordilleras andinas, presenta una gran distribución y variedad de estructuras geológicas como fallas, pliegues y lineamientos estructurales. La actual configuración es el resultado de la evolución geológica y configuración estructural de sus diferentes sectores. Con el levantamiento final de las cordilleras andinas se formó la cuenca del Magdalena, en el Plio-Pleistoceno. Movimientos en bloques con desplazamientos verticales predominaron, aunque también afectados por fallas transversales, y llevaron a la subdivisión de la cuenca en las subcuencas actuales (IDEAM & CORMAGDALENA, 2001).

En general, los sectores alto, medio y bajo del río Magdalena tienen un rumbo noreste-suroeste, en el cual el modelo de evolución involucra fallamiento que afecta el basamento,

y se originaron estructuras apareadas (sinclinal - anticlinal por doblamiento de un bloque del basamento fallado. La mayoría de fallas que afecta la cuenca, son de sentido longitudinal (sur - norte) y transversal (sureste - noroeste). Las principales fallas son de rumbo, cabalgamiento y transversales y se ubican en los bordes de la cuenca (IDEAM & COR-MAGDALENA, 2001).

A.2.3   Cuenca Magdalena-Cauca y Orogenia Andina

La esquina noroccidental de Suramérica, donde está localizada Colombia, ha experimentado diferentes eventos geológicos que controlan la distribución, génesis, relleno de las cuencas y los límites estructurales de las cuencas sedimentarias. A lo largo del tiempo la Tierra ha sufrido constantes cambios, entre ellos la generación de nuevas estructuras y cadenas montañosas a partir de la deformación por compresión de los sedimentos de una cuenca sedimentaria. Este proceso es lo que se denomina orogenia (Sierra, García, Nieto, & Ortiz, 2013).

Tal y como ilustran Sierra, García, Nieto, and Ortiz (2013), la primera cordillera colombiana que tuvo lugar en el territorio fue la Central, durante el Triásico - Jurásico (225 - 145 Ma). Al tiempo en que Pangea se divide en Laurasia al norte y Gondwana al sur (durante el Triásico Medio), una transgresión marina habría cubierto el oriente de lo que hoy es Colombia. Durante el Jurásico, período de actividad ígnea intrusiva y extrusiva, varias formaciones se generaron. Durante el Cretáceo ocurre una nueva transgresión marina que hace que el mar existente al oriente de la Cordillera Central avance por el sur. Este evento favorece a la deposición de sedimentos marinos. Por otro lado, en el occidente de la Cordillera Central continua la sedimentación hacia el mar.

Durante el Paleoceno y Mioceno los mares se retiran, dando luz a la mayor parte del territorio. Al occidente de la Cordillera Central, se conserva una franja con gruesa sedimentación marina, y el resto del país es continente con extensas zonas pantanosas (mares poco profundos rodeados por montañas) que representan hoy formaciones carboníferas. Un nuevo plegamiento hace desplazar las rocas más rígidas de la Cordillera Central. En este proceso se empieza a dar la elevación de la Cordillera Occidental, luego de que la Oriental ha adquirido ya alguna extensión (Sierra, García, Nieto, & Ortiz, 2013).

Hace aproximadamente un millón de años ocurrió el Pulso Orogénico Andino Tardío con un nuevo levantamiento hasta la altura actual desde donde se reanuda la erosión. En este periodo ocurrió el recubrimiento de extensas regiones por glaciares continentales. Du-

rante este tiempo en la Cordillera Central y al sur de la Cordillera Occidental se genera una intensa actividad volcánica, mucha de la cual continua en la actualidad. Como lo mencionan Sierra, García, Nieto, and Ortiz (2013), la actividad tectónica de los Andes aún no ha cesado. El territorio colombiano sufre los efectos de la colisión y movimiento de tres grandes placas de la corteza terrestre: la de Nazca al occidente, la Placa Suramericana al oriente y la Placa Caribe al norte. En la Figura A.6 se intenta mostrar cortes de las 3 cordilleras por la cuales los ríos Magdalena y Cauca fluyen.

A.3   Hidrogeología

Pese a que en el territorio de Colombia el 75% de su extensión posee condiciones adecuadas para el almacenamiento de agua subterránea, menos del 15% ha sido estudiado, a escalas 1:25:00 o 1:100.000; por esta razón los recursos de las aguas subterráneas del país no han sido cuantificados. Tradicionalmente el agua superficial ha sido considerada como la fuente principal de abastecimiento. Sin embargo, desde hace algunos años se ha empezado a reconocer la importancia actual y futura de las aguas subterráneas, tanto desde el punto de vista de abastecimiento como de sus funciones ecosistémicas. Tomando como referencia el estudio de Aguas Subterráneas: una visión general (IDEAM, 2013a), y la Figura A.7, a continuación se describen brevemente las provincias y sistemas hidrogeológicos identificados en la cuenca Magdalena-Cauca.

A partir del modelo geológico básico, se produce una división del país en provincias hidrogeológicas, que agrupan cuencas geológicas con características litológicas, estructurales y geomorfológicas similares y que, además, presenten un comportamiento hidrogeológico homogéneo reconocible espacialmente. Las provincias están limitadas por barreras impermeables, correspondientes a rasgos estructurales o estratigráficos regionales, y pueden subdividirse, a su vez, en cuencas y subcuencas hidrogeológicas (Sistemas Acuíferos). Hacen parte de la cuenca Magdalena Cauca las provincias: Sinú – San Jacinto (SAC1), Valle Bajo del Magdalena (SAC2), Cesar (SAC4), Valle Medio del Magdalena (SAM1), Valle Alto del Magdalena (SAM2), Valle del Cauca – Patía (SAM3), Cordillera Oriental (SAM4) y los Andes centrales (SAM6).

En la Cordillera Oriental se localizan seis Sistemas Acuíferos montanos e intramontanos siendo los más conocidos los Sistemas Acuíferos de la Sabana de Bogotá (SAM4.6) y Tunja (SAM4.3) que corresponden a acuíferos clásticos desarrollados en rocas sedimenta-
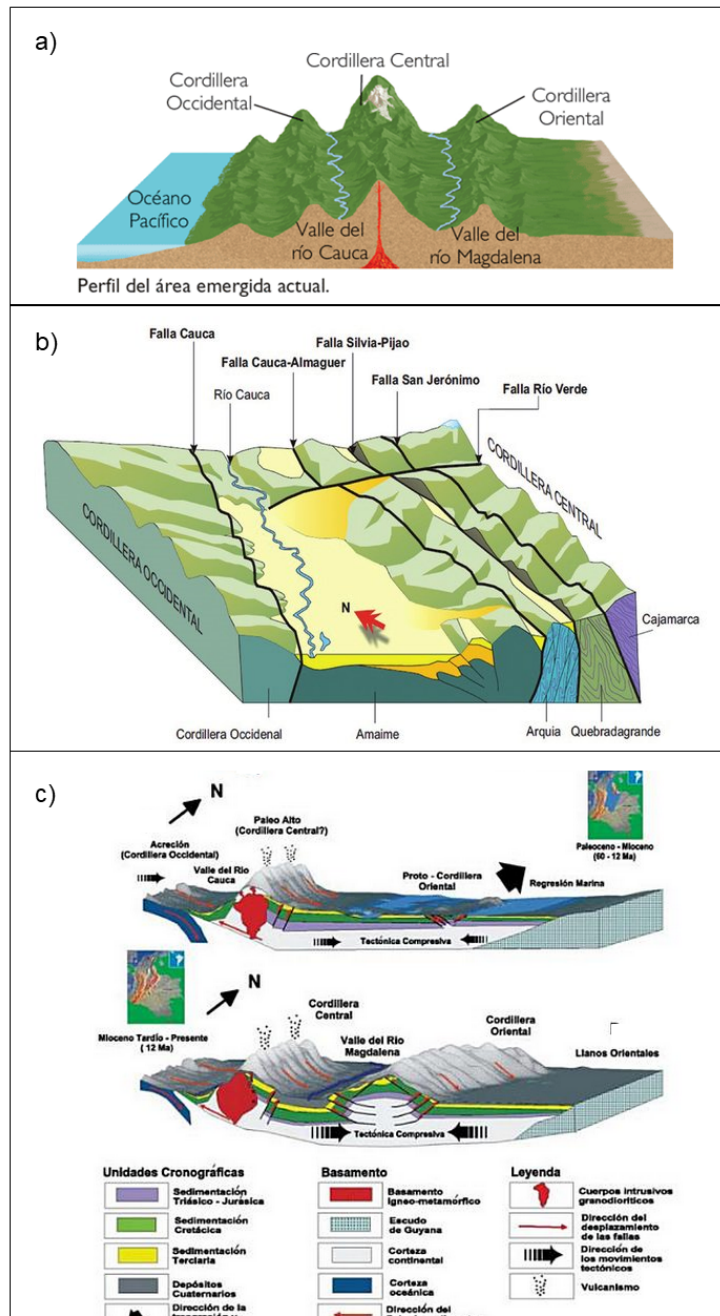
Figure A.6: Corte de las tres cordilleras colombianas. En a): Representación del perfil actual de las cordilleras colombianas (Tomado de: (Carranza Torres, 2016)). En b): Esquema del sistema de fallas en la Cordillera Central: al occidente del río Cauca, la Falla Cauca también conocidacomo Cauca-Patía y al oriente del río Cauca, las fallas Cauca-Almaguer, Silvia-Pijao y San Jerónimo. (Tomado de: (López, 2006)). En c): Esquema de evolución geológica del Magdalena desde el Paleoceno (60 m.a) hasta el presente (Tomado de: (Restrepo Ángel, 2005)).
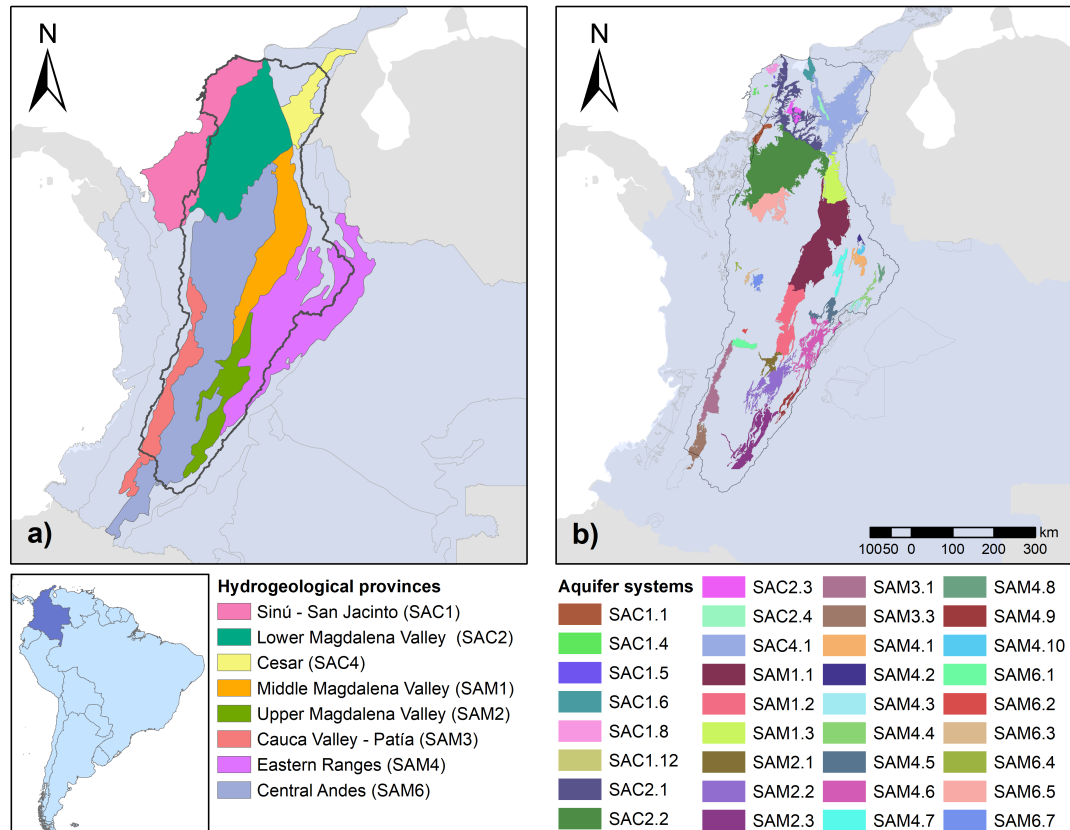
Figure A.7: Hydrogeological provinces and aquifer systems of the Magdalena-Cauca river basin. Source: Estudio Nacional del Agua 2018.

rias con buenas posibilidades en las secuencias cretácicas, Paleógeno-Neógeno y sedimentos recientes del cuaternario. Así mismo, se cuentan con estudios y modelo hidrogeológico conceptual del Sistema Acuífero San Gil-Barichara (SAM4.1) que se desarrolla en ambientes cársticos de rocas carbonatadas cretácicas. En el valle del Cauca se identifica el Sistema Acuífero más conocido del país (SAM3.1) cuya sostenibilidad es estratégica para el desarrollo del Valle del Cauca pues de él depende la agroindustria, principal renglón de la economía de esta región. Este Sistema Acuífero se desarrolla en secuencias de sedimentos clásticos interconectados del valle estructural del río Cauca que son recargados desde la Cordillera Central.

Bajo el Valle Alto del río Magdalena y asociados a depósitos aluviales, terrazas y secuencias sedimentarias silisiclásticas del Paleógeno- Neógeno principalmente se identifican y conocen los Sistemas Acuíferos de Ibagué, Purificación- Saldaña y Neiva-Tatacoa (SAM2.1, SAM2.2, SAM2.3) que se utilizan para agricultura, abastecimiento doméstico e

industria petrolera principalmente. En el Valle Medio del río Magdalena se encuentran los Sistemas Acuíferos de Mariquita-Dorada-Salgar, Nare-Berrio-Yondó y Simití (SAM1.1, SAM1.2, SAM1.3) constituidos por sedimentos aluviales, terrazas y secuencia de areniscas y conglomerados del Paleógeno Neógeno que presentan variaciones de facies y poca continuidad lateral. Estos Sistemas Acuíferos se utilizan para actividades agropecuarias, uso doméstico y desarrollos de hidrocarburos.

En la región Andina, dentro de la cuenca Magdalena-Cauca se reconocen adicionalmente Sistemas Acuíferos que no están asociados a las Provincias Hidrogeológicas por constituir coberteras que suprayacen ambientes ígneos y metamórficos de las Cordilleras Central y Occidental. El Sistema Acuífero del Glacis del Quindío se ubica en el piedemonte de la Cordillera Central en vecindades de los departamentos de Quindío y Risaralda. Este Sistema Acuífero (SAM6.1) se desarrolla a partir de secuencias de flujos de piroclastos y lavas que provienen de la actividad volcánica de la Cordillera Central y depósitos aluviales que conforman acuíferos discontinuos de moderada productividad los cuales son usados en la región para fines recreativos, abastecimiento público y doméstico y la agricultura. De características similares es el Sistema Acuífero de Santagueda que es aprovechado para satisfacer necesidades recreativas y que está constituido por sedimentos recientes y del Paleógeno–Neógeno conformando acuíferos de poca continuidad y rápidos cambios laterales de facies litológicas. En ambientes restringidos y suprayaciendo rocas cristalinas se reconocen los Sistemas Acuíferos del Bajo Cauca antioqueño y Santa Fé de Antioquia (SAM6.5 y SAM 6.4) que se desarrollan en depósitos aluviales principalmente. Restringido al Valle de Aburrá se encuentra el Sistema Acuífero del Valle de Aburrá (SAM6.3) que es aprovechado en vecindades de Medellín para uso doméstico e industrial principalmente y en el Valle de San Nicolás, el acuífero del Valle de San Nicolás y la Unión (SAM6.7).

En la cuenca Magdalena-Cauca también se identifican Acuíferos asociados a Provincias Hidrogeológicas Costeras, por ejemplo los Sistemas Acuíferos de Morroa, Turbaco, Sabanalarga, el Sistema acuífero asociado a la Mojana, y el Cesar (SAC1.1, SAC1.4, SAC1.5, SAC 2.2, SAC4.1) que explotan secuencias detríticas cuaternarias y del Paleógeno Neógeno que suprayacen espesas secuencias de rocas sedimentarias cretácicas que conforman el subsuelo de la costa Caribe y el valle inferior del Magdalena. El Sistema Acuífero del Valle del Río Cesar (SAC4.1) está conformado por los depósitos aluviales del río Cesar y secuencias detríticas del Paleógeno-Neógeno. Se trata de una estructura alargada restringida al valle del río Cesar donde se aprovecha el agua subterránea para uso doméstico, agropecuario y en la explotación del carbón a cielo abierto por mediana y gran minería.

APPENDIX B

SUPPORTING INFORMATION FOR CHAPTER 2: "SPATIAL AND TEMPORAL SHIFTS OF TOTAL WATER STORAGE FIELDS IN A MEDIUM-SIZE TROPICAL BASIN INFERRED FROM GRACE DATA"

Contents of this file

1. Figure B.1. Monthly anomalies of TWS and their corresponding trends at the MC basin as a whole and its major sub-basins.

2. Figure B.2. Seasonal maps for GRACE mean, GRACE JPL mascon and GRACE CSR mascon anomalies

3. Figure B.3. Map of statistically significant (p<0.05) trends in TWS_{GLDAS} anomalies.

4. Figure B.4. Map of statistically significant (p<0.05) trends in GWS anomalies.
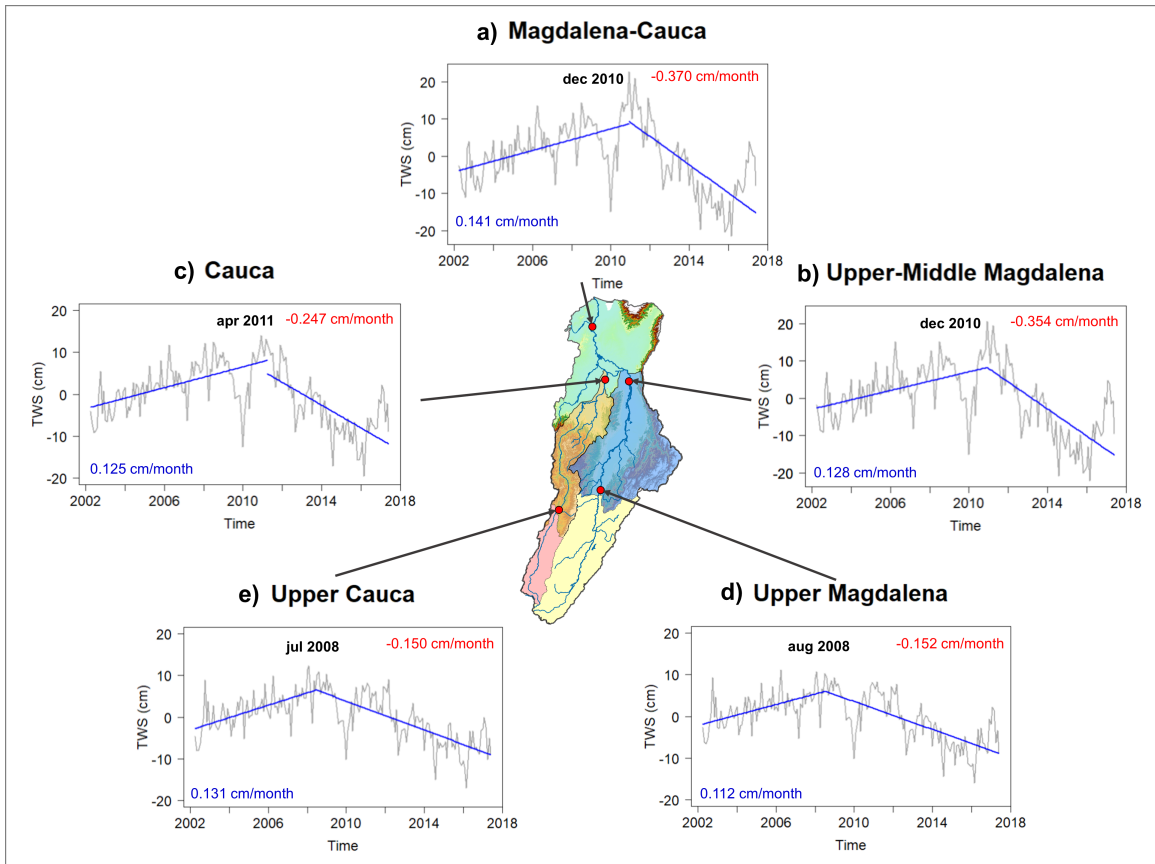
Figure B.1: Monthly anomalies of TWS (grey line) and their corresponding trends (solid blue lines) at the MC basin as a whole and its major sub-basins. Seasonality is removed from data. Only statistically significant trends ($p < 0.05$) are plotted.
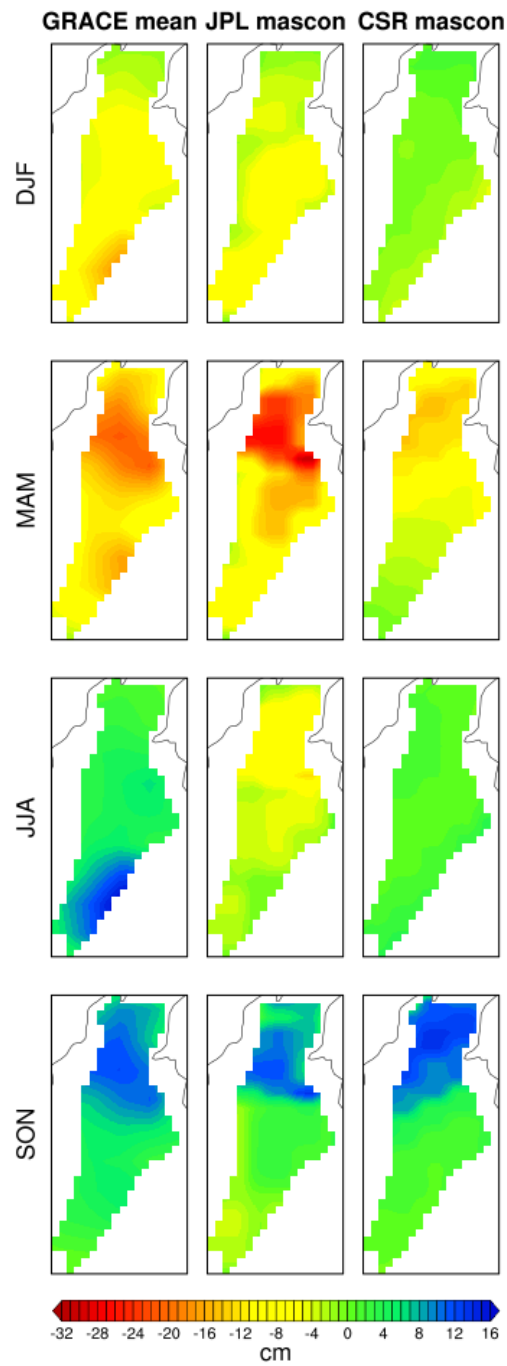
Figure B.2: Seasonal maps for GRACE mean, GRACE JPL mascon and GRACE CSR mascon anomalies.
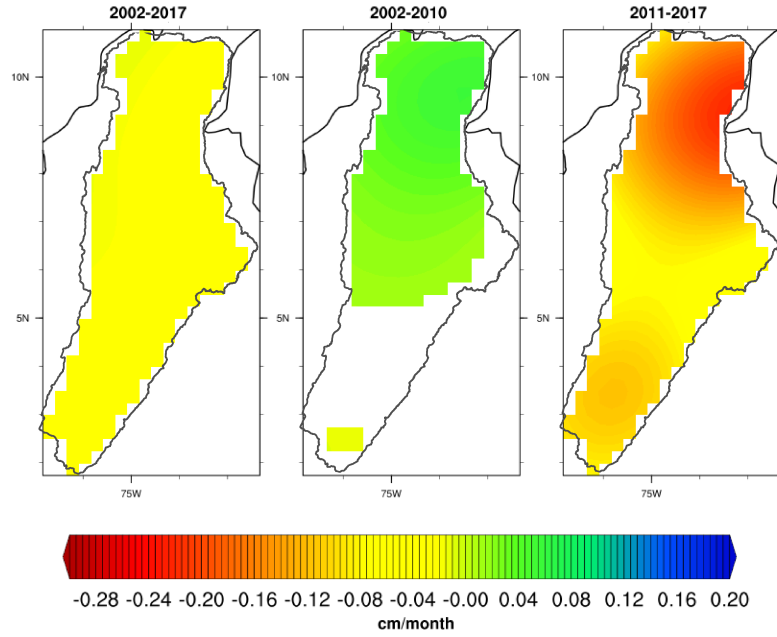
Figure B.3: Map of statistically significant (p<0.05) trends in TWS_{GLDAS} anomalies.
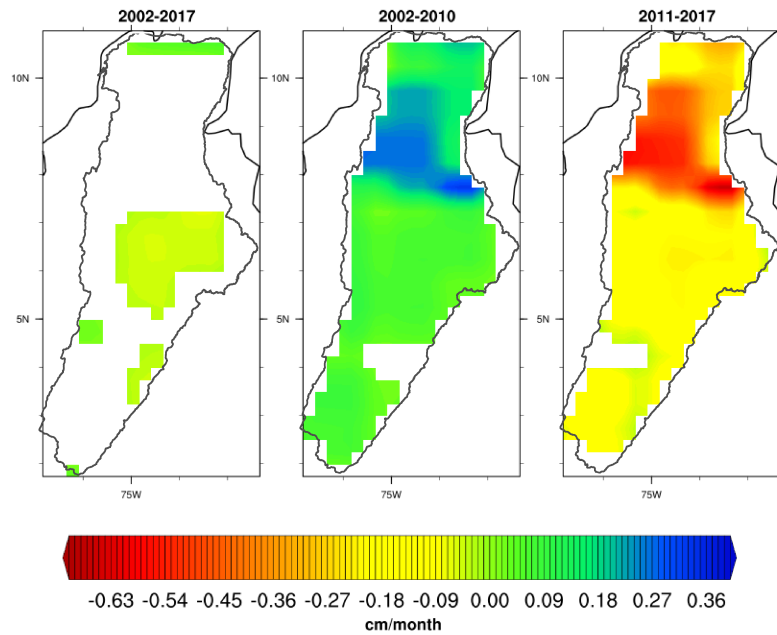
Figure B.4: Map of statistically significant (p<0.05) trends in GWS anomalies.

APPENDIX C

SUPPORTING INFORMATION FOR CHAPTER 3: "COMPARATIVE ASSESSMENT OF GLOBAL MODELS IN REPRESENTING GRACE IN A MEDIUM-SIZE TROPICAL BASIN"

Contents of this file

1. Figure C.1. Hydrographic zoning of the Magdalena-Cauca basin. The annual precipitation cycle is shown for each zone. Source: (Zapata, 2019).

2. Figure C.2. RSR between GRACE and the GHMs (blue and yellow points for WRR1 and WRR2 respectively) and LSMs (yellow and green points for WRR1 and WRR2) at different scales. In a) for the monthly series, b) for the seasonality, and c) for the long-term trends. The basins are organized from major to minor area, and the data is standardized and normalized.

3. Figure C.3. Seasonal maps for GRACE JPL and each GHM WRR1 and WRR2.

4. Figure C.4. Seasonal maps for GRACE JPL and each LSM WRR1 and WRR2.

5. Figure C.5. Long-term trends time series for the models and GRACE for a) UMM, b) UC and c) UMP basins. The black line indicates the GRACE JPL, the blue and red lines the GHMs WRR1 and WRR2 respectively, the yellow lines the LSM WRR1 and the green lines LSM WRR2.
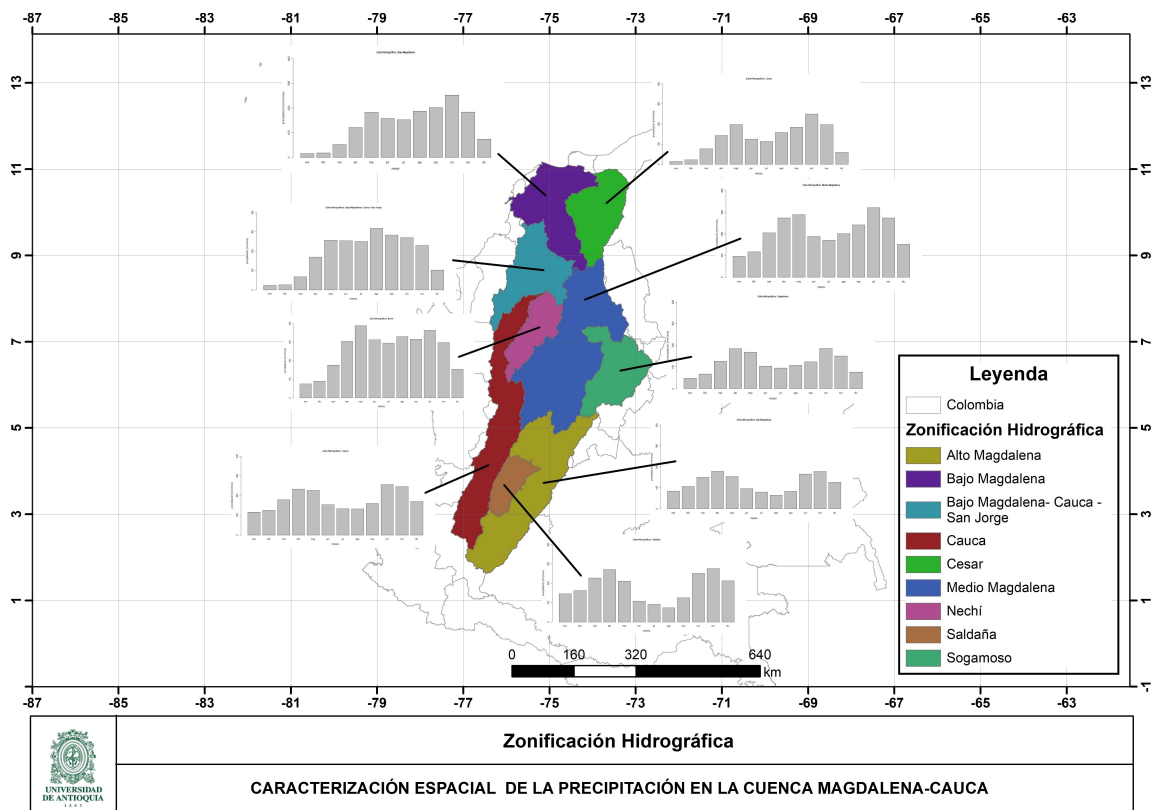
Figure C.1: Hydrographic zoning of the Magdalena-Cauca basin. The annual precipitation cycle is shown for each zone. Source: (Zapata, 2019).
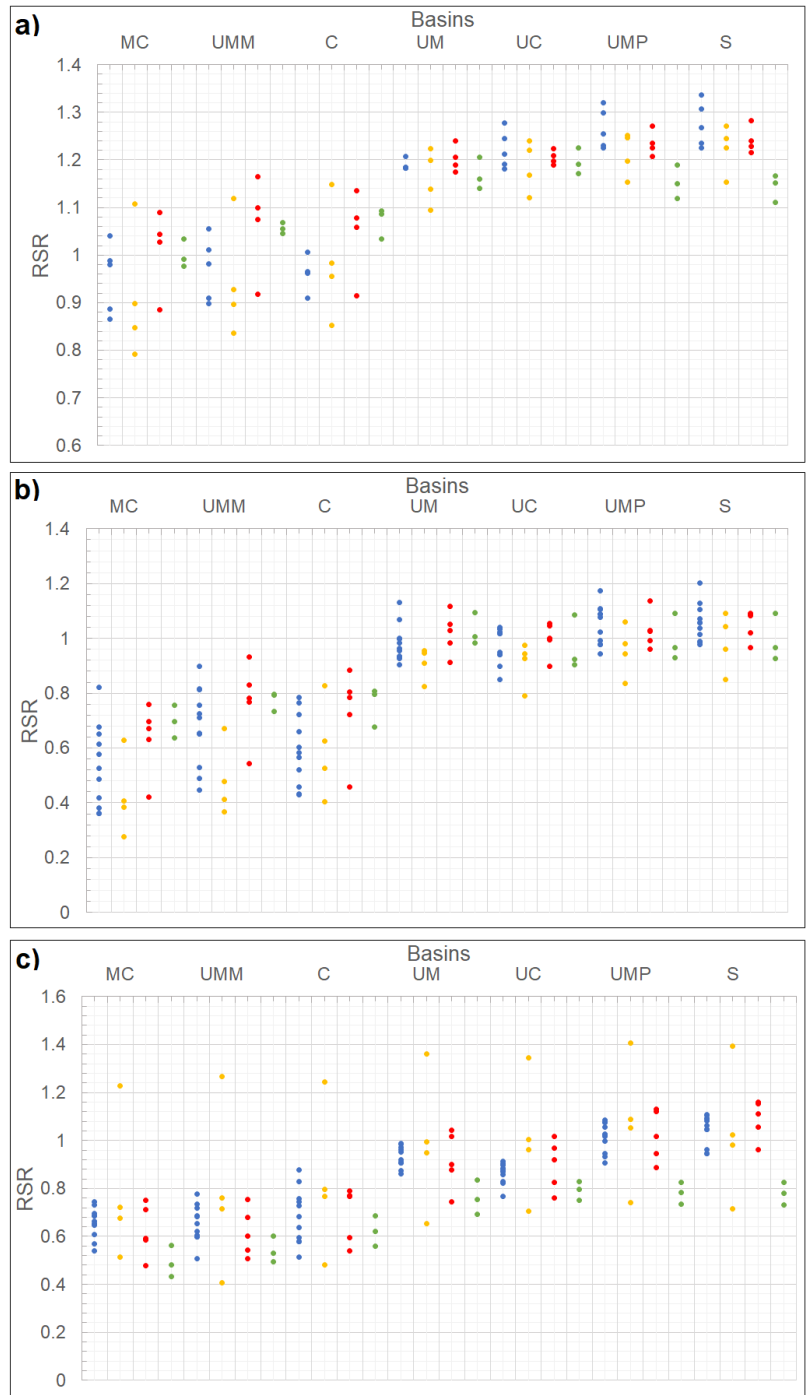
Figure C.2: RSR between GRACE and the GHMs (blue and yellow points for WRR1 and WRR2 respectively) and LSMs (yellow and green points for WRR1 and WRR2) at different scales. In a) for the monthly series, b) for the seasonality, and c) for the long-term trends. The basins are organized from major to minor area, and the data is standardized and normalized.
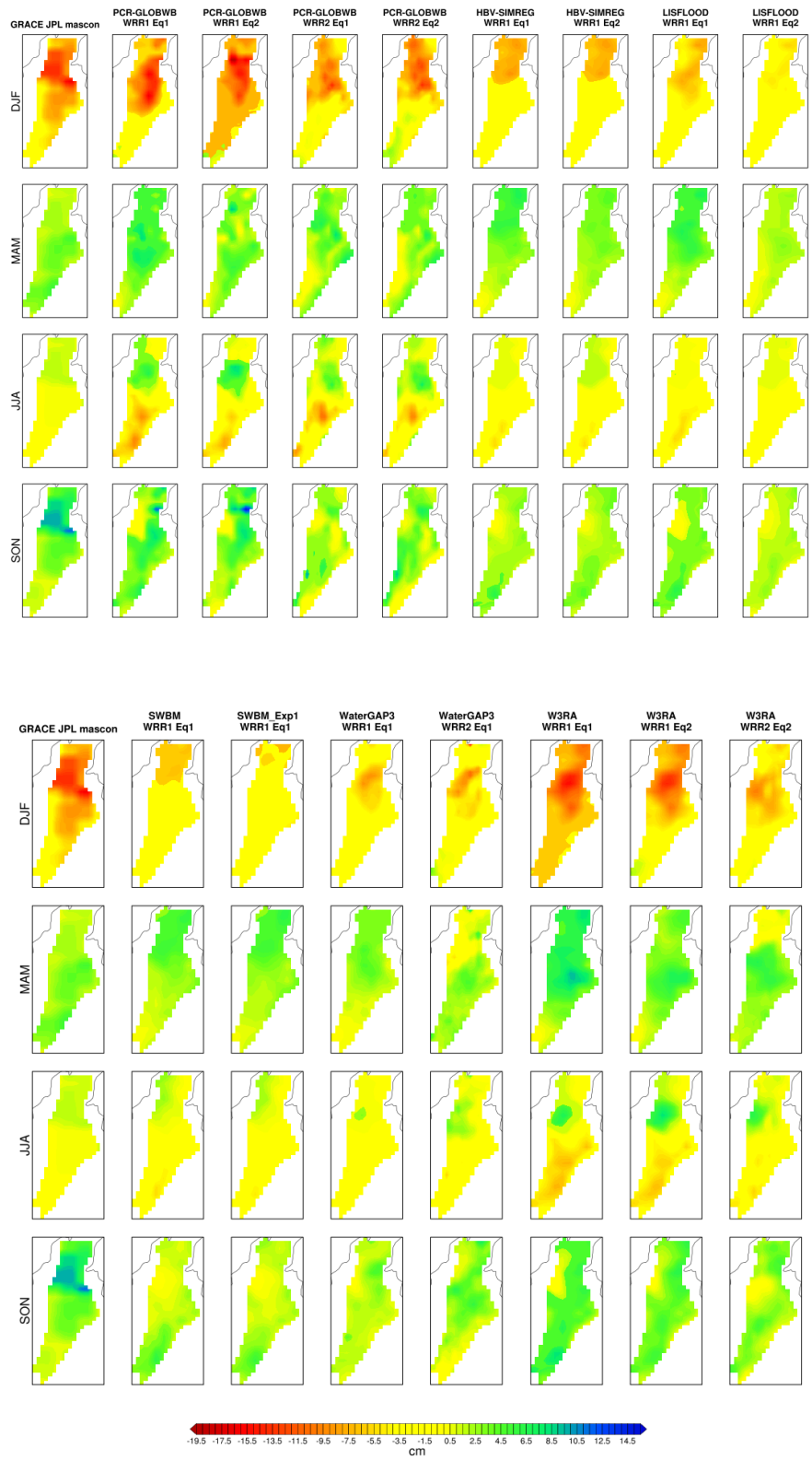
Figure C.3: Seasonal maps for GRACE JPL and each GHM WRR1 and WRR2.
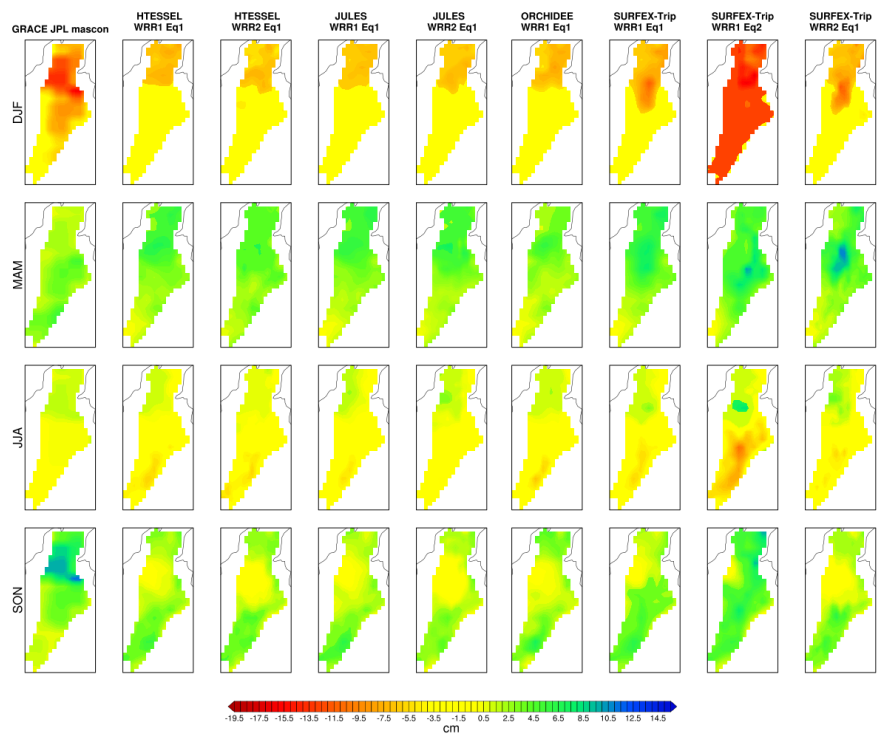
Figure C.4: Seasonal maps for GRACE JPL and each LSM WRR1 and WRR2.
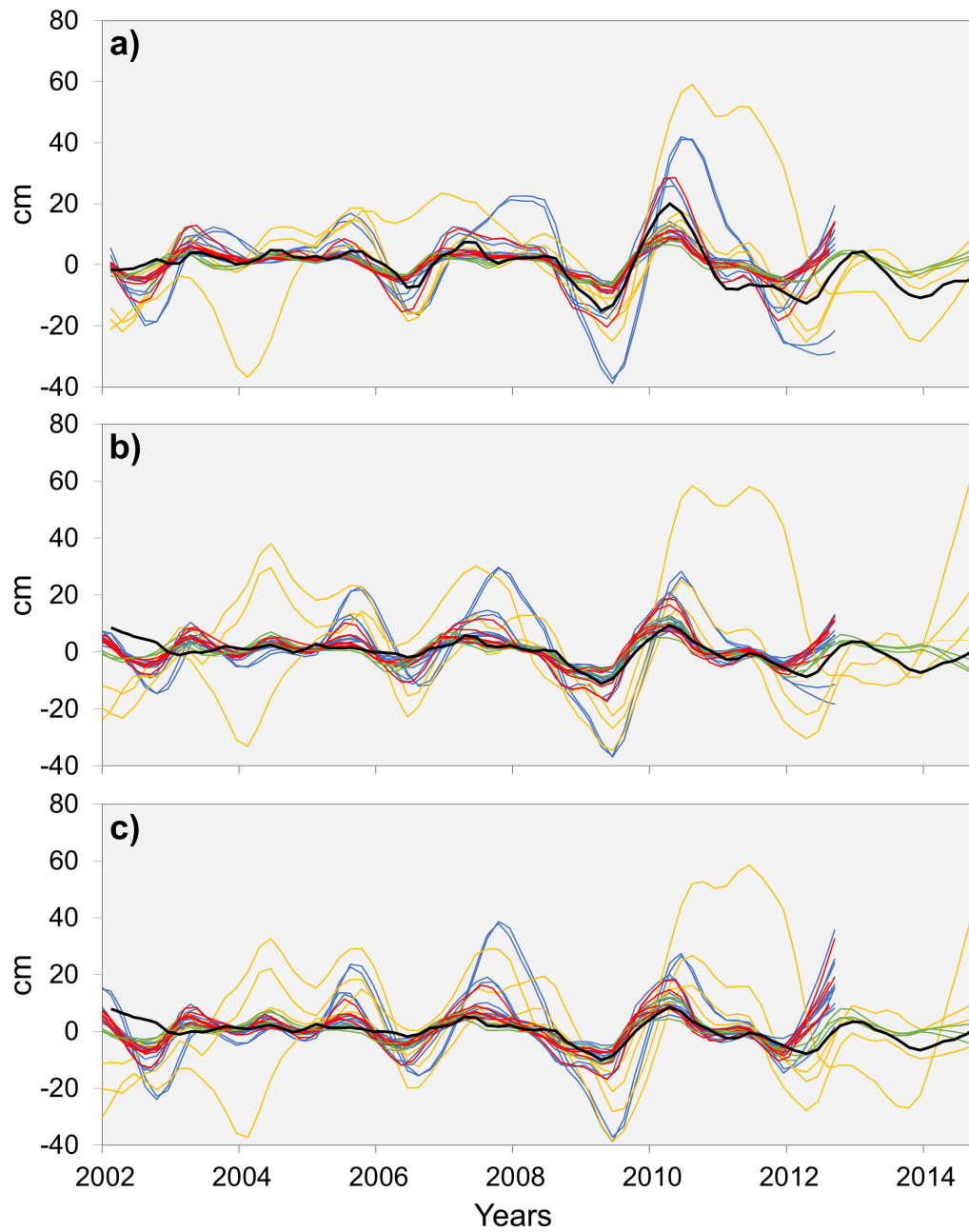
Figure C.5: Long-term trends time series for the models and GRACE for a) UMM, b) UC and c) UMP basins. The black line indicates the GRACE JPL, the blue and red lines the GHMs WRR1 and WRR2 respectively, the yellow lines the LSM WRR1 and the green lines LSM WRR2.

REFERENCES

Abiy, A. Z., & Melesse, A. M. (2017). Evaluation of watershed scale changes in ground-water and soil moisture storage with the application of grace satellite imagery data. *Catena*, *153*, 50–60.

Alley, W. M., & Konikow, L. F. (2015). Bringing grace down to earth. *Groundwater*, *53*(6), 826–829.

Álvarez, A. J. (1983). Geologıa de la cordillera central y el occidente colombiano y petroquımica de los intrusivos granitoides mesocenozóicos. *Boletın Geológico*, *26*(2), 1–175.

Álvarez, J. J., Ordóñez, O., Martens, U. C., & Correa, A. M. (2009). Terrenos, complejos y provincias en la cordillera central de colombia. *Ingenierıa Investigación y Desarrollo: I2+ D*, *9*(2), 49–56.

Anaya-Acevedo, J. A., Escobar-Martínez, J. F., Massone, H., Booman, G., Quiroz-Londoño, O. M., Cañón-Barriga, C. C., . . . Palomino-Ángel, S. (2017). Identification of wetland areas in the context of agricultural development using remote sensing and gis. *Dyna*, *84*(201), 186–194.

Angarita, H., Wickel, A. J., Sieber, J., Chavarro, J., Maldonado-Ocampo, J. A., Herrera-R, G. A., . . . Purkey, D. (2018). Basin-scale impacts of hydropower development on the mompós depression wetlands, colombia. *Hydrology and Earth System Sciences*, *22*(5), 2839.

Arduini, G., Fink, G., Martinez de la Torre, A., Nikolopoulos, E., Anagnostou, E., Balsamo, G., & Boussetta, S. (2017). End-user- focused improvements and descriptions of the advances introduced between the wrr tier1 and wrr tier2. Tech. rep., eartH2Observe.

Arnesen, A. S., Silva, T. S., Hess, L. L., Novo, E. M., Rudorff, C. M., Chapman, B. D., & McDonald, K. C. (2013). Monitoring flood extent in the lower amazon river floodplain using alos/palsar scansar images. *Remote Sensing of Environment*, *130*, 51–61.

Awange, J., Forootan, E., Kuhn, M., Kusche, J., & Heck, B. (2014). Water storage changes and climate variability within the nile basin between 2002 and 2011. *Advances in water resources*, *73*, 1–15.

Bastidas, B., Betancur, T., & Martinez, J. A. (2019). Spatial distribution of precipitation and evapotranspiration estimates from worldclim and chelsa datasets: Improving long-term water balance at the watershed-scale in the urabá region of colombia. *International Journal of Sustainable Development and Planning*, *14*(2), 105–117.

Beck, H. E., Van Dijk, A. I., Levizzani, V., Schellekens, J., Gonzalez Miralles, D., Martens, B., & De Roo, A. (2017). Mswep: 3-hourly 0.25 global gridded precipitation (1979-2015) by merging gauge, satellite, and reanalysis data. *Hydrology and Earth System Sciences*, *21*(1), 589–615.

Becker, M., LLovel, W., Cazenave, A., Güntner, A., & Crétaux, J.-F. (2010). Recent hydrological behavior of the east african great lakes region inferred from grace, satellite altimetry and rainfall observations. *Comptes Rendus Geoscience*, *342*(3), 223–233.

Bedoya-Soto, J. M., Poveda, G., Trenberth, K. E., & Vélez-Upegui, J. J. (2019). Interannual hydroclimatic variability and the 2009–2011 extreme enso phases in colombia: From andean glaciers to caribbean lowlands. *Theoretical and Applied Climatology*, *135*(3-4), 1531–1544.

Betancur-Vargas, T., García-Giraldo, D. A., Vélez-Duque, A. J., Gómez, A. M., Flórez-Ayala, C., Patiño, J., & Ortíz-Tamayo, J. Á. (2017). Aguas subterráneas, humedales y servicios ecosistémicos en colombia. *Biota Colombiana*, *18*(1).

Billah, M. M., Goodall, J. L., Narayan, U., Reager, J., Lakshmi, V., & Famiglietti, J. S. (2015). A methodology for evaluating evapotranspiration estimates at the watershed-scale using grace. *Journal of Hydrology*, *523*, 574–586.

Bolaños-Chavarría, S., & Betancur-Vargas, T. (2018). Estado del arte sobre el cambio climático y las aguas subterráneas. ejemplos en colombia. *Revista Politécnica*, *14*(26), 52–64.

Bradley, R. S., Vuille, M., Diaz, H. F., & Vergara, W. (2006). Threats to water supplies in the tropical andes. *Science*, *312*(5781), 1755–1756.

Buytaert, W., Cuesta-Camacho, F., & Tobón, C. (2011). Potential impacts of climate change on the environmental services of humid tropical alpine regions. *Global Ecology and Biogeography*, *20*(1), 19–33.

Buytaert, W., & De Bièvre, B. (2012). Water for cities: The impact of climate change and demographic growth in the tropical andes. *Water Resources Research*, *48*(8).

Cai, W., Borlace, S., Lengaigne, M., Van Rensch, P., Collins, M., Vecchi, G., . . . Wu, L. et al. (2014). Increasing frequency of extreme El Niño events due to greenhouse warming. *Nature climate change*, *4*(2), 111–116.

Cai, W., Santoso, A., Wang, G., Yeh, S.-W., An, S.-I., Cobb, K. M., . . . Kug, J.-S. et al. (2015). ENSO and greenhouse warming. *Nature Climate Change*, *5*(9), 849–859.

Camacho, L., Rodríguez, E., & Pinilla, G. (2008). Modelación dinámica integrada de cantidad y calidad del agua del canal del dique y su sistema lagunar, colombia. In *Xxiii latinamerican congress on hydraulic (iarh)*.

Carmona, A. M., & Poveda, G. [Germán]. (2014). Detection of long-term trends in monthly hydro-climatic series of colombia through empirical mode decomposition. *Climatic Change*, *123*(2), 301–313.

Carranza Torres, L. F. (2016). Colombia y su biodiversidad. Available in http://linacarranza14.blogspot.com/2016/03/cordilleras-colombia-posee-tres.html. Retrieved 4 June 2020.

Casson, D. R., Werner, M., Weerts, A., & Solomatine, D. (2018). Global re-analysis datasets to improve hydrological assessment and snow water equivalent estimation in a sub-arctic watershed. *Hydrology and Earth System Sciences*, *22*(9), 4685–4697.

Chen, J. [JL], Famigliett, J. S., Scanlon, B. R., & Rodell, M. (2016). Groundwater storage changes: Present status from grace observations. In *Remote sensing and water resources* (pp. 207–227). Springer.

Chen, J. [JL], Wilson, C. R. [Clark R], & Tapley, B. D. [Byron D]. (2010). The 2009 exceptional amazon flood and interannual terrestrial water storage change observed by grace. *Water Resources Research*, *46*(12).

Chen, J. [JL], Wilson, C. R. [Clark R], Tapley, B. D. [Byron D], Scanlon, B., & Güntner, A. (2016). Long-term groundwater storage change in victoria, australia from satellite gravity and in situ observations. *Global and Planetary change*, *139*, 56–65.

Chen, J. [JL], Wilson, C., Tapley, B., Blankenship, D., & Ivins, E. (2007). Patagonia icefield melting observed by gravity recovery and climate experiment (grace). *Geophysical Research Letters*, *34*(22).

Chen, J. [JL], Wilson, C., Tapley, B., Yang, Z., & Niu, G. (2009). 2005 drought event in the amazon river basin as measured by grace and estimated by climate models. *Journal of Geophysical Research: Solid Earth*, *114*(B5).

Cleveland, R. B., Cleveland, W. S., McRae, J. E., & Terpenning, I. (1990). Stl: A seasonal-trend decomposition. *Journal of official statistics*, *6*(1), 3–73.

Clifton, C., Evans, R., Hayes, S., Hirji, R., Puz, G., & Pizarro, C. (2010). Water and climate change: Impacts on groundwater resources and adaptation options. World Bank.

CORMAGDALENA. (2007). *Atlas cuenca del río grande de la magdalena*. Corporación Autónoma Regional del Río Grande de la Magdalena, Barrancabermeja.

Dabrowska-Zielinska, K., Budzynska, M., Tomaszewska, M., Bartold, M., Gatkowska, M., Malek, I., . . . Napiorkowska, M. (2014). Monitoring wetlands ecosystems using alos palsar (l-band, hv) supplemented by optical data: A case study of biebrza wetlands in northeast poland. *Remote Sensing*, *6*(2), 1605–1633.

Dee, D. P., Uppala, S., Simmons, A., Berrisford, P., Poli, P., Kobayashi, S., . . . Bauer, d. P. et al. (2011). The era-interim reanalysis: Configuration and performance of the data assimilation system. *Quarterly Journal of the royal meteorological society*, *137*(656), 553–597.

Deus, D. (2016). Integration of alos palsar and landsat data for land cover and forest mapping in northern tanzania. *Land*, *5*(4), 43.

Döll, P. [Petra], Hoffmann-Dobrev, H., Portmann, F. T., Siebert, S., Eicker, A., Rodell, M., . . . Scanlon, B. R. (2012). Impact of water withdrawals from groundwater and surface water on continental water storage variations. *Journal of Geodynamics*, *59*, 143–156.

Duque-Villegas, M., Salazar, J. F., & Rendón, A. M. (2019). Tipping the enso into a permanent el niño can trigger state transitions in global terrestrial ecosystems. *Earth System Dynamics*, *10*(4), 631–650.

Dutra, E., Balsamo, G., Calvet, J., Minvielle, M., Eisner, S., Fink, G., . . . van Dijk, A. [AI] et al. (2015). Report on the current state-of-the-art water resources reanalysis. Tech. Rep. D. 5.1, eartH2Observe.

Dutra, E., Balsamo, G., Calvet, J., Munier, S., Burke, S., Fink, G., . . . de Roo, A. et al. (2017). Report on the improved water resources reanalysis (wrr2). *EartH2Observe, Report*, (5.2), 94.

Ek, M., Mitchell, K., Lin, Y., Grunmann, P., Rogers, E., Gayno, G., . . . Tarpley, J. (2003). Implementation of the upgraded noah land-surface model in the ncep operational mesoscale eta model. *J. Geophys. Res*, *108*(8851), 530–543.

Eom, J., Seo, K.-W., & Ryu, D. (2017). Estimation of amazon river discharge based on eof analysis of grace gravity data. *Remote sensing of environment*, *191*, 55–66.

Escobar Martínez, J. F. (2011). *Plataforma SIG para el modelamiento de sistemas acuíferos en medios tropicales* (Doctoral dissertation, Universidad de Antioquia).

Etter, A., McAlpine, C., & Possingham, H. (2008). Historical patterns and drivers of landscape change in colombia since 1500: A regionalized spatial approach. *Annals of the Association of American Geographers*, *98*(1), 2–23.

Famiglietti, J. (2004). Remote sensing of terrestrial water storage, soil moisture and surface waters. *Washington DC American Geophysical Union Geophysical Monograph Series*, *150*, 197–207.

Famiglietti, J. S. (2014). The global groundwater crisis. *Nature Climate Change*, *4*(11), 945.

Famiglietti, J. S., Lo, M. [Minhui], Ho, S. L., Bethune, J., Anderson, K., Syed, T. H., . . . Rodell, M. (2011). Satellites measure recent rates of groundwater depletion in california's central valley. *Geophysical Research Letters*, *38*(3).

Famiglietti, J. S., & Rodell, M. [Matthew]. (2013). Water in the balance. *Science*, *340*(6138), 1300–1301.

Fatolazadeh, F., Voosoghi, B., & Naeeni, M. R. (2016). Wavelet and gaussian approaches for estimation of groundwater variations using grace data. *Groundwater*, *54*(1), 74–81.

Feng, W., Zhong, M., Lemoine, J.-M., Biancale, R., Hsu, H.-T., & Xia, J. (2013). Evaluation of groundwater depletion in north china using the gravity recovery and climate experiment (grace) data and ground-based measurements. *Water Resources Research*, *49*(4), 2110–2118.

Frappart, F., Ramillien, G., & Famiglietti, J. S. (2011). Water balance of the arctic drainage system using grace gravimetry products. *International journal of remote sensing*, *32*(2), 431–453.

García-Giraldo, D., Betancur-Vargas, T., & Villegas, J. C. (2018). Expandiendo el concepto de ecosistema en sistemas acuífero-humedal: Modelo de funcionamiento hidrológico. In *El agua subterránea: Recurso sin fronteras: Humedales vinculados al agua subterránea* (pp. 221–227). Editorial de la Universidad Nacional de Salta.

Gleeson, T., & Cardiff, M. (2013). The return of groundwater quantity: a mega-scale and interdisciplinary "future of hydrogeology"? *Hydrogeology Journal*, *21*(6), 1169–1171.

Green, T. R., Taniguchi, M., Kooi, H., Gurdak, J. J., Allen, D. M., Hiscock, K. M., . . . Aureli, A. (2011). Beneath the surface of global change: Impacts of climate change on groundwater. *Journal of Hydrology*, *405*(3-4), 532–560.

Grings, F., Salvia, M., Karszenbaum, H., Ferrazzoli, P., Kandus, P., & Perna, P. (2009). Exploring the capacity of radar remote sensing to estimate wetland marshes water storage. *Journal of environmental management*, *90*(7), 2189–2198.

Gründemann, G. J., Werner, M., & Veldkamp, T. I. (2018). The potential of global re-analysis datasets in identifying flood events in southern africa. *Hydrology and Earth System Sciences*, *22*(9), 4667–4683.

Guarín Giraldo, G. W., & Poveda, G. [Germán]. (2013). Variabilidad espacial y temporal del almacenamiento de agua en el suelo en colombia. *Revista de la Academia Colombiana de Ciencias Exactas, Físicas y Naturales*, *37*(142), 89–113.

Gudmundsson, L., Wagener, T., Tallaksen, L., & Engeland, K. (2012). Evaluation of nine large-scale hydrological models with respect to the seasonal runoff climatology in europe. *Water Resources Research*, *48*(11).

Gupta, H. V., Kling, H., Yilmaz, K. K., & Martinez, G. F. (2009). Decomposition of the mean squared error and nse performance criteria: Implications for improving hydrological modelling. *Journal of hydrology*, *377*(1-2), 80–91.

Hachborn, E., Berg, A., Levison, J., & Ambadan, J. T. (2017). Sensitivity of grace-derived estimates of groundwater-level changes in southern ontario, canada. *Hydrogeology Journal*, *25*(8), 2391–2402.

Han, S.-C., Kim, H., Yeo, I.-Y., Yeh, P., Oki, T., Seo, K.-W., . . . Luthcke, S. B. (2009). Dynamics of surface water storage in the amazon inferred from measurements of inter-satellite distance change. *Geophysical Research Letters*, *36*(9).

Harris, I., & Jones, P. (2017). Cru ts3.24: Climatic research unit (cru) time-series (ts) version 3.24 of high resolution gridded data of month-by-month variation in climate (jan. 1901–dec. 2015). *Centre for Environmental Data Analysis*.

Hassan, A., & Jin, S. (2016). Water storage changes and balances in africa observed by grace and hydrologic models. *Geodesy and Geodynamics*, *7*(1), 39–49.

Hoffmann, J. (2005). The future of satellite remote sensing in hydrogeology. *Hydrogeology Journal*, *13*(1), 247–250.

Hoyos, N., Correa-Metrio, A., Sisa, A., Ramos-Fabiel, M., Espinosa, J., Restrepo, J., & Escobar, J. (2017). The environmental envelope of fires in the colombian caribbean. *Applied geography*, *84*, 42–54.

Hoyos, N., Escobar, J., Restrepo, J., Arango, A., & Ortiz, J. (2013). Impact of the 2010–2011 la niña phenomenon in colombia, south america: The human toll of an extreme weather event. *Applied Geography*, *39*, 16–25.

Huang, J., Pavlic, G., Rivera, A., Palombi, D., & Smerdon, B. (2016). Mapping groundwater storage variations with grace: A case study in alberta, canada. *Hydrogeology Journal*, *24*(7), 1663–1680.

Huang, Y., Salama, M., Krol, M. S., Van Der Velde, R., Hoekstra, A. Y., Zhou, Y., & Su, Z. (2013). Analysis of long-term terrestrial water storage variations in the yangtze river basin. *Hydrology and earth system sciences*, *17*(5), 1985.

Huffman, G. J., Bolvin, D. T., Nelkin, E. J., Wolff, D. B., Adler, R. F., Gu, G., ... Stocker, E. F. (2007). The trmm multisatellite precipitation analysis (tmpa): Quasi-global, multiyear, combined-sensor precipitation estimates at fine scales. *Journal of hydrometeorology*, *8*(1), 38–55.

IDEAM. (2013a). *Aguas subterráneas en colombia: Una visión general.* Bogotá DC.

IDEAM. (2013b). *Zonificación y codificación de unidades hidrográficas e hidrogeológicas de colombia*. IDEAM Bogotá DC.

IDEAM. (2015). *Estudio nacional del agua 2014*. IDEAM Bogotá DC.

IDEAM. (2019). *Estudio nacional del agua 2018*. IDEAM Bogotá DC.

IDEAM, & CORMAGDALENA. (2001). *Estudio Ambiental de la Cuenca Magdalena - Cauca y Elementos para su Ordenamiento Territorial - Resumen Ejecutivo*. Bogotá D. C.

IDEAM, PNUD, MADS, DNP, & CANCILLERÍA. (2015). *Nuevos escenarios de cambio climático para colombia 2011-2100 herramientas científicas para la toma de decisiones–enfoque nacional-regional: Tercera comunicación nacional de cambio climático*. Bogotá DC: IDEAM.

Jaramillo Villa, Ú., Flórez-Ayala, C., Cortés-Duque, J., Cadena-Marín, E. A., Estupiñán-Suárez, L. M., Rojas, S., ... Aponte, C. et al. (2016). Colombia anfibia. un país de humedales. volumen i.

Jaramillo-Mejía, M. C., & Chernichovsky, D. (2019). Impact of desertification and land degradation on colombian children. *International journal of public health*, *64*(1), 67–73.

Jiang, D., Wang, J., Huang, Y., Zhou, K., Ding, X., & Fu, J. (2014). The review of grace data applications in terrestrial hydrology monitoring. *Advances in Meteorology*, *2014*.

Josse, C., Cuesta, F., Navarro, G., Barrena, V., Becerra, M. T., Cabrera, E., ... Saito, J. et al. (2011). Physical geography and ecosystems in the tropical andes. *SK Herzog, R. Martínez, PM Jørgensen y H. Tiessen (comps.), Climate Change and Biodiversity in the Tropical Andes. São José dos Campos y París: Instituto Interamericano para la Investigación del Cambio Global y Comité Científico sobre Problemas del Medio Ambiente*.

Kim, J.-W., Lu, Z., Lee, H., Shum, C., Swarzenski, C. M., Doyle, T. W., & Baek, S.-H. (2009). Integrated analysis of palsar/radarsat-1 insar and envisat altimeter data for mapping of absolute water level changes in louisiana wetlands. *Remote Sensing of Environment*, *113*(11), 2356–2365.

Kleidon, A., Renner, M., & Porada, P. (2014). Estimates of the climatological land surface energy and water balance derived from maximum convective power. *Hydrology and Earth System Sciences*, *18*, 2201–2218.

Landerer, F. W., & Swenson, S. [SC]. (2012). Accuracy of scaled grace terrestrial water storage estimates. *Water resources research*, *48*(4).

Lee, H., Beighley, R. E., Alsdorf, D., Jung, H. C., Shum, C., Duan, J., . . . Andreadis, K. (2011). Characterization of terrestrial water dynamics in the congo basin using grace and satellite radar altimetry. *Remote Sensing of Environment*, *115*(12), 3530–3538.

Lettenmaier, D. P., & Famiglietti, J. S. (2006). Hydrology: Water from on high. *Nature*, *444*(7119), 562.

Li, J. [Jin], Chen, J., Ni, S., Tang, L., & Hu, X. (2019). Long-term and inter-annual mass changes of patagonia ice field from grace. *Geodesy and Geodynamics*, *10*(2), 100–109.

Liesch, T., & Ohmer, M. (2016). Comparison of grace data and groundwater levels for the assessment of groundwater depletion in jordan. *Hydrogeology Journal*, *24*(6), 1547–1563.

Liesenberg, V., Galvão, L. S., & Ponzoni, F. J. (2007). Variations in reflectance with seasonality and viewing geometry: Implications for classification of brazilian savanna physiognomies with misr/terra data. *Remote Sensing of Environment*, *107*(1-2), 276–286.

Long, D. [Di], Chen, X., Scanlon, B. R., Wada, Y., Hong, Y., Singh, V. P., . . . Yang, W. (2016). Have grace satellites overestimated groundwater depletion in the northwest india aquifer? *Scientific reports*, *6*, 24398.

Long, D. [Di], Longuevergne, L., & Scanlon, B. R. (2015). Global analysis of approaches for deriving total water storage changes from grace satellites. *Water Resources Research*, *51*(4), 2574–2594.

Long, D. [Di], Pan, Y., Zhou, J., Chen, Y., Hou, X., Hong, Y., . . . Longuevergne, L. (2017). Global analysis of spatiotemporal variability in merged total water storage changes using multiple grace products and global hydrological models. *Remote sensing of environment*, *192*, 198–216.

Long, D. [Di], Scanlon, B. R., Longuevergne, L., Sun, A. Y., Fernando, D. N., & Save, H. (2013). Grace satellite monitoring of large depletion in water storage in response to the 2011 drought in texas. *Geophysical Research Letters*, *40*(13), 3395–3401.

Long, D. [Di], Shen, Y., Sun, A., Hong, Y., Longuevergne, L., Yang, Y., . . . Chen, L. (2014). Drought and flood monitoring for a large karst plateau in southwest china using extended grace data. *Remote Sensing of Environment*, *155*, 145–160.

López López, P., Immerzeel, W. W., Rodríguez Sandoval, E. A., Sterk, G., & Schellekens, J. (2018). Spatial downscaling of satellite-based precipitation and its impact on discharge simulations in the magdalena river basin in colombia. *Frontiers in Earth Science*, *6*.

López, M. (2006). Análisis de deformación tectónica en los pie de montes de las cordilleras central y occidental, valle del cauca, colombia-contribuciones paleosısmicas. *Universidad Eafit, Medellın, Colombia*.

Lv, M., Ma, Z., Yuan, X., Lv, M., Li, M., & Zheng, Z. (2017). Water budget closure based on grace measurements and reconstructed evapotranspiration using gldas and water use data for two large densely-populated mid-latitude basins. *Journal of hydrology*, *547*, 585–599.

Magrin, G., Marengo, J., Boulanger, J.-P., Buckeridge, M., Castellanos, E., Poveda, G., . . . Vicuña, S. (2014). Regional aspects: Central and south america. In *Climate change 2014: Impacts, adaptation, and vulnerability, contribution of working group ii to the fifth assessment report of the intergovernmental panel on climate change, volume ii*. Cambridge University Press.

Martens, B., Gonzalez Miralles, D., Lievens, H., Van Der Schalie, R., De Jeu, R. A., Fernández-Prieto, D., . . . Verhoest, N. (2017). Gleam v3: Satellite-based land evaporation and root-zone soil moisture. *Geoscientific Model Development*, *10*(5), 1903–1925.

Martínez, R., Zambrano, E., Nieto, J. J., Hernández, J., & Costa, F. (2017). Evolución, vulnerabilidad e impactos económicos y sociales de el niño 2015-2016 en américa latina. *Investigaciones geográficas*, (68), 65–78.

Miralles, D., Holmes, T., De Jeu, R., Gash, J., Meesters, A., Dolman, A. et al. (2011). Global land-surface evaporation estimated from satellite-based observations.

Moiwo, J. P., Lu, W., & Tao, F. (2012). Grace, gldas and measured groundwater data products show water storage loss in western jilin, china. *Water Science and Technology*, *65*(9), 1606–1614.

Mojica, J., & Macía, C. (1983). Breve síntesis sobre el estado actual del conocimiento del jurásico en colombia. manuscrito presentado a la iv reunión del igco, durante la 10a. conferencia deolóica del caribe, 24p. cartagena. Manuscrito presentado a la IV Reunión del IGCO, durante la 10a. Conferencia deolóica del Caribe, 24p. Cartagena.

Montanari, A., Young, G., Savenije, H., Hughes, D., Wagener, T., Ren, L., . . . Grimaldi, S. et al. (2013). "panta rhei—everything flows": Change in hydrology and society—the iahs scientific decade 2013–2022. *Hydrological Sciences Journal*, *58*(6), 1256–1275.

Moriasi, D. N., Arnold, J. G., Van Liew, M. W., Bingner, R. L., Harmel, R. D., & Veith, T. L. (2007). Model evaluation guidelines for systematic quantification of accuracy in watershed simulations. *Transactions of the ASABE*, *50*(3), 885–900.

Muggeo, V. M. et al. (2008). Segmented: An r package to fit regression models with broken-line relationships. *R news*, *8*(1), 20–25.

Nanteza, J., de Linage, C., Thomas, B., & Famiglietti, J. (2016). Monitoring groundwater storage changes in complex basement aquifers: An evaluation of the grace satellites over e ast a frica. *Water Resources Research*, *52*(12), 9542–9564.

Nardini, A., & Franco Idarraga, F. (2016). A qualitative hydro-geomorphic prediction of the destiny of the mojana region (magdalena-cauca basin, colombia), to inform large scale decision making. *Resources*, *5*(3), 22.

Ni, S., Chen, J., Wilson, C. R., Li, J., Hu, X., & Fu, R. (2018). Global terrestrial water storage changes and connections to enso events. *Surveys in Geophysics*, *39*(1), 1–22.

Ning, S., Ishidaira, H., & Wang, J. (2014). Statistical downscaling of grace-derived terrestrial water storage using satellite and gldas products. *B1 ()*, *70*(4), I_133–I_138.

O'Loughlin, F., Neal, J. C., Schumann, G., Beighley, E., & Bates, P. D. (2018). Inundation extents and volumes of the congo's wetlands. In *Agu fall meeting abstracts*.

Ortiz, M. A. D., González, J. D. N., & López, T. S. (2005). Páramos: Hidrosistemas sensibles. *Revista de ingeniería*, (22), 64–75.

Ospina M, D. L., & Vargas J, C. A. (2018). Monitoring runoff coefficients and groundwater levels using data from grace, gldas, and hydrometeorological stations: Analysis of a colombian foreland basin. *Hydrogeology Journal*.

Ouma, Y. O., Aballa, D., Marinda, D., Tateishi, R., & Hahn, M. (2015). Use of grace time-variable data and gldas-lsm for estimating groundwater storage variability at small basin scales: A case study of the nzoia river basin. *International Journal of Remote Sensing*, *36*(22), 5707–5736.

Pabón Caicedo, J. D. (2012). Cambio climático en colombia: Tendencias en la segunda mitad del siglo xx y escenarios posibles para el siglo xxi. *Revista de la Academia Colombiana de Ciencias Exactas, Físicas y Naturales*, *36*(139), 261–278.

Palomino-Ángel, S., Anaya-Acevedo, J. A., Simard, M., Liao, T.-H., & Jaramillo, F. (2019). Analysis of floodplain dynamics in the atrato river colombia using sar interferometry. *Water*, *11*(5), 875.

Papa, F., Frappart, F., Malbeteau, Y., Shamsudduha, M. [Mohammad], Vuruputur, V., Sekhar, M., ... Pandey, R. K. et al. (2015). Satellite-derived surface and sub-surface water storage in the ganges–brahmaputra river basin. *Journal of Hydrology: Regional Studies*, *4*, 15–35.

Phillips, T., Nerem, R., Fox-Kemper, B., Famiglietti, J., & Rajagopalan, B. (2012). The influence of enso on global terrestrial water storage using grace. *Geophysical Research Letters*, *39*(16).

Pope, K. O., Rejmankova, E., Paris, J. F., & Woodruff, R. (1997). Detecting seasonal flooding cycles in marshes of the yucatan peninsula with sir-c polarimetric radar imagery. *Remote Sensing of environment*, *59*(2), 157–166.

Poveda, G., & Mesa, O. (1996). Extreme phases of the enso phenomenon(el nino and la nina) and its effects on the hydrology of colombia. *ING. HIDRAL. MEXICO*, *11*(1), 21–37.

Poveda, G., & Pineda, K. (2009). Reassessment of colombia's tropical glaciers retreat rates: Are they bound to disappear during the 2010–2020 decade? *Advances in Geosciences*, *22*, 107–116.

Poveda, G. [Germán]. (2004). La hidroclimatología de colombia: Una síntesis desde la escala inter-decadal hasta la escala diurna. *Rev. Acad. Colomb. Cienc*, *28*(107), 201–222.

Rabatel, A., Francou, B., Soruco, A., Gomez, J., Cáceres, B., Ceballos, J. L., ... Wagnon, P. (2013). Current state of glaciers in the tropical andes: A multi-century perspective on glacier evolution and climate change. *The Cryosphere*, *7*(1), 81–102.

Ramillien, G., Frappart, F., Güntner, A., Ngo-Duc, T., Cazenave, A., & Laval, K. (2006). Time variations of the regional evapotranspiration rate from gravity recovery and climate experiment (grace) satellite gravimetry. *Water resources research*, *42*(10).

Rangel-Ch, J. O. (2015). La biodiversidad de colombia: Significado y distribución regional. *Revista de la Academia Colombiana de Ciencias Exactas, Físicas y Naturales*, *39*(151), 176–200.

Rangel, J. O. (2005). La biodiversidad de colombia. *Palimpsestvs*, (5).

Reager, J., & Famiglietti, J. S. (2013). Characteristic mega-basin water storage behavior using grace. *Water resources research*, *49*(6), 3314–3329.

Reager, J., Thomas, B., & Famiglietti, J. (2014). River basin flood potential inferred using grace gravity observations at several months lead time. *Nature Geoscience*, *7*(8), 588.

Resende, T. C., Longuevergne, L., Gurdak, J. J., Leblanc, M., Favreau, G., Ansems, N., . . . Aureli, A. (2019). Assessment of the impacts of climate variability on total water storage across africa: Implications for groundwater resources management. *Hydrogeology Journal*, *27*(2), 493–512.

Restrepo Ángel, J. D. (2005). *Los sedimentos del rıo magdalena: Reflejo de la crisis ambiental*. Universidad Eafit.

Restrepo, J., & Kjerfve, B. (2000). Magdalena river: Interannual variability (1975–1995) and revised water discharge and sediment load estimates. *Journal of hydrology*, *235*(1-2), 137–149.

Rodell, M. [Matthew], Chen, J. [Jianli], Kato, H., Famiglietti, J. S., Nigro, J., & Wilson, C. R. (2007). Estimating groundwater storage changes in the mississippi river basin (usa) using grace. *Hydrogeology Journal*, *15*(1), 159–166.

Rodell, M. [Matthew], Houser, P., Jambor, U., Gottschalck, J., Mitchell, K., Meng, C.-J., . . . Bosilovich, M. et al. (2004). The global land data assimilation system. *Bulletin of the American Meteorological Society*, *85*(3), 381–394.

Rodell, M. [Matthew], Velicogna, I., & Famiglietti, J. S. (2009). Satellite-based estimates of groundwater depletion in india. *Nature*, *460*(7258), 999.

Rodríguez, E., Sánchez, I., Duque, N., Arboleda, P., Vega, C., Zamora, D., . . . García, C. et al. (2019). Combined use of local and global hydro meteorological data with hydrological models for water resources management in the magdalena-cauca macro basin–colombia. *Water Resources Management*, 1–21.

Rodríguez, N., & Armenteras, D. (2005). Ecosistemas naturales de la cuenca del río magdalena. In *Los sedimentos del río magdalena: Reflejo de la crisis ambiental* (pp. 79–98). Universidad Eafit.

Rosenqvist, A., Shimada, M., Ito, N., & Watanabe, M. (2007). Alos palsar: A pathfinder mission for global-scale monitoring of the environment. *IEEE Transactions on Geoscience and Remote Sensing*, *45*(11), 3307–3316.

Rowlands, D., Luthcke, S., McCarthy, J., Klosko, S., Chinn, D., Lemoine, F., . . . Sabaka, T. (2010). Global mass flux solutions from grace: A comparison of parameter estimation strategies—mass concentrations versus stokes coefficients. *Journal of Geophysical Research: Solid Earth*, *115*(B1).

Running, S., Mu, Q., & Zhao, M. (2017). Mod16a2 modis/terra net evapotranspiration 8-day l4 global 500m sin grid v006. *NASA EOSDIS Land Processes DAAC https://doi. org/10.5067/MODIS/MOD16A2*, *6*.

Sakumura, C., Bettadpur, S., & Bruinsma, S. (2014). Ensemble prediction and intercomparison analysis of grace time-variable gravity field models. *Geophysical Research Letters*, *41*(5), 1389–1397.

Salazar, J. F., Villegas, J. C., Rendón, A. M., Rodríguez, E., Hoyos, I., Mercado-Bettín, D., & Poveda, G. (2018). Scaling properties reveal regulation of river flows in the amazon through a forest reservoir. *Hydrology and Earth System Sciences*, *22*(3), 1735–1748.

Save, H. [Himanshu], Bettadpur, S., & Tapley, B. D. (2016). High-resolution csr grace rl05 mascons. *Journal of Geophysical Research: Solid Earth*, *121*(10), 7547–7569.

Scanlon, B., Zhang, Z., Rateb, A., Sun, A., Wiese, D., Save, H., . . . Döll, P. et al. (2019). Tracking seasonal fluctuations in land water storage using global models and grace satellites. *Geophysical Research Letters*, *46*(10), 5254–5264.

Scanlon, B., Zhang, Z., Save, H., Sun, A., Schmied, H., van Beek, L., . . . Reedy, R. C. et al. (2018). Global models underestimate large decadal declining and rising water storage trends relative to grace satellite data. *Proceedings of the National Academy of Sciences*, *115*(6), E1080–E1089.

Scanlon, B. R., Longuevergne, L., & Long, D. (2012). Ground referencing grace satellite estimates of groundwater storage changes in the california central valley, usa. *Water Resources Research*, *48*(4).

Scanlon, B. R., Zhang, Z. [Zizhan], Save, H., Wiese, D. N., Landerer, F. W., Long, D., . . . Chen, J. (2016). Global evaluation of new grace mascon products for hydrologic applications. *Water Resources Research*, *52*(12), 9412–9429.

Schellekens, J., Dutra, E. [Emanuel], la Torre, A. M.-d., Balsamo, G. [Gianpaolo], van Dijk, A. [Albert], Weiland, F. S., . . . Eisner, S. [Stephanie] et al. (2017). A global water resources ensemble of hydrological models: The earth2observe tier-1 dataset. *Earth System Science Data*, *9*, 389–413.

Schneider, U., Fuchs, T., Meyer-Christoffer, A., & Rudolf, B. (2008). Global precipitation analysis products of the gpcc. *Global Precipitation Climatology Centre (GPCC), DWD, Internet Publikation*, *112*.

Seo, J. Y., & Lee, S.-I. (2016). Integration of grace, ground observation, and land-surface models for groundwater storage variations in south korea. *International journal of remote sensing*, *37*(24), 5786–5801.

Seyoum, W. M., & Milewski, A. M. (2016). Monitoring and comparison of terrestrial water storage changes in the northern high plains using grace and in-situ based integrated hydrologic model estimates. *Advances in water resources*, *94*, 31–44.

Shamsudduha, M., Taylor, R., & Longuevergne, L. (2012). Monitoring groundwater storage changes in the highly seasonal humid tropics: Validation of grace measurements in the bengal basin. *Water Resources Research*, *48*(2).

Shamsudduha, M. [Mohammad], Taylor, R. G., Jones, D., Longuevergne, L., Owor, M., & Tindimugaya, C. (2017). Recent changes in terrestrial water storage in the upper nile basin: An evaluation of commonly used gridded grace products. *Hydrology and Earth system sciences*, *21*(9), 4533–4549.

Sheffield, J., Ferguson, C. R., Troy, T. J., Wood, E. F., & McCabe, M. F. (2009). Closing the terrestrial water budget from satellite remote sensing. *Geophysical Research Letters*, *36*(7).

Shen, H., Leblanc, M., Tweed, S., & Liu, W. (2015). Groundwater depletion in the hai river basin, china, from in situ and grace observations. *Hydrological Sciences Journal*, *60*(4), 671–687.

Sierra, A. M., García, C., Nieto, E., & Ortiz, N. (2013). Orogenia de las cordilleras colombianas: Oriental, central y occidental. geología y geomorfología. Available in https: //geoloygeomorfoubosque.blogspot.com/2013/03/orogenia-de-las-cordilleras-colombianas.html. Retrieved 27 May 2020.

Šiklomanov, I. (1997). *Comprehensive assessment of the freshwater resources of the world*. WMO.

Sproles, E., Leibowitz, S., Reager, J. et al. (2015). Grace storage-runoff hystereses reveal the dynamics of regional watersheds. *Hydrology and Earth System Sciences*, *19*(7).

Swenson, S., & Wahr, J. (2009). Monitoring the water balance of lake victoria, east africa, from space. *Journal of Hydrology*, *370*(1-4), 163–176.

Swenson, S. [SC], & Lawrence, D. (2015). A grace-based assessment of interannual groundwater dynamics in the community land model. *Water Resources Research*, *51*(11), 8817–8833.

Swenson, S. [Sean], & Wahr, J. [John]. (2006). Post-processing removal of correlated errors in grace data. *Geophysical Research Letters*, *33*(8).

Syed, T. H., Famiglietti, J. S., Rodell, M., Chen, J., & Wilson, C. R. (2008). Analysis of terrestrial water storage changes from grace and gldas. *Water Resources Research*, *44*(2).

Tang, J., Cheng, H., & Liu, L. (2014). Assessing the recent droughts in southwestern china using satellite gravimetry. *Water Resources Research*, *50*(4), 3030–3038.

Tang, Q., & Zhang, X. (2011). Mapping evapotranspiration using modis and grace data. In *2011 19th international conference on geoinformatics* (pp. 1–4). IEEE.

Tangdamrongsub, N., Ditmar, P., Steele-Dunne, S., Gunter, B., & Sutanudjaja, E. (2016). Assessing total water storage and identifying flood events over tonlé sap basin in cambodia using grace and modis satellite observations combined with hydrological models. *Remote sensing of environment*, *181*, 162–173.

Tapley, B. D. [Byron D], Bettadpur, S., Watkins, M., & Reigber, C. (2004). The gravity recovery and climate experiment: Mission overview and early results. *Geophysical Research Letters*, *31*(9).

Taylor, K. E. (2001). Summarizing multiple aspects of model performance in a single diagram. *Journal of Geophysical Research: Atmospheres*, *106*(D7), 7183–7192.

Taylor, R. G., Scanlon, B. [Bridget], Döll, P. [Petra], Rodell, M. [Matt], Van Beek, R., Wada, Y. [Yoshihide], . . . Edmunds, M. et al. (2013). Ground water and climate change. *Nature climate change*, *3*(4), 322–329.

Tiwari, V., Wahr, J., & Swenson, S. (2009). Dwindling groundwater resources in northern india, from satellite gravity observations. *Geophysical Research Letters*, *36*(18).

Toussaint, J. F., & Restrepo, J. J. (1982). Magmatic evolution of the northwestern andes of colombia. *Earth-Science Reviews*, *18*(3-4), 205–213.

Vargas, G., Hernández, Y., & Pabón, J. D. (2018). La niña event 2010–2011: Hydroclimatic effects and socioeconomic impacts in colombia. In *Climate change, extreme events and disaster risk reduction* (pp. 217–232). Springer.

Vishwakarma, B. D., Devaraju, B., & Sneeuw, N. (2018). What is the spatial resolution of grace satellite products for hydrology? *Remote Sensing*, *10*(6), 852.

Voss, C. (2005). The future of hydrogeology. *Hydrogeology Journal*, *13*(1), 1–6.

Voss, K. A., Famiglietti, J. S., Lo, M., De Linage, C., Rodell, M., & Swenson, S. C. (2013). Groundwater depletion in the middle east from grace with implications for transboundary water management in the tigris-euphrates-western iran region. *Water resources research*, *49*(2), 904–914.

Vuille, M. (2013). *Climate change and water resources in the tropical andes*. Inter-American Development Bank.

Wada, Y. [Yoshihide], Van Beek, L. P., Van Kempen, C. M., Reckman, J. W., Vasak, S., & Bierkens, M. F. (2010). Global depletion of groundwater resources. *Geophysical research letters*, *37*(20).

Wahr, J. [John], Swenson, S., Zlotnicki, V., & Velicogna, I. (2004). Time-variable gravity from grace: First results. *Geophysical Research Letters*, *31*(11).

Wang, H., Guan, H., Gutiérrez-Jurado, H. A., & Simmons, C. T. (2014). Examination of water budget using satellite products over australia. *Journal of Hydrology*, *511*, 546–554.

Wang, S., & Li, J. [Junhua]. (2016). Terrestrial water storage climatology for canada from grace satellite observations in 2002–2014. *Canadian Journal of Remote Sensing*, *42*(3), 190–202.

Watkins, M. M., Wiese, D. N., Yuan, D.-N., Boening, C., & Landerer, F. W. (2015). Improved methods for observing earth's time variable mass distribution with grace using spherical cap mascons. *Journal of Geophysical Research: Solid Earth*, *120*(4), 2648–2671.

Waylen, P., & Poveda, G. [Germán]. (2002). El niño–southern oscillation and aspects of western south american hydro-climatology. *Hydrological Processes*, *16*(6), 1247–1260.

Weedon, G. P., Balsamo, G., Bellouin, N., Gomes, S., Best, M. J., & Viterbo, P. (2014). The wfdei meteorological forcing data set: Watch forcing data methodology applied to era-interim reanalysis data. *Water Resources Research*, *50*(9), 7505–7514.

Wiese, D. N., Landerer, F. W., & Watkins, M. M. (2016). Quantifying and reducing leakage errors in the jpl rl05m grace mascon solution. *Water Resources Research*, *52*(9), 7490–7502.

Winter, T. C. (1999). Relation of streams, lakes, and wetlands to groundwater flow systems. *Hydrogeology Journal*, *7*(1), 28–45.

Wolter, K., & Timlin, M. S. (1993). Monitoring enso in coads with a seasonally adjusted principal. In *Proc. of the 17th climate diagnostics workshop, norman, ok, noaa/nmc/cac, nssl, oklahoma clim. survey, cimms and the school of meteor., univ. of oklahoma, 52* (Vol. 57).

Xiao, R., He, X., Zhang, Y., Ferreira, V., & Chang, L. (2015). Monitoring groundwater variations from satellite gravimetry and hydrological models: A comparison with in-

situ measurements in the mid-atlantic region of the united states. *Remote Sensing*, *7*(1), 686–703.

Xie, Z., Huete, A., Ma, X., Restrepo-Coupe, N., Devadas, R., Clarke, K., & Lewis, M. (2016). Landsat and grace observations of arid wetland dynamics in a dryland river system under multi-decadal hydroclimatic extremes. *Journal of Hydrology*, *543*, 818–831.

Yang, P., & Chen, Y. (2015). An analysis of terrestrial water storage variations from grace and gldas: The tianshan mountains and its adjacent areas, central asia. *Quaternary International*, *358*, 106–112.

Yang, P., Xia, J., Zhan, C., Qiao, Y., & Wang, Y. (2017). Monitoring the spatio-temporal changes of terrestrial water storage using grace data in the tarim river basin between 2002 and 2015. *Science of the Total Environment*, *595*, 218–228.

Yeh, P. J.-F., Swenson, S. C., Famiglietti, J. S., & Rodell, M. (2006). Remote sensing of groundwater storage changes in illinois using the gravity recovery and climate experiment (grace). *Water Resources Research*, *42*(12).

Yi, H., & Wen, L. (2016). Satellite gravity measurement monitoring terrestrial water storage change and drought in the continental united states. *Scientific reports*, *6*(1), 1–9.

Yuan, T., Lee, H., & Jung, H. (2015). Toward estimating wetland water level changes based on hydrological sensitivity analysis of palsar backscattering coefficients over different vegetation fields. *Remote Sensing*, *7*(3), 3153–3183.

Zaitchik, B. F., Rodell, M., & Reichle, R. H. (2008). Assimilation of grace terrestrial water storage data into a land surface model: Results for the mississippi river basin. *Journal of Hydrometeorology*, *9*(3), 535–548.

Zapata, A. F. (2019). *Caracterización espacial de la precipitación en la cuenca del magdalena - cauca* (Universidad de Antioquia, Ingeniería Ambiental).

Zaveri, E., Grogan, D. S., Fisher-Vanden, K., Frolking, S., Lammers, R. B., Wrenn, D. H., . . . Nicholas, R. E. (2016). Invisible water, visible impact: Groundwater use and indian agriculture under climate change. *Environmental Research Letters*, *11*(8), 084005.

Zhang, L. (2017). *Terrestrial water storage from grace gravity data for hydrometeorological applications* (Doctoral dissertation).

Zhang, L., Dobslaw, H., Stacke, T., Güntner, A., Dill, R., & Thomas, M. (2017). Validation of terrestrial water storage variations as simulated by different global numerical models with grace satellite observations.

Zhang, Z. [Zizhan], Chao, B., Chen, J., & Wilson, C. (2015). Terrestrial water storage anomalies of yangtze river basin droughts observed by grace and connections with enso. *Global and Planetary Change*, *126*, 35–45.